EXTRACTION OF NICKEL AND COBALT FROM LATERITIC ORES BY NITRIC ACID

A THESIS SUBMITTED TO
THE GRADUATE SCHOOL OF NATURAL AND APPLIED SCIENCES
OF
MIDDLE EAST TECHNICAL UNIVERSITY

BY

ONUR SAKA

IN PARTIAL FULFILLMENT OF THE REQUIREMENTS
FOR
THE DEGREE OF MASTER OF SCIENCE
IN
METALLURGICAL AND MATERIALS ENGINEERING

DECEMBER 2014

Approval of the thesis:

EXTRACTION OF NICKEL AND COBALT FROM LATERITIC ORES BY NITRIC ACID

submitted by **ONUR SAKA** in partial fulfillment of the requirements for the degree of **Master of Science in Metallurgical and Materials Engineering Department, Middle East Technical University** by,

Prof. Dr. Gülbin Dural Ünver _____
Dean, Graduate School of **Natural and Applied Sciences**

Prof. Dr. Hakan C. Gür _____
Head of Department, **Metallurgical and Materials Engineering**

Prof. Dr. Yavuz A. Topkaya _____
Supervisor, **Metallurgical and Materials Engineering Dept., METU**

Examining Committee Members:

Prof. Dr. Abdullah Öztürk _____
Metallurgical and Materials Engineering Dept., METU

Prof. Dr. Yavuz A. Topkaya _____
Metallurgical and Materials Engineering Dept., METU

Prof. Dr. İshak Karakaya _____
Metallurgical and Materials Engineering Dept., METU

Prof. Dr. M. Ümit Atalay _____
Mining Engineering Dept., METU

Assist. Prof. Dr. Mert Efe
Metallurgical and Materials Engineering Dept., METU _____

Date: 05.12.2014

I hereby declare that all information in this document has been obtained and presented with academic rules and ethical conduct. I also declare that, as required by those rules and conduct, I have fully cited and referenced all material and results that are not original to this work.

Name, Last Name: Onur Saka

Signature:

ABSTRACT

EXTRACTION OF NICKEL AND COBALT FROM LATERITIC ORES BY NITRIC ACID

Saka, Onur

M.S., Department of Metallurgical and Materials Engineering

Supervisor: Prof. Dr. Yavuz A. Topkaya

December 2014, 132 pages

This thesis study is related to the extraction kinetics of nickel and cobalt from lateritic nickel ores from Gördes/Manisa region of Turkey. The experimental studies involved the optimization of nitric acid leaching of nickel laterite ores at atmospheric pressure for high nickel and cobalt extraction. The main parameters optimized after the characterization of laterites were the nitric acid concentration, leaching temperature, duration of leaching and the particle size of the ore sample.

The atmospheric leaching experiments were conducted on the 70% limonitic 30% nontronitic ore mixture obtained from the Gördes open pit mine. Considering the similar studies from literature and highest nickel and cobalt extraction into account, the process parameters optimized as; leaching at 104°C with 378 g/L nitric acid concentration, 48 hours of experiment duration, -600 μm particle size using S/L ratio of 1/5 wt/vol. 95.4% nickel and 96.6% cobalt were extracted at the given leaching conditions.

Atmospheric leaching produced a contaminated pregnant leach solution (PLS) due to high iron and aluminum contents. A stock of PLS was produced for the selective precipitation for the impurities. Iron, aluminum and chromium which are the main impurity elements were almost completely removed from leach liquor with low nickel and cobalt losses.

Keywords: Laterite, Atmospheric Leaching, Nickel, Cobalt, Nitric Acid

ÖZ

NİKEL VE KOBALTIN LATERİTİK CEVHERLERDEN NİTRİK ASİT İLE EKSTRAKSİYONU

Saka, Onur

Yüksek Lisans, Metalurji ve Malzeme Mühendisliği Bölümü

Tez Yöneticisi: Prof. Dr. Yavuz A. Topkaya

Aralık 2014, 132 sayfa

Bu tez çalışması Manisa-Gördes bölgesinden alınan lateritik tipteki cevherden nikel ve kobalt ektraksiyonu ile ilgilidir. Deneysel çalışmalar lateritik cevherin atmosferik nitrik asit liçi ile yüksek verimde nikel ve kobalt ektraksiyonu için parametreleri optimize etmeyi kapsar. Nitrik asit konsantrasyonu, liç sıcaklığı, süresi ve deneyde kullanılan cevherin parçacık boyutu deneyler yoluyla optimize edilen temel değişkenlerdir.

Atmosferik liç deneyleri Gördes açık maden ocağından elde edilen %70 limonitik cevher %30 nontronitik cevher içeren bir cevher karışımı ile yapılmıştır. Daha önce yapılan benzer çalışmaları göz önünde tutarak, ayrıca deneysel çalışmalarda en yüksek nikel ve kobalt extraksiyonu gözeterek optimum deney parametreleri şu şekilde belirlenmiştir: 104°C de 1/5 katı/sıvı oranı kullanarak 378 g/L nitrik asit, ve 600 µm altı parçacık boyutu kullanarak 48 saat süreyle liç edilmesi sonucunda nikelin %95,4 ü ve kobaltın %96,6 sı liç çözeltisine alınmıştır.

Atmosferik liç işlemi demir ve alüminyum'un yüksek miktarlarda liç çözeltisine alınması nedeniyle kirli bir liç çözeltisi oluşturmuştur. Empürite çöktürme çalışmaları için bir stok oluşturulmuştur. Liç çözeltisi, nikel ve kobalt kayıpları kabul edilebilir sınırlarda tutularak, içerdiği ana safsızlıklar olan demir, alüminyum ve kromdan neredeyse tamamen arındırılmıştır.

Anahtar Kelimeler: Laterit, Atmosferik Liç, Nikel, Kobalt, Nitrik Asit

To my dear family;

ACKNOWLEDGEMENTS

First and foremost, I would like to express my sincere appreciation and gratitude to my supervisor Prof. Dr. Yavuz A. Topkaya for his limitless and continuous guidance, wisdom, never-ending belief and his endless patience and understanding in preparation of this thesis.

META Nikel Kobalt A.Ş. is gratefully acknowledged for providing the original nickel laterite ore samples and conducting the chemical analyses for the experimental leach residues.

I would like to thank my colleagues and friends Erman Kondu, Şerif Kaya, Recai Önal, Bengi Yağmurlu, Gülten Kılıç, Güher Tan, Orkun Muğan and Utku Olgun who were with me and helped me along the way with their emotional support, guidance, suggestions, and valuable friendships along my study. I would like to present my special thanks to my friends Mehmet Dincer and Kıvanç Korkmaz whom we spent most our time together throughout my journey which was full of laughter and joy.

My best friend Can Sönmez who was always with me from the beginning of my life and boosted my morale whenever I felt down also deserves a special acknowledgement. My dearest friends Özgün Yalçın, Deniz Gürkan Uzlu, Arman Güngör and Cansu Yanardağ also deserve many thanks for their moral support and valuable friendships.

Burcu Aksoy is the precious one who was with me throughout the most important span of my life. She helped and encouraged me to make the right choices in my life. Her existence in my life did not only enlighten my perspective but also encouraged me to complete this thesis by giving my best.

At last but not the least, I would like to express my gratitude to my family for their support and patience throughout this study. My mother Eser Saka is my greatest motivator who sacrificed all her life to help me become who I am. I also would like thank to my grandmothers Necla Saka and Pakize Türkistanlı for their endless love and support. I also would like to present my appreciation to my dearest uncle Haydar Saka who is my mentor and idol, has influenced me with his vision, perspective on life and philosophy.

TABLE OF CONTENTS

LIST OF TABLES

TABLES

LIST OF FIGURES

FIGURES

CHAPTER 1

INTRODUCTION

Nickel is a widely used element in thousands of products such as in industrial, military, aerospace, marine and architectural applications. Nickel is also used in many of everyday used products, including coins, magnets and rechargeable batteries. The magnetic properties and the electrical conductivity of nickel make it very important for use in computer hard drives and many other electronics applications. But the main use of nickel is in stainless steel industry. About 65% of the Nickel produced is used in stainless steel industry. Another 20% goes into superalloys or nonferrous alloys. Nickel is also used in heat and electrical resistant alloys [1].

According to international nickel study group data, usage of nickel had grown about seven percent to 1.77 million tons in 2013. The future for nickel look promising as an increase in the demand for stainless steel and superalloys are expected on the forthcoming years [1]. Statistics show that the nickel prices are unstable and open to rapid changes due to worldwide economics and nickel stocks. Nickel prices took a slump below 14000 USD/t in July 2013 but climbed up to 21500 USD/t by May 2014, However, there is a decreasing trend in the nickel prices over the past few months and up-to date price of nickel has dropped back to 15535 USD/t as retrieved from London Metal Exchange on 12.11.2014 [2].

Although the lateritic ores contain about 70% of the world's nickel resources, most of the nickel production has been done from sulphide ores until recently, due to their higher nickel grade and cheaper production. Due to the decline in

the global reserves of sulphide ores, and developing hydrometallurgical production methods from lateritic ores, there is an increase in the production from laterites [3, 4].

Three major routes can be used for laterite processing which are; pyrometallurgical, hydrometallurgical processes and the Caron process. The Caron process is combination of pyrometallurgical and hydrometallurgical steps but it is not seen as a viable option anymore because it is energy intensive, and has low cobalt recovery values [3]. Since pyrometallurgical processes need higher grade ores, they have higher energy requirements and have lower cobalt recoveries compared to hydrometallurgical techniques thus; hydrometallurgical methods are more frequently preferred since they are more applicable to limonitic ores [5].

High pressure acid leaching (HPAL) and atmospheric pressure acid leaching (AL) are the primary hydrometallurgical processes that are commercially applied. The feasibility of HPAL is highly dependent on the ore grade since the capital cost is very high as it requires titanium autoclaves to operate. Atmospheric leaching is conducted at open vessels or tanks; therefore the capital cost is much lowered as it avoids the need for an autoclave. In HPAL the dissolved iron, re-precipitates as hematite at high temperatures. However atmospheric leaching produces contaminated pregnant leach solution (PLS) containing iron and aluminum in high concentrations which should be selectively precipitated from the leach liquor [6].

Iron removal by hydrolytic precipitation, with the addition of an alkali is a possible method. Another method which can be used is the thermal hydrolysis in an autoclave for the iron precipitation [7, 8].

Throughout this study, the main objective was to investigate the leachability of the lateritic nickel ores from Gördes/Manisa region of Turkey with the atmospheric nitric acid leaching method as an alternative to HPAL. The optimum leaching conditions for the highest Ni and Co extraction values were

investigated. Also efficient removal of iron for purification of the PLS was studied on the course of this thesis content.

CHAPTER 2

LITERATURE SURVEY

2.1 Nickel and Its Application Areas

Nickel is a transition metal which lies on the 4^{th} period and 8B group in the periodic table with an atomic weight 58.71. It has a density of 8.912 g/cm^3, and has a silvery white appearance. Generally nickel forms FCC crystal structure, although hexagonal form can also be encountered which transforms to cubic structure at 250°C.

It is a poor thermal and electrical conductor but shows ferromagnetic properties at room temperature when it is in cubic form. Nickel can form multiple chemical compounds with various elements as its position on the periodic table suggests. The main usage of nickel is as an alloying element. Nickel bearing alloys and materials are widely used in thousands of products in our everyday lives. They are selected over other materials because they have excellent corrosion resistance, reasonably high strength and toughness at low temperatures and have unique magnetic properties. As an exceptional property, nickel's corrosion resistance to alkalis shines out among others [9, 10].

2.2 Nickel Reserves

According to Boldt, earth's crust contains 0.008% of nickel which makes it the 24th most abundant element in it [11]. However the reserves which can be feasibly mined and processes are more limited. The nickel ores which are of commercial significance are fewer compared to copper, zinc or lead, although it is a more abundant element than them. Nickel reserves are land based deposits which are mineable, and economically processable. On the other hand nickel resources which is nearly the twice amount of nickel reserves, are not profitable for mining. Developments of new technologies and processes will most probably result in some of the nickel resources be converted into nickel reserves. According to 2014 issue of mineral commodity summary, there is at least 130 million tons of nickel on worldwide land based resources which has Ni grade over 1% [12].

There are mainly two types of ore deposits that the nickel is processed. The first one is sulfide ore deposits which are magmatic. The second source of nickel is laterites and the principal ore minerals are nickeliferrous limonite, saprolitic clay layers and transition layers (nontronite) [13].

Nickel, which is to be extracted from its ores, does not occur in metallic form. It is generally found in some nickel minerals or, as a substitution element in other mineral lattices. The divalent ions of iron, magnesium and nickel has similar diameters, due to this, nickel is generally associated with them. Boldt states that, the observations on igneous rocks shows that the increase in iron and magnesium also result in a higher nickel content, whereas nickel quantity is inversely proportional with aluminum and silicon content [11].

The distribution of nickel production worldwide according to 2011 data of mineral commodity summaries is given in Figure 1.

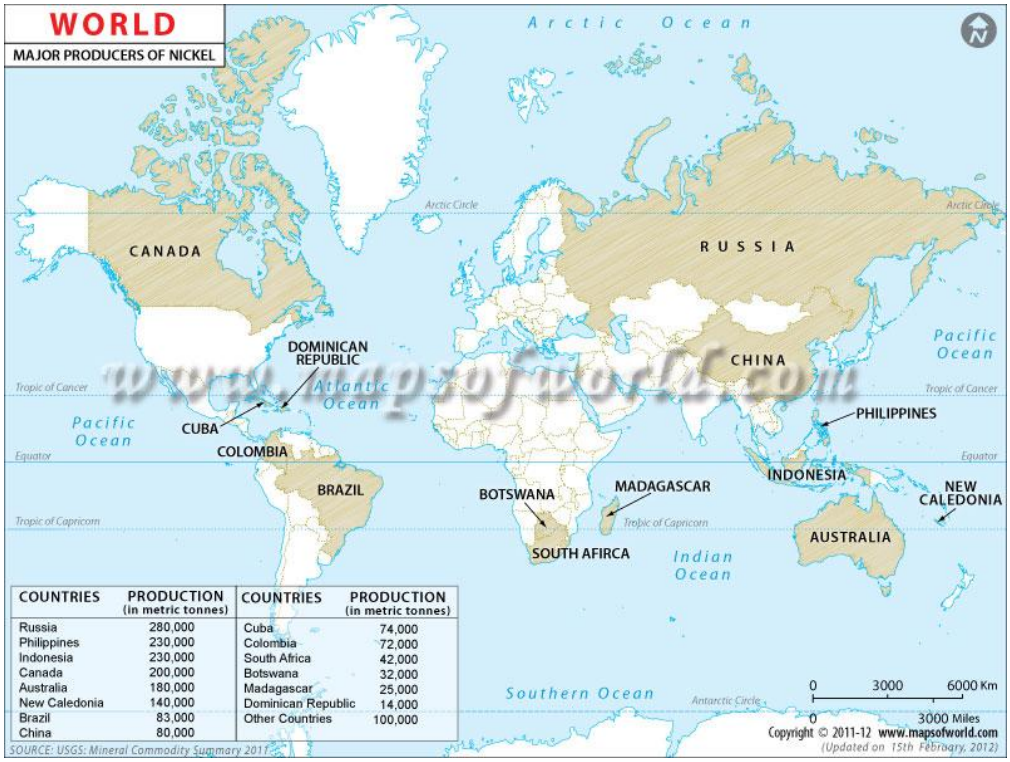

Figure 1**:** Nickel production throughout the world [14].

The global nickel production is led by Russia, Canada, Indonesia, and Philippines but there are plenty of others producers ranging from moderate to minor in terms of production [15].

Global nickel production by ore types over time can be seen in Figure 2. It shows that the early source of nickel was laterites, but the production from sulfides dominated the nickel market, in the 20th century. However, the increase in the laterite processing, which has ended the dominance of sulfides, is observed in recent years.

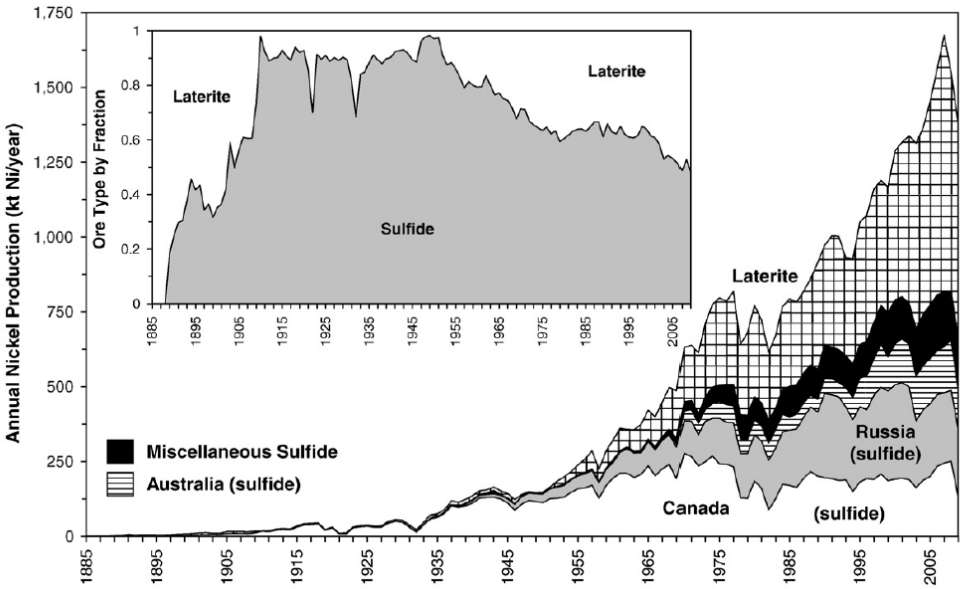

Figure 2: Worldwide nickel production by ore type [16]

Even though Turkey can be considered rich for some ore deposits due to its rich diversity of mineral types, thanks to its complicated geology, it can be classified as relatively poor in terms nickel reserves. But with the start of the 21st century, there has been an increasing effort for nickel production headed by the private enterprises, especially accelerated by the increase in nickel prices. As a result several nickel-cobalt ore reserves were discovered which may lead to significant production in the future. Currently active production facilities are in Manisa-Turgutlu Çaldağ, Manisa Gördes and Eskişehir-Mihalıççık-Yunus Emre [17].

From the two pits opened in Gördes nickel facility, since 2003, 230000 tons of nickel was produced and 150000 tons were exported to Greece, FYROM, and China. Some of the remaining nickel ore has been kept for the pilot testing [18].

2.2.1 Sulfide Type Nickel Ores

Sulfide type nickel ores can be found in magmatic rocks, formed by the volcanic and hydrothermal processes. They usually contain 0.4-2.0% of nickel, 0.2-2.0% copper, 10-30% iron, 5-20% sulfur and several other minerals including silica, magnesia, alumina, calcium oxide and copper. Occasionally other precious metals such as gold, platinum and palladium can be encountered within these sulfide ores. Most of the global nickel production are supplied form pentlandite $(Fe,Ni)_9S_8$; which is the primary ore mineral is in sulfide type of deposits, and has about 34% Ni in its content. Nickeliferous pyrrhotite (Fe_7S_8), and chalcopyrite ($CuFeS_2$) are the other major sulfide minerals. Magnetite (Fe_3O_4), pyrite (FeS_2), ilmenite ($FeTiO_3$), chromite ($FeCr_2O_4$), cubanite ($CuFe_2S_3$) and violarite (Ni_2FeS_4) are the other commonly encountered minerals but usually occur in small amounts. [10, 15, 19].

About 30-40% of worldwide nickel reserves are found in sulfide deposits however; most of the nickel has been produced from sulfide ores until today. The main reason is the difficulty of laterite processing compared to sulfides. Sulfide ores can be concentrated by physical methods with ease, whereas laterites require more complex treatment [16]. The nickel production from oxide ores, consume up to two or three times the energy compared to production from sulfide ores, which makes the production more expensive and sensitive to fuel oil and electrical power costs. Recovery of by-products, also favor the production form sulfide ores. The political and geographical factors have also influenced the nickel production. Sulfide nickel deposits are mostly found close to major nickel markets [10]. Sulfide ores generally have higher nickel grades and can be found on larger areas especially vertically which makes their mining cheaper. Major sulfide mineral deposits are found in Canada, Russia, Republic of South Africa, Zimbabwe, Finland and Australia [19].

However; the decrease of the grades of the sulfide ores, since the richer ores are consumed, and the expected long-term depletion in discovery of new sulfide deposits in traditional mining districts has forced the nickel industry to shift its production to more challenging locations like east-central Africa and the Subarctic and also to make use of oxide ore deposits more [10, 12].

Pyrometallurgical processing of sulfide ores, are very similar to other base metals. The general nickel production from a sulfide body starts with an open cut, or underground mining. It is followed by concentration by flotation. Afterwards concentrates are smelted to produce a Ni-Cu matte and then refined to produce pure metal. Smelters and refineries can be at different locations depending on geographical factors. Copper is an important co-product, and precious metals such as silver, gold and platinum are also often extracted from sulfide ore bodies [16].

2.2.2 Oxide Type Nickel Ores

As specified by Boldt, laterites were the main source of nickel towards the end of 19th century, before the sulfides deposits were discovered in Ontario, Canada. As stated previously in the explanation of sulfide deposits, about 60-70% of worldwide nickel reserves are found in oxide deposits however; most of the nickel production was supplied from sulfide ores throughout the 20th century [11]. This was mainly due to, higher nickel grades of the sulfides, and relatively complex and challenging processing of the lateritic ores because the nickel is present in the mineral crystal structures in them. The capital cost of laterite projects being high, and the processes being very resource intensive, was deterring factors. However, with the depletion of the sulfide deposits, and the growing demand of the nickel market, has forced the utilization of oxide ores. Thus, also with the development of new processing techniques, the production from laterites has an increasing trend. This trend can be observed

in Figure 2. But the economics and feasibility of the laterite projects are highly sensitive to feed grade of the plant and the global nickel prices.

Nickel is concentrated by rock-weathering process, in other words erosion. Nickel containing olivine-rich igneous rocks, are weathered and concentrated, by the chemical and mechanical activity of nature, up to a level that they can be considered as nickel ores. This process is called lateritic weathering [11, 20].

Upon weatherization of ultramafic rocks, minerals, which constitutes the olivine, decomposes with the help of atmosphere and rainfall or underground waters with acidic character, leading to iron, magnesium and nickel go into solution with ground waters. Afterwards iron oxidizes and precipitates as ferric hydroxide, which will then lose its water and form goethite, FeO(OH), and hematite Fe_2O_3. The iron oxide precipitates closer to the earth's surface, and nickel, which is less soluble compared to magnesium also precipitates. The nickel is in solid solution with these iron oxides. But the remaining nickel, magnesium and silica in the solution flow downwards and precipitate as hydrous silicate as the solution is neutralized in earth.

The nickel concentration generally increases upon descending to the bottom zone, but depending on the weathering factors, more nickel may also be retained in the upper part of the bedrock. The top part primarily consists of ferric oxides, which are entitled as limonite. The nickel deposit in this zone is called limonitic type or nickeliferous iron ore. The main component in this part is goethite, FeO(OH). The bottom silicate part of nickel deposit is called serpentine, $Mg_3Si_2O_5(OH)_4$, or saprolite zone. These two zones are encountered in almost all lateritic nickel deposits. A transition layer which consists of nontronite, $Na_{0.6}(Ni,Fe)_4(Al,Si)_8O_{20}(OH)_4(H_2O)_8$, which is an iron rich smectite, can also be present within the laterite profile. The compositions of the minerals serpentine and nontronite may differ depending on the laterite profile [11]. The solubility of the minerals limits the depth of laterite profile [20].

Since plentiful rainfall and humid climates favor the weatherization process, most lateritic ore deposits occur in tropical regions, or places where the climate was tropical or sub-tropical in the past ages [11].

The nickel and cobalt grades, of the lateritic deposits, generally are in the range between 0.66-2.4% and 0.01-0.15%, respectively; for Ni and Co (1.3%, ad 0.08% as an average) and the range in size changes from 2.5 to about 400 million tonnes [21]. Most of the lateritic nickel deposits are found in: New Caledonia, Cuba, Indonesia and the Philippines. Many laterite projects have started and grown all around the world, starting from the 1950's. Some larger scaled projects were established in New Caledonia and in the western Pacific archipelago, and other smaller projects around Eastern Europe and Russia. It can be foreseen that growth in the laterite processing will continue considering the existing production facilities and the planned projects in the development phase. Ferronickel is produced by a number of producers, but other intermediate products are also produced such as Ni-sulfide, Ni-hydroxide or Ni-carbonate. Cobalt is generally produced as a by-product [16]. Turkey as previously mentioned, can be classified as relatively poor in terms of nickel reserves. But there are several lateritic ore deposits located in the western part of Turkey. Currently on-going nickel projects are in: Manisa-Turgutlu Çaldağ, Manisa Gördes and Eskişehir-Mihalıççık-Yunus Emre.

Nickel occurs embodied within other oxide or silicate minerals, and nickel minerals are not encountered individually within the nickel laterites. In the review by Whittington and Muir, it is emphasized that nickel and cobalt substitution occur at the defect sites, in the goethite or hematite lattice, and this was supported by a number of authors in their studies on Ni-Co substitution on synthetic goethites. It is also expressed that the hematite has less substantial capacity for nickel, compared to goethite [20].

Laterites may be classified based on their mineralogy based on the predominant nickel hosting minerals. There are mainly three types of nickel deposits; Silicate nickel deposits mainly composed of hydrated Mg-Ni

silicates such as garnierite, silicate nickel deposits dominated by smectite clays such as nontronite, and oxide deposits mainly composed of iron oxides [22].

A cross-sectional illustration of typical laterite profile can be seen in Figure 3.

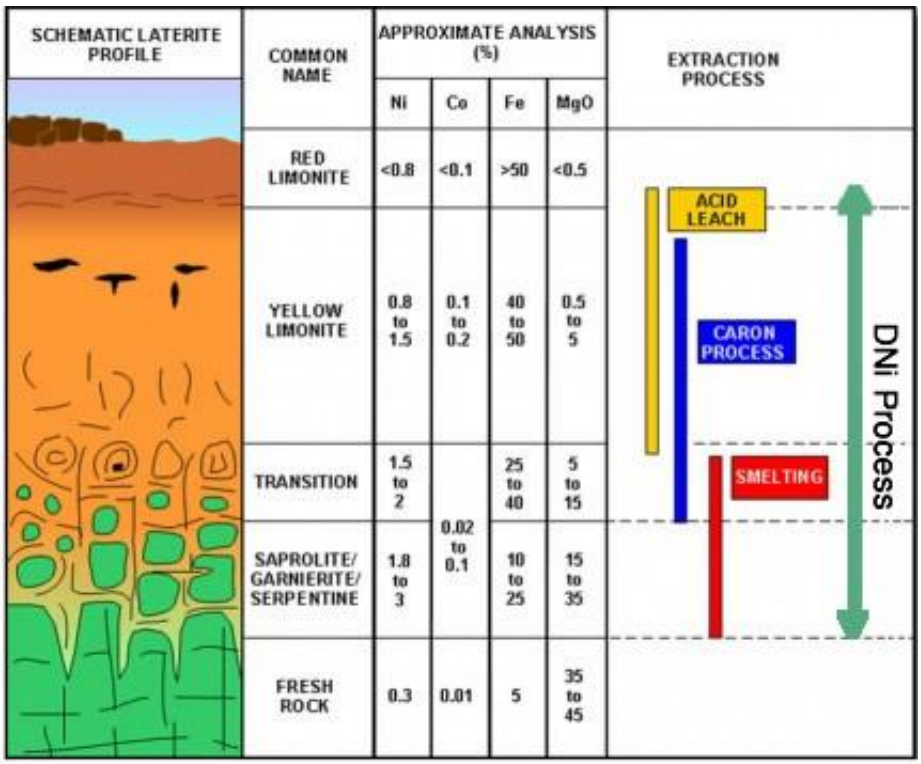

Figure 3: Cross-sectional view of a laterite profile [23]

The laterite profile begins with ferricrete (iron cap) at the top, followed by limonite, dominated by goethite. Two different classifications can be made for limonitic zone for some laterites. Top part of the limonite containing high amount of iron with low magnesium, and silicon content, is termed as red limonite, and lower part of the limonite higher in aluminosilicates and clays are called yellow limonite [24]. Smectite transition zone comes afterwards if the drainage is poor. Saprolite zone comes next and the deposit finishes with the unweathered rock at the base [21]. Laterites are easier to mine, since their

deposits are near surface, and can be mined by open pit method, whereas sulfides need underground mining which is more costly.

Whittington and Muir, pointed out that the limonitic part is not generally suited to upgrading, but upgrading can be applied, to an extent, for some of the magnesium rich-saprolitic ores. Ion exchange can take place for serpentines, smectite clays, garnierite, and some other minerals with variable chemical compositions such as:

$$Mg_3Si_2O_5(OH)_4 + 3Ni^{2+}_{(aq)} = Ni_3Si_2O_5(OH)_4 + 3Mg^{2+}_{(aq)} \qquad \text{Rx. 2.1}$$

Ion-exchange can also occur for nontronite, and they may contain up to 2% nickel [20].

2.3 Production Methods of Nickel from Lateritic Ores

Processing of oxide ores is more complex and difficult than of sulfides. Basic beneficiation of the ore is applied before processing, but efficient physical concentration of nickel is not possible in lateritic ores, since they are not suitable for most of the conventional beneficiation techniques which are used on sulfides, such as flotation or magnetic separation, because the nickel is substituted in the lattice of other minerals.

Both pyrometallurgical and hydrometallurgical processes are applied on lateritic ores for the extraction of nickel and cobalt, and downstream processes vary for the production of both intermediate and final products. Raw oxide ores usually have very high moisture content, and have high melting temperature components, in high amounts; therefore the energy requirement is very high for their fusion. Thus leaching may be more feasible from an economic standpoint [11]. Limonite and nontronite are suitable for

Caron process, acid leaching processes. But drying or calcining should be employed prior to processing for vaporization of the high water content [16].

Pyrometallurgical techniques are generally employed on saprolitic part of the laterite. Especially silicate rich garnierite ores are suitable for pyrometallurgical processes to produce high carbon ferronickel [4].

2.3.1 Pyrometallurgical Routes

Pyrometallurgical processes are the oldest and the most widely used processes to produce ferronickel or nickel matte. Smelting is a high energy consuming process since all the material need firstly to be calcined and then heated up to 1600°C to be melted and form a slag, but it is still a popular production technique for large scaled producers. Conventional route is followed, for most of the pyrometallurgical laterite processes. Commercial pyrometallurgical techniques use either, melting and sulfiding to separate an iron-nickel matte, or melting and reduction to obtain to separate and iron-nickel metal, from the gangue [3, 11].

Magnesium, iron and nickel content are critical for smelting. Silicate rich, high nickel (preferably >2%), high magnesium (10-15%) and low iron (13-20%) containing saprolites are suitable for nickel matte and ferronickel production [24]. Especially garnierite ores are very suitable for high carbon ferronickel production [4]. Limonites generally contain less than 2% nickel, and more than 25% iron, and has high water containing nature, so they cannot be treated via pyrometallurgical route, so they are best suited for hydrometallurgical processes. Lateritic ores with has high nickel grade (>2.2% Ni), low Fe/Ni ratio (5-6) and high MgO content are workable to produce high carbon ferronickel. If the Fe/Ni ratio is relatively higher (6-12) but the nickel grade is slightly lower (>1.5% Ni), and the ore has a high melting point slag (>1600°C) it is most suitable to produce low carbon

ferronickel. The ores with relatively high ratio (>6), but has a lower melting point slag (<1600°C); SiO_2/MgO ratio in the range 1.8 to 2.2, matte smelting is the most suitable way [3].

The basic principles in matte smelting for treatment of sulfides also apply to laterites. The only difference is that sulfide minerals do not need external sulfur sources but the oxide ores need sulfur bearing minerals, to be added to the furnace charge. Gypsium, $CaSO_4.H_2O$ which is a hydrated calcium sulfate is the most commonly used sulfiding agent.

Drying/dehydrating is carried out as a preliminary treatment in rotary kilns, multi hearth roasters, sintering machines or pelletizing machines. The ore, gypsium, limestone and the coke are charged in the furnace. As the charge goes down, while the hot reducing gas is going up, it is melted and reduced to produce matte and slag. The matte which consists of nickel iron and sulfur is then charged into converters and air is blown on it. Iron oxidizes preferentially than nickel, and forms a slag with the added silica. Converting continues until all the iron is taken away from the matte. The remaining slag is also recycled to minimize the nickel loss [11]. A conventional flowsheet for smelting to matte is given in Figure 4.

The growing need for nickel alloy steels increased the production of ferronickel, so ferronickel is the most commonly produced smelting product. The process is also called the Rotary Kiln-Electric Furnace (RKEF) process**.** The process procedure is almost the same as matte smelting procedure, except there is no need for sulfiding agent addition in the charge, for ferronickel production.

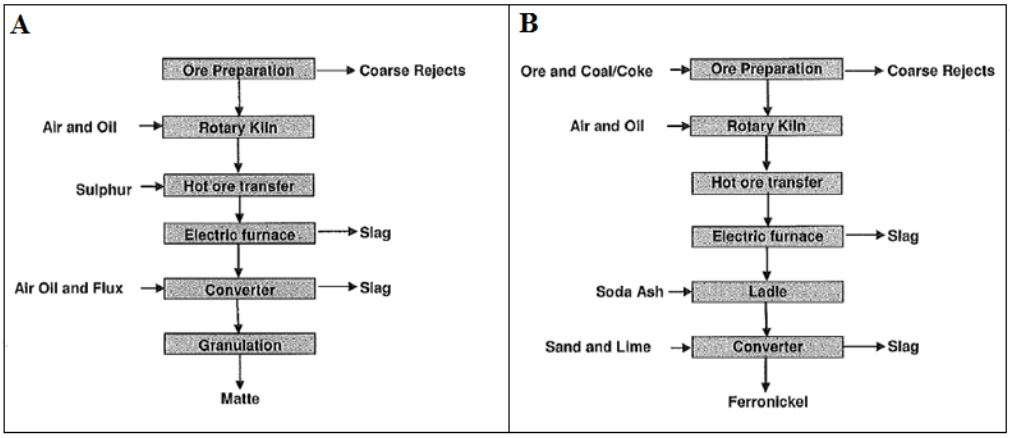

Figure 4: A: Schematic flowsheet for smelting to matte, B: Schematic flowseet for smelting to ferronickel [24]

Calcination of the ore, with coke addition in the charge, is achieved in rotary kilns at 900-1000°C. Some iron and nickel is pre-reduced in this step. Afterwards the calcine is smelted in an electric furnace at 1550°C with additional coke. This smelting operation produces ferronickel by reducing most of the iron and all of the nickel. Slag is formed with the remaining magnesium, iron and silica [24]. Carbon monoxide gas reduces the nickel and iron in the furnace. Iron oxide reduction takes place in three stages, hematite to magnetite, then to ferrous oxide, finally to metallic iron [11]. Some part of the reduction, occur with the reaction of solid carbon and oxides. Nickel and overall iron reduction reactions are as follows:

$$NiO + CO = Ni + CO_2 \qquad \text{Rx. 2.2}$$

$$Fe_2O_3 + 3CO = 2Fe + 3CO_2 \qquad \text{Rx. 2.3}$$

Then, the produced ferronickel is refined from its impurities, which are S, C, Si, Cr and P, with controlled oxidation. Recovery of nickel is generally high, usually in the 90-95% range [3].

Kyle summarized the pros and cons of ferronickel production by smelting as follows [24]:

- High magnesium containing ores can be treated (when Ni content is also high)
- Easily disposable residues
- High nickel recovery (≈90%)
- Reagents are easily available and inexpensive
- High capital costs
- High energy consumption, therefore operations are very sensitive to energy prices.
- Low magnesium ores cannot be handled, blending needed to maintain (SiO_2/MgO) ratios
- Cobalt is not recovered

According to Taylor, established hydrometallurgical options looks more appealing for both laterite and saprolite, than the pyrometallurgical processes [25]. However; Kyle stresses that major proportion of the nickel from laterites are still produced by smelting and further projects being developed. Some of the active smelting operations are Cerro Matoso in Columbia, Donaiambo and Konaniambo in New Caledonia, Pomalaa and Soroako in Indonesia, Onça Puma in Brazil, and several smelters in Japan which are using imported ores [24].

2.3.2 Caron Process

The Caron process which is applied on lateritic ores, developed and patented by M. H. Caron in 1924 is a hybrid process which utilizes both the pyrometallurgical and hydrometallurgical techniques. It is based on reduction of nickel and cobalt by roasting in the front end and leaching with ammonium carbonate on the back end. First commercial application was started in Nicaro,

Cuba in 1944 by US Government [10]. According to Taylor, there are currently 4 Caron facilities in the world; Yabulu in Australia, and Toctains in Brazil, Nicaro and Punta Gorda in Cuba. Although not officially confirmed, Nicaro was reported to be closed in 2012 [25].

The extraction values of nickel and cobalt goes down, as the saprolite content increases, because Ni and Co which are locked in the silicate matrix, cannot be reduced at roasting temperatures, so the Caron process is suitable for limonitic type of ores which are low in magnesium content and has a minimum iron level of 35%. [3, 24]. The flowsheet of Caron process is given in Figure 5:

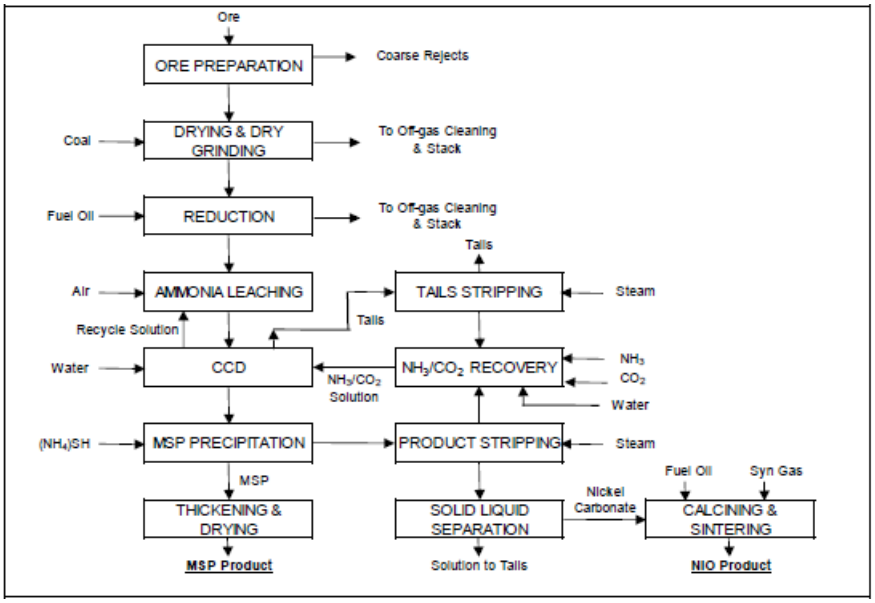

Figure 5: Caron process flowseet [25]

Crushed and screened ore is dried in a rotary kiln, followed by a reduction roasting operation in multi-hearth furnaces at 700-750°C. The reduced calcine is then cooled and leached selectively with ammonia-ammonium carbonate solution in agitated tanks. The obtained leach pulp is passed through a 7 stage CCD washing circuit and the tailings are separated for recovering ammonia.

Cobalt is recovered as cobalt sulphide, and sent for refining. Steam stripping is applied to take away the ammonia and carbon dioxide, which are recycled and re-used in leaching, and recover the nickel as nickel carbonate. Finally, calcination and sintering is applied to nickel carbonate to get a nickel oxide (NiO) product. The pros and cons of Caron process can be given as follows [24, 25]:

The positive sides of Caron Process are:

- It is a proven technology which can be applied to low grade ores
- Nickel and cobalt products can be obtained separately
- High selectivity of ammonia leaching and recycling of ammonia
- Mild operating conditions and minimal corrosion problems

The negative sides are:

- Low nickel and cobalt recovery compared to HPAL (80-85% for Ni, 35-55% for Co)
- Highly energy intensive drying and calcining steps
- Limitation to limonites (low magnesium ores)

The acid leaching processes is generally preferred over Caron process due to its negative aspects.

2.3.3 Hydrometallurgical Routes

As previously mentioned, for pyrometallurgical processes and Caron process to be economically practicable, the lateritic ores should have high nickel grades, and low humidity. However with the need of utilization of lower grade limonitic-nontronitic ores with high moisture content (25-50%), direct extraction methods which are based on acid leaching have emerged. The

temperature range of leaching processes is between 25-275°C, which significantly lowers the energy costs, compared to much more energy intensive pyrometallurgical routes. These leaching processes are also more environmental friendly since they do not emit toxic gases like SO_2. The efficient recovery of cobalt also makes the hydrometallurgical processes more feasible in the treatment of laterites.

Hydrometallurgical processes can be classified under two main topics, processes operated at atmospheric pressure and processes performed at high pressures, however there are some processes which combine both methods. Although high pressure acid leaching (HPAL) seems to be the most established process for the treatment of these ores, it is still a process in progress, and there are also number other developing methods both at atmospheric pressure and at high pressure such as DNi process, Neomet process, EPAL etc. The details of these processes will be summarized from literature in the following topics.

2.3.3.1 High Pressure Acid Leaching

High pressure acid leaching (HPAL) is the most established and widely used hydrometallurgical process for low grade laterites. The expected nickel extraction is high for HPAL, around 90-95%, and cobalt is also recovered as a valuable by product with high efficiency. HPAL dates back to 1959, when the first plant was built in Moa Bay in Cuba. Second generation PAL plants, Murrin, Cawse, and Bulong which are located at western region of Australia were engaged in 1990's, although Cawse and Bulong plants were closed down. Third generation plants, Goro in New Caledonia and Coral Bay in Philippines, were started in 2000's. Several other HPAL projects in the world are Ramu, Ravensthorpe, Taganito and Ambatovy [26, 27]. Another HPAL

plant is soon to begin production in Gördes project of META Nikel Kobalt A.Ş in Turkey.

HPAL operation is conducted in titanium autoclaves, under high pressure (35-55 atm) and temperatures between 240-255°C [28]. Commercially accepted lixiviant is sulphuric acid for the HPAL. Acid consumption for HPAL process is dependent on the mineralogy of the laterite, but usually is in the range 300-400 kg sulphuric acid/ton of ore. An abbreviated flowsheet of HPAL process is given in Figure 6.

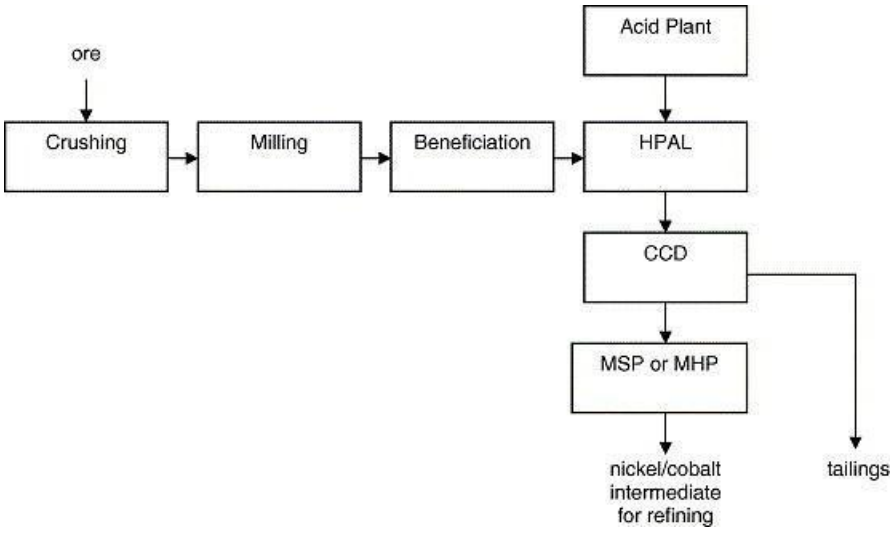

Figure 6: Simplified sketch of HPAL flowsheet [29]

Upgrading and concentration techniques are not very successful on lateritic ores, rather simple beneficiation techniques such as crushing and milling is applied to the ore before leaching. The ore is fed as slurry into the autoclave. Maximization of the amount of solid content is important for minimizing the costs, but slurries with too much viscosity will result in the disfunction of pumping systems. Firstly, the charged slurry is heated prior to acid leaching. Concentrated sulphuric acid, along with high pressure steam are injected to the autoclave when the desired temperature is reached. Few examples of the important leaching reactions are [26]:

$$NiO + H_2SO_4 = NiSO_4 + H_2O \quad \text{Rx. 2.4}$$

$$2FeO(OH) + 3H_2SO_4 = Fe_2(SO_4)_3 + 4H_2O \quad \text{Rx. 2.5}$$

$$2AlOOH + 3H_2SO_4 = Al_2(SO_4)_3 + 4H_2O \quad \text{Rx. 2.6}$$

This sketch in Figure 6 is a simplified representation and the details of downstream operations, MSP and MHP are not given, also alternative techniques such as direct solvent extraction is not shown. The pregnant leach solution can be treated by a number of methods after leaching, such as: production by nickel sulphide (MSP) intermediate used by Murrin Murrin and Moa Bay, production by nickel hydroxide (MHP) intermediate used by Cawse (closed), production by direct solvent extraction (DSX) used by Bulong (closed). The intermediate nickel hydroxide or nickel sulphide products are sent for further refining via solvent extraction/electrowinning [20].

HPAL is applied most efficiently for limonitic type, or limonitic/saprolitic mixture type of ores with low magnesium content (Mg not exceeding 5%). This is due to reaction chemistry of iron and magnesium at high temperatures. The ferric iron chemistry at elevated temperatures results in the dissolved iron to re-precipitate as ferric oxide (hematite in the HPAL temperatures), releasing the acid back into the solution. Magensium does not re-precipitate, which results in a much higher acid consumption for this operation, even though magnesium minerals are more easily dissolved in the acidic medium than iron oxides. Due to this thermal hydrolysis phenomenon, limonite is much more suited then saprolite for HPAL, since it contains much more iron oxides, and much less magnesium silicates. The regeneration of acid due to hematite and alunite precipitation results in two advantages which are; lower sulphuric acid consumption, and an easier solid-liquid separation. The decrease in the iron and aluminum cations in the PLS due to precipitation also provides convinience in downstream processing [25, 26]. The re-precipitation reactions of iron and aluminum are:

$$Fe_2(SO_4)_3 + 3H_2O = Fe_2O_3 + 3H_2SO_4 \quad \text{Rx. 2.7}$$

$$3Al_2(SO_4)_3 + 14H_2O = 2(H_3O)Al_3(SO_4)_2(OH)_6 + 5H_2SO_4 \quad \text{Rx. 2.8}$$

The first autoclave in Moa Bay project was constructed with lead-lined acid bricks, but the modern autoclaves are made of titanium alloy covered carbon steel vessels which are divided into several separate compartments with their own titanium agitators. Titanium alloys have high resistance both to sulfuric acid and to the attack from chloride present in the process water. They are also strong enough to withstand high internal pressure [26].

The constructed autoclave in Gördes is a horizontal type and it is 32 m wide, 7 m long, and has a weight of 580 tons. The planned capacity of the new plant is 33000 tons/year MHP which corresponds 10000 tons/year nickel. The required sulfuric acid consumption is estimated as 350000 tons/year. The ore feed will have 35% pulp density and the leaching operation will be conducted at 255°C [30, 31].

Although most of the reported extraction efficiencies of nickel and cobalt are high in the literature for HPAL, Korkmaz, on his study on the limonitic type of ores obtained from Gördes, reported the extraction efficiencies of nickel and cobalt as 73.2% and 76.8% respectively. The same ore was used, but as a limonitic-nontronitic ore mixture, in this study. The inhibiting effect of precipitating iron, by coating the surface of undissolved iron minerals was claimed to be the reason for low extraction values by Korkmaz [32].

Several two stage processes are developed which utilizes atmospheric leaching for elimination the unfeasible leaching of saprolites in HPAL. The Best known two-stage leaching process is the AMAX process patented by Queneau and Chou [33]. Another contemporary two-stage process which employs the basic principles of AMAX process is called EPAL. The brief

summaries for these processes are given in the atmospheric leaching chapter. See section 2.3.3.2.

Another study by Ma et al focuses on pressure acid leaching with nitric acid (NAPL) on an Indonesian limonitic laterite. NAPL was developed and patented in China in 2008. Extraction efficiencies of both nickel and cobalt were reported to have increased from 75% to 85% upon using nitric acid as a lixiviant instead of sulphuric acid. It is also claimed that the residual acid in case of NAPL is lower compared to HPAL. A commercial plant with a capacity of 30000 tons/year, which will utilize NAPL technology, was stated to be in preparation stage [34, 35].

2.3.3.2 Atmospheric Leaching

The researches on atmospheric leaching (AL) of laterites date back to 1950's. Nevertheless, AL was not a preferred route upon processing of laterites on commercial stage and remained mostly at development and pilot and trial stages. However; due to commissioning problems confronted at Cawse, Bulong and Murrin Murrin HPAL operations, there is and increasing attention for AL [36]. Especially for smaller scale ore bodies where the ore tonnage cannot counterbalance the capital cost and operational expenses AL provides an appealing alternative. Reid and Barnett asserted that AL operations need high nickel recovery, tolerable acid consumption and a low iron concentration in the PLS in order to be competitive with HPAL [27].

All direct leaching operations conducted under atmospheric pressure (1 atm) using either organic or mineral acids as a lixiviant can be classified as atmospheric leaching. Some AL processes are; in-situ, heap (column in laboratory practice), agitation (tank or vat in industrial scale) leaching. The temperature of the AL ranges from ambient temperatures up to boiling point

(105°C). Heap and agitation leaching are the two most important AL processes which will be summarized.

Since re-precipitation does not occur at low temperatures, iron and aluminum is extracted in high amounts in AL. Therefore, AL is considered more feasible for saprolitic ores rather than high iron-containing limonite. Inverse solubility phenomena of magnesium sulfate occurs upon cooling from 270 to 180 °C in HPAL operation, therefore high Mg-containing saprolites do not pose a problem for AL [26, 37].

The dissolution reactions in AL by sulphuric acid are the same as in HPAL, except there are no re-precipitation reactions of iron and aluminum afterwards.

Heap leaching operation has advantages of lower capex and lower operation costs over HPAL and tank leaching. It is also a simple and continuous process [38]. Sulphuric acid is the most commonly used lixiviant for heap leaching of nickel. Heap leaching plant displaces the titanium autoclaves and CCD in HPAL, which decreases its capital cost about 15-20%, but has all the remaining downstream processes of HPAL. However, the metal recoveries are also 15-20% lower compared to HPAL. Since the operation takes place at ambient temperatures and only force is gravitational, the reaction kinetics are very low, thus completion of the heap leaching process takes months, instead of hours in HPAL or agitation leach. Kinetics of the reactions depends on permeability of the heap, chemical dissolution rate and the environmental conditions (rain, humidity). Acid consumption may vary between 500 to 700 kg/ton of ore. Another drawback is that 20-30% of the lateritic ore need to be dissolved to achieve 65-85% nickel extraction (1-3% in copper heap leach) which increases the acid expenditure and causes the permeability-enhancing agglomerates to dissolve, decreasing the permeability by a factor of 10. Due to lower metal recoveries than HPAL and agitation leaching, heap leaching is mostly preferred for low grade laterites or small ore bodies that cannot counterbalance the investment costs of HPAL or AL. General verdict is that

heap leaching is more suitable for saprolitic ores with low clay content, rather than limonite; however hematite rich limonites are an exception [25, 26]. Greek lateritic ores are good examples for high hematite containing limonites, making them very suitable for heap leaching. Oxley et al expressed that Turkish and Balkan laterites are also suitable for heap leaching as they contain low amounts of clay. Also the average hematite content for the Çaldağ nickel laterite is given as 30.97% in the same study [39].

Heap leaching research and development began in 1990's at National Technical University of Athens on low-grade nickeliferous lateritic deposit in Greece. HELLAS (HEap Leach LAteriteS), patented by Agatzini-Leonardou, was the first process which applied heap leaching with diluted acid on limonitic ores with high hematite quantity. These ores were very suitable for heap leaching since the iron was present in the hematite rather than goethite, therefore acid consumption was low [36]. The process was also successful on selective leaching of nickel over iron. Extraction of nickel was close to 85%, whereas the iron extraction was below 50% upon leaching less than 40 days. Sulphuric acid consumption was varying, 10-25 kg/kg nickel extracted whereas the acid usage was 41-72 kg/kg nickel for agitation leaching and 27-34 for HPAL for the same ore [4, 40].

Çaldağ nickel project was also initially planned as a heap leach plant by European Nickel PLC, due to its low clay, high silicate and high hematite content, and several pilot plant tests on heap leaching were conducted over the years. On the study by Oxley et al on Çaldağ ore, the extractions of important metals were given as 79.4% Ni, 82.7% Co, 30.0% Fe after 548 days of heap leaching [39]. However; the heap leach project was cancelled, and agitated tank leaching was selected for the processing of the ore instead. This radical change was stated to be made due to restrictions placed on the site and for economic reasons [41].

McDonald and Whittington reviewed several other studies on heap leaching developments [4]. Miller and Liu performed beneficiation, to separate a

coarse, siliceous low-grade part (containing 0.3-0.7% Ni, 0.01-0.03% Co), from fine parts and clay particles, and separately processed the upgraded ore. Rejected low-grade part leached afterwards with an acid supplemented solution. It was noted that maximum nickel extractions were obtained from limonite rejects, and saprolite rejects were used for neutralization and enhancing iron rejection [42]. Duyvesteyn et al suggested the positive effect of pelletizing, which secures the column permeability for high clay-containing ores [43]. Liu stressed the importance of process water and suggested the use of saline water with 50-150 g/L dissolved salt [44]. Purkiss proposed the addition of 5 g/L metabisulphite to the sulphuric acid leach solution which enhanced the nickel and cobalt extractions [45].

A counter-current heap leaching is argued to have lower acid consumptions, lower iron and high nickel extractions, then single heap process by Panagiotopoulos et al [46]. Thus a cleaner PLS with lower residual acid is claimed to have obtained. A comparison between open circuit leaching and leaching with PLS recirculation with controlled acid concentration; i.e. counter-current multi-stage leaching, was studied by Perreira and Gobbo. It is expressed that although open circuit leaching had higher extractions, the acid consumption was drastically higher, 560 kg/t ore versus 280 kg/t ore in counter-current leaching. The leaching durations were also noted to be much shorter in counter-current circuit [47].

An illustrative sketch for a counter-current two-stage heap leaching sketch is given in Figure 7.

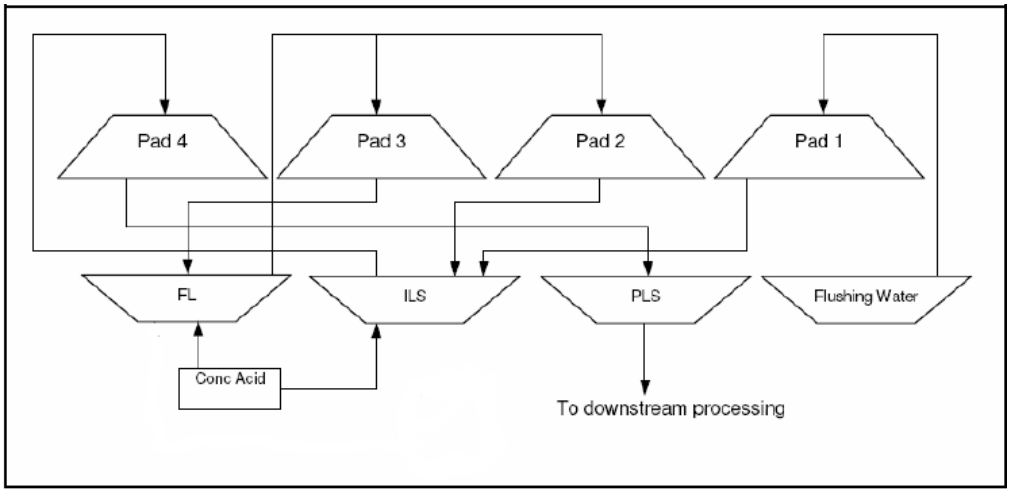

Figure 7 : Typical counter-current two-stage heap leach illustration [48]

Two stage counter-current configurations are generally selected as an effective heap leaching process. Crushing, screening and agglomeration is applied to the ore before stacking into the leach pads. The agglomerates are given some rest for curing, and then the heap is irrigated by slowly spraying or dripping with diluted sulphuric acid solution, in a two-stage counter-current system. The leach cycle is divided into two main stages, primary and secondary leaching and the total process will take up at least 18 months to finalize. The produced intermediate leach solution (ILS) after the secondary stage is fed back to the primary stage to increase the solution tenor. Each heap pad is leached in stages to fulfill the acid neutralization and nickel extraction. The depleted heap is rinsed with water and decommissioned afterwards. Residual Ni and Co in the ILS pond is washed for collection. The produced PLS is send to downstream processes for MHP production which are similar in other AL and EPAL. However heap leaching produces solid free leach liquor, so there is no CCD thickeners needed for S/L separation [25, 26]. Column leach experiments are used for simulation the heap leaching at laboratory conditions.

Agitation leaching, also named as tank leaching on industrial scale, aims to accelerate the reaction kinetics and shorten the leaching durations, by operating at higher temperatures (<105°C) than heap leaching, and also by mechanically stirring the leach solution and the ore, within tanks. Tank leach is most suitable for saprolitic ores with high nickel grade and low iron content. A simplified process flowsheet, showing only the upstream processes for a single stage agitated atmospheric leaching for the treatment of saprolite is given in Figure 8.

Nickel and cobalt extractions are generally in the 85-95% range and the acid consumption varies between 700-1000 kg/t of ore, depending on the mineralogy, and the process details. Sulphuric acid is generally used for agitation leaching; however there are several studies which employ the usage of another type of acid, some of which are: nitric acid, hydrochloric acid and several other organic acids. Several atmospheric leaching approaches were researched and developed up to now. Some of these are; single stage leaching to treat a saprolite or a limonite/saprolite blend, two-stage leaching for treating the limonite and saprolite separately, and also a counter-current system for two stage process. Although many pilot plant studies were carried out, and there are still some operations are at pilot plant stage, only commercialized AL process was as a secondary stage to PAL, in Ravensthorpe EPAL facility [25].

Typical procedure in agitative leaching starts with crushing, grinding and screening as ore preparation step, followed by leaching at atmospheric pressure in acid-brick lined tanks with heat input. Steam injection system can be used to support heat input when required. Generally AL discharge is treated with limestone for neutralization and iron removal step, but several other reagents and methods can be used. The downstream processes are similar to HPAL and heap leaching and will be discussed in the following sections. A simplified atmospheric flowsheet is given in Figure 8.

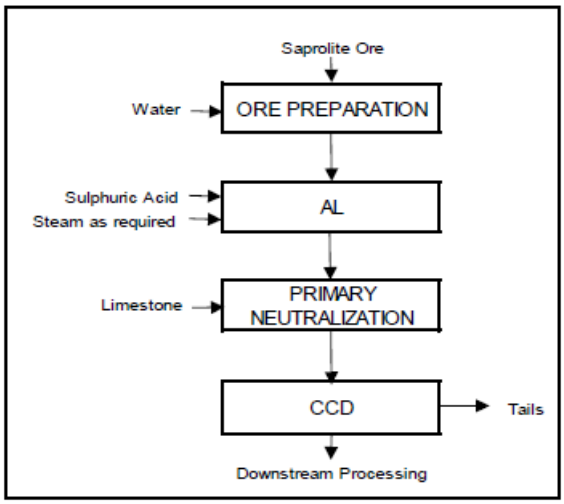

Figure 8: AL flowsheet for saprolite [25]

One of the first studies on atmospheric leaching using sulfuric acid was done by Apostolidis et al. Reduction roasting using hydrogen gas was performed at 500-900°C before leaching, to promote the selectivity of the leaching operation. So 80% nickel extraction was achieved by leaching at 70°C [49].

On an agitation leach study on Australian laterites, Canterford reported 90% of nickel was extracted, although the sulphuric acid consumption was pretty high, 1000 kg/t ore. It was stressed that, the extraction efficiencies were dependent on the mineralogy of the ore, the leaching temperature, and concentration of the acid [50].

According to several studies from literature, multi-stage counter-current atmospheric leaching (CCAL) lowers the acid requirement, by utilizing acid recycling via feeding the discharge from the second stage to the first stage. The agitative leaching of Greek lateritic ores was studied by Panagiotpoulos et al. 75-80% nickel and cobalt extractions were reported, whereas iron and magnesium extractions were given as 55% and 80% respectively, upon leaching at 95°C for 4 h, using a sulphuric concentration of 3 N and pulp density of 15%. Grain size of the ore and pulp density was claimed to have negligible effect on extractions, however temperature and acid concentration

was stated to be directly proportional with extraction values. It was also reported using counter-current two or three-stage leaching, instead of single stage leaching, reduced the acid consumption from 1600 kg/t to 650 kg/t [46]. In another study by Panagiotopoulos et al., it was reported that acid consumption on a simulated three-stage counter current experiment, the acid consumption would be close to 500 kg/t ore and high nickel extraction and an iron to nickel ratio of 7.5 in the PLS would be obtained. However in a six-stage counter-current extraction, both the acid consumption (650-850 kg/t ore), and the iron extraction had increased [51].

Curlook practiced on high magnesium containing highly serpentized saprolitic ores, and reported that 90% of nickel was collected in the PLS within an hour, upon leaching at 80-100°C with an addition of 800-1000 kg acid per ton of ore using 15-33% pulp density. It was stressed that longer leaching durations were needed, when the leaching temperature and the pulp densities are higher, or the ore was less serpentized [52].

Studies by Das et al. (1997), Senanayake and Das (2004), and Das et al. (2010), on atmospheric sulphuric acid leaching of goethite based limonitic ores, supported the positive effect using sulphur dioxide (SO_2) gas as a reductant. Das et al. (1997) observed that the extraction of nickel increased from 40% to 85% when the redox potential was decreased from 840 mV to 560 mV via bubbling SO_2 gas through the acid solution upon leaching at 90°C for 6 h [53]. Senanayake and Das stated that manganese and cobalt extractions was not affected as much as iron and nickel extractions upon SO_2 bubbling [54]. A more recent study by Das et al. (2010) reported that, leaching smectite ores with 700 kg H_2SO_4/t of ore in the absence of SO_2 gave 75-86% Ni and 51-59% Fe extractions, whereas 94% Ni and 80-85% Fe extractions were obtained in the presence of SO_2. Limonitic ores also displayed similar behavior; extraction values after 10 h of leaching, pre-sulphur dioxide treatment was, <75% Ni and 55-60% Fe. SO_2 addition boosted the extractions to 92% Ni and 85-94% Fe [55].

SO_2 addition is also used in sulphation atmospheric leach process (SAL). The primary difference of the process from AL is in the ore preparation stage. Concentrated sulphuric acid is added onto the limonitic ore in a pug mill prior to leaching which leads to sulphation of nickel and cobalt. Overall leach extractions of the process are given as 87% Ni and 88% Co using 600 H_2SO_4 kg/t ore [56].

According to O'Neill, grinding does not affect the leaching kinetic of serpentine ores considerably. Leaching of coarser silicates gave insignificantly lower extraction efficiencies but the processing of their leach residue reported to have easier downstream processing due to better settling properties [57].

Girgin et al. studied the atmospheric sulphuric acid leaching beahaviour of Adatepe (Eskişehir) Turkish lateritic ores. The nickel extraction was given as 99.2% for 120 minutes of leaching at 95°C, with a sulphuric acid concentration of 60%. Girgin et al. interpreted from XRD analysis that, full dissolution of goethite was not necessary. The leaching was claimed to be controlled by external diffusion and chemical reactions since the activation energy for nickel dissolution was found as 30.36 kj/mole [58].

As previously mentioned, heap leaching was given up and atmospheric tank leaching was selected for the processing of Çaldağ project. Willis stated that in the agitated tank leaching studies on Çaldağ, 96% Ni and 94% Co extractions were achieved in 6 h for leaching at 92°C, while the residual free acid was 35-40 g/L in the PLS. Willis also stressed that nickel extractions exceeding 90% can be achieved with only 5 g/L residual free acid; which shows the suitability of the Çaldağ ore for counter-current atmospheric leaching [41].

The atmospheric leaching study of Büyükakıncı on Gördes lateritic ore is a good example for comparison of heap versus agitation leaching. Extractions were given as 96.0% Ni and 63.4% Co for limonite, and 93.1% Ni and 75.0%

Co for nontronite after leaching for 24 h at 95°C via agitation leaching. Column leaching experiment results were given as; 43.9% Ni and 55.2% Co extractions for the limonitic ore after leaching for 228 days, and 83.9% Ni and 55.2% Co extractions for the nontronitic ore after leaching for 122 days. It was concluded that the limonitic ore was unsuitable for heap leaching [59].

Various multi-stage processes which may involve AL steps, or both HPAL and AL steps were developed and patented. Generally, high magnesia containing ores are used in a second stage for neutralizing the PLS produced by HPAL in the first stage. Alternatively, reverse process can also be applied.

Büyükakıncı and Topkaya carried out multi-step leaching experiments at atmospheric pressure. Limonite was initially leached; nontronite was leached in the pregnant liquor afterwards. The residual acid concentration of PLS was decreased from 97 g/L to 27 g/L after neutralization with nontronite. The extraction efficiencies from nontronite during neutralization were reported as 75-88% for Ni and 15-39% for Co depending on the added nontronite amount. These extraction values were lower compared to single stage leaching of nontronite which were; 96% Ni and 63.4% Co. But also as a plus along with decreased residual acid, there was a decrease in the Fe extraction [60].

Due to problematic situation of saprolites in HPAL, an alternative process called the AMAX process was developed and patented by Queneau and Chou [33]; which is a two-stage leaching variation of pressure acid leaching process, and it allows the processing of both limonitic and saprolitic ores containing a maximum amount of magnesium of 15% [20]. The high magnesium containing part of the ore is used for neutralizing the HPAL liquor with atmospheric leaching, and the leach residue of AL is recycled to HPAL to be leached along with limonite to recover remaining nickel [4]. Taylor reported that the pilot plant of AMAX process was operated at 270°C. It was noted that the higher temperature yielded faster kinetics, therefore; the need of larger autoclaves were avoided, the acid consumption decreased, and the resulting PLS had better purity. However direct steam injection was needed to

achieve such high temperatures and with the increased pressure, thicker autoclave walls were needed [61].

Enhanced pressure acid leaching (EPAL) is another process which uses two-stage leaching to be able to treat saprolitic components along with limonitic ores. EPAL process has a similar flowsheet with AMAX and the process is patented by BHP operations [62]. These two processes (AMAX and EPAL) can also be classified as HPAL processes, since it also employs a leaching step at high pressure. The process starts with high pressure acid leaching of the limonite ore slurry containing 5-35% solids with sulphuric acid. Sulphur dioxide gas is used as a reductant to keep the reduction potential between 900-1000 mV to minimize the ferrous ion production and increase cobalt recovery by reducing manganese minerals. The saprolitic parts are leached at atmospheric pressure, utilizing the regenerated acid from the HPAL, with additional fresh acid input. This atmospheric leaching step neutralizes the acidic leach liquor by consuming the free acid. The overall nickel extraction is dependent on the mineralogy of the ore [63]. High magnesium saprolites are reported to neutralize the acid more effectively. For the iron precipitation step, alkali metals, or ammonium salts are added to favor jarosite, $NaFe_3(SO_4)_2(OH)_5$, precipitation [26].

$$3Fe_2(SO_4)_3 + 2NaCl + 12\ H_2O = 2NaFe_3(SO_4)_2(OH)_5 + 5H_2SO_4 + 2HCl \quad \text{Rx. 2.9}$$

EPAL was the planned process for Ravensthorpe Nickel Operations by BHP-Billiton, but the plant was closed before reaching full capacity production, due to economic concerns [63].

A two-stage process patented by Liu et al, gave the description for the process as; separating the low and high Mg-containing ores by selective mining or classification, then leaching the low Mg ore with concentrated sulphuric acid,

followed by the introduction of the high Mg-containing ore as a slurry to finalize primary leaching step. Precipitation of iron as goethite or another form of iron oxide or iron hydroxide, and utilizing the released sulphuric acid in leaching the high Mg-containing ore as a secondary leaching step [42].

There are several other developing techniques which employ the utilization of another type of acid, such as HCl, HNO_3, various organic acids, or utilizing bacterial leaching.

According to the review by McDonald, citric acid has proven to be the most effective organic acid for leaching of serpentinic or Greek limonitic ores where nickel is mostly found in other minerals rather than iron oxides. Heterotrophic bacteria are also used in many in-situ leaching studies, since it generates citric acid [64].

A recent study by Li et al. focuses on the atmospheric leaching of a leateritic ore, using hydrochloric acid. The extraction efficiencies are given as 92.3% Ni, 61.5% Co and 56.3% Fe for leaching for 120 minutes at 80°C with the optimized conditions of 8mol HCl/L with a S/L ratio of 1/4, and a particle size below 0.15 mm. According to Li et al, the dissolution rates of the minerals are ranked as: goethite>lizardite>magnetite>hematite [65].

The comparison of positive and negative aspects of HPAL and AL are summarized in Table 1.

Table 1: Comparison of HPAL and AL [4, 66]

HPAL	AL
High capex	Low to moderate capex
High maintenance cost	Low maintenance cost
Harder process control	Easier process control
Low acid consumption	High acid consumption
Moderate energy consumption	Low energy consumption
High extractions	Variable extractions
Easier downstream processing	Pregnant solutions harder to treat
Short residence time	Moderate to long residence time
Suitable for limonite ores	Suitable for saprolite (Conventional AL)
Commercially proven	Not yet commercially proven

Chander pointed out that the acid consumption in AL is high for satisfactory Ni and Co recoveries, but this acid cost would be reduced if there was a way the regenerate the acid [67]. Processes like DNi, Jaguar process (atmospheric chloride leaching process), Nichromet and Neomet were developed based on this acid regeneration aim. Jaguar process, Nichromet and Neomet are all chloride based processes which utilizes hydrochloric acid regeneration and recycle.

Neomet process is a being developed by Neomet Technologies (Canada) and was introduced by Bryn Harris at the ALTA 2011 Ni/Co conference [68]. It is promoted as a potentially low capex process which can treat both limonitic and saprolitic ores. The leaching process is a hydrochloric acid atmospheric leaching process which takes place in a special atmospheric acid tank, patented as "atmospheric autoclave" system, to be able to regenerate the acid. The reported nickel and cobalt extractions are above 90%. It was also stated that secondary neutralization is not needed for removal of residual iron, and

nickel and cobalt are recovered as basic chlorides [25]. Scandium, a rare earth element which is rising in value with the developing technologies, can be recovered as a by-product in Neomet, giving an edge to this process. A flowsheet for this process is given in Figure 9.

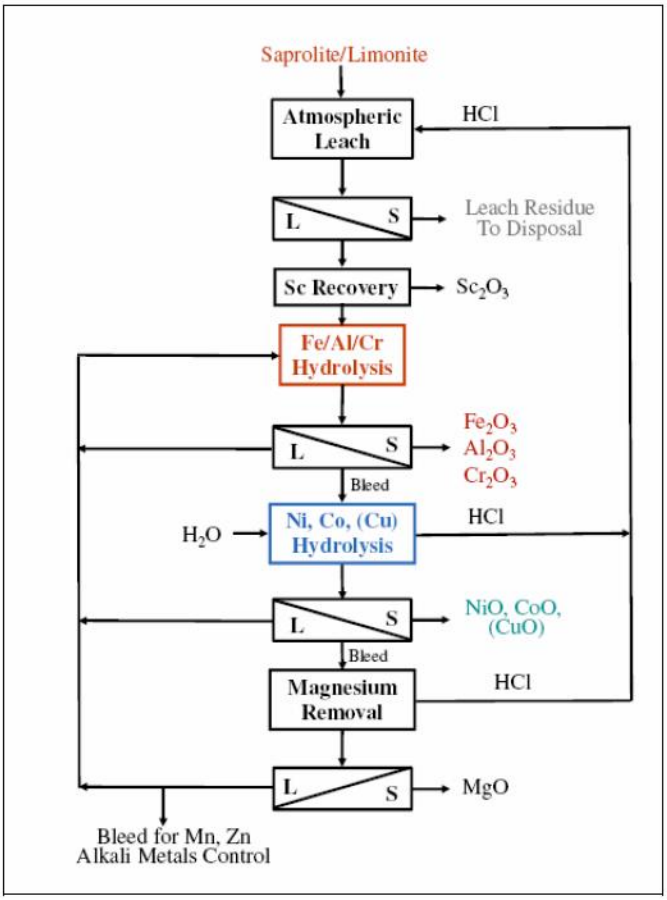

Figure 9: Neomet process flowsheet for saprolite/limonite [26]

Leaching in Neomet takes place between 100-110°C under atmospheric pressure with the recycled HCl. After S/L separation by a vacuum belt filter, scandium recovery is done as a by product. The pregnant liquor is concentrated and subjected to hydrolysis later on, at 180-190°C for the precipitation and removal of iron and aluminum as oxides while regenerating acid. The solvent matrix which is open to the atmosphere remains fluid at 200-250°C allowing the HCl removal from the system. The solvent matrix is

taken and injected with steam for recovery of nickel and cobalt as tri-basic chlorides. Calcination is done to produce a Ni/Co oxide product, and the released HCl is fed back to the leaching tank [25].

A detailed survey of the DNi process will be given in the following section since the subject of this thesis is closely related to the process. Summarized reviews of Jaguar Process and Nichromet can be found elsewhere [26, 64].

2.3.3.2.1 Atmospheric Nitric Acid Leaching and DNi process

The direct nickel process (DNi) is owned and led by Direct Nickel Pty Ltd. It is a process based on the precursor processes developed and patented by Drinkard Metalox Inc. The DNi employs the methods developed by Drinkard [69]. The novel part of the process is based on recovery and regeneration of NO_x gas [70].

The unique features of DNi process is that it recovers over 95% of its reagents, and +95% (theoretically 99%) of the nitric acid for re-using in the process. DNi process is claimed to be tested on, around 50 different ores, and be able to treat the full laterite profile, including all the limonite, saprolite and clay zones. A plant size with a minimum of 5000 tpa and 1.5% nickel was seen feasible for DNi process [23].

The DNi process liquors are rich in magnesium nitrate, which is thermally decomposed to magnesia for recycling. The most critical component is the recycling of this magnesium nitrate to recover magnesia and nitric acid. Most of the obtained magnesia is returned to the precipitation cycle which is also a saleable quality product. This method also resolves the magnesium disposal problem faced in HPAL.

The nitric acid is more aggressive than sulphuric acid in dissolving the nickel-bearing ores, and its metal salts are more soluble than both sulphuric and

hydrochloric acid. This is also advantageous for elements such as calcium, because the sulphate form of it is solid gypsium salt which causes scaling and build-up increasing the downtime and maintenance costs. Another advantage of nitric acid is that lower temperatures are needed for thermal hydrolysis compared to sulphuric acid. Acid distillation and recycle of nitric acid is also possible.

The reported advantages of DNi over HPAL are [23, 71]:

- Reduced capex, replacing the titanium autoclaves with stainless steel tanks
- Simpler and safer operation, as the process is under atmospheric pressure
- Lower operating and maintenance costs
- 20-40 kg/t ore acid consumption due to acid recycling compared to 500 kg /t consumption for HPAL
- Recycling of key reagents (+95%) and producing saleable quality hematite and magnesium oxide by-products
- Environmental friendly since NO_x gas is retained, and tailings are reduced, by the production of magnesium and iron by-products

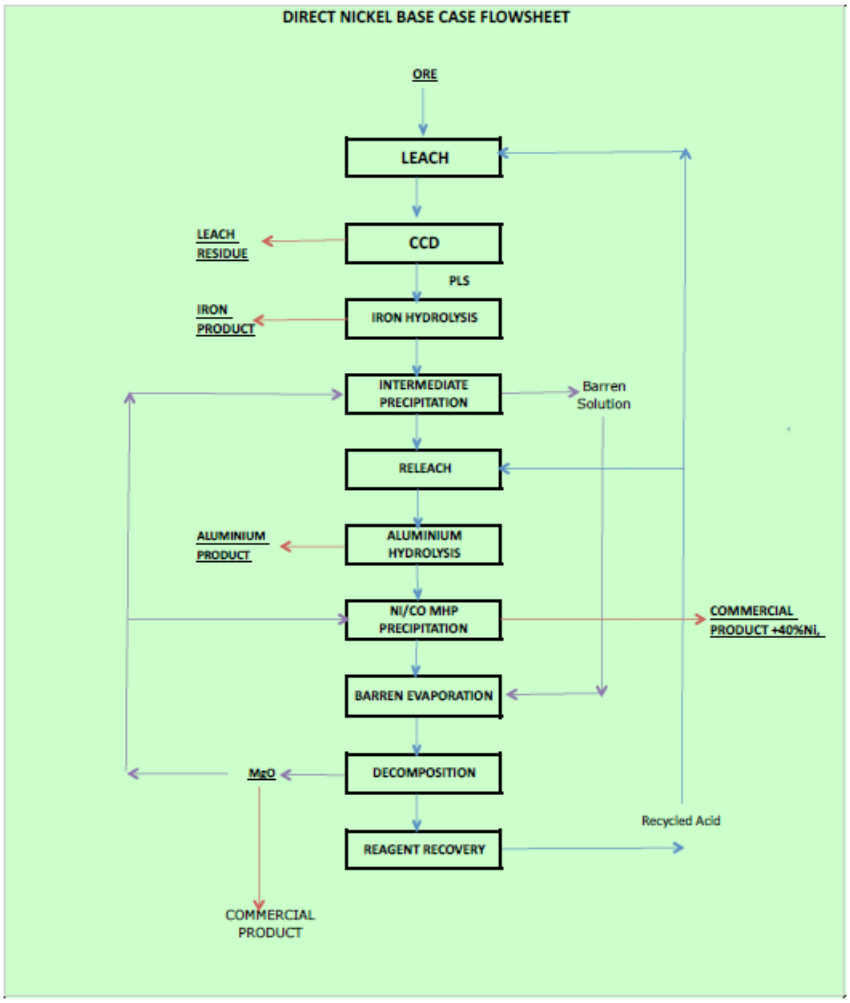

Figure 10: The direct nickel process flowsheet [72]

The process starts with the leaching of the ore which is achieved in less than 5 h; at a temperature just over 100°C under atmospheric pressure using recycled HNO_3 with freshly added acid in closed tanks. Extraction efficiencies are reported to be higher than 90% for Ni, Co, Mn, Mg and other base metals. S/L separation is done in a series of CCD thickeners. Dissolution reactions of several important oxides are given as:

$$Ni(OH)_2 + 2HNO_3 = Ni^{2+} + 2NO_3^- + 2H_2O \qquad \text{Rx. 2.10}$$

$$Co(OH)_2 + 2HNO_3 = Co^{2+} + 2NO_3^- + 2H_2O \qquad \text{Rx. 2.11}$$

$$Fe_2O_3 + 6HNO_3 = 2Fe^{3+} + 6NO_3^- + 3H_2O \quad \text{Rx. 2.12}$$

$$Mg_3SiO_2(OH)_4 + 6HNO_3 = 3Mg^{2+} + 6NO_3^- + 5H_2O + 2SiO_2 \quad \text{Rx. 2.13}$$

The PLS is concentrated via evaporation prior to thermal hydrolysis, until the boiling point reaches 140°C. The evaporated nitric acid and steam is retained for recycle. Iron hydrolysis, which will be explained in more detail in the following sections, takes place at 160-180°C and almost all of the iron and most of the chromium is precipitated as hematite. The iron precipitate is almost 50% of the ore feed. The pH of the iron-free solution is raised for precipitation of an intermediate product by the addition of recycled MgO. Intermediate product, which contains Ni, Co, Al and several other base metals, separated from the barren solution by filtering and thickening and re-dissolved with recycled acid afterwards. The re-leached PLS is heated for aluminum removal by thermal hydrolysis. The resultant gaseous nitric acid from hydrolysis reactions is also recycled. The thermal hydrolysis reactions of iron and aluminum are:

$$2Fe(NO_3)_3 + 3H_2O = Fe_2O_3 + 6HNO_3 \quad \text{Rx. 2.14}$$

$$2Al(NO_3)_3 + 3H_2O = Al_2O_3 + 6HNO_3 \quad \text{Rx. 2.15}$$

MgO is added once again, this time to the aluminum and iron free solution to increase the pH and precipitate a Ni/Co hydroxide product. The Ni/Co hydroxide precipitation reactions are as follows:

$$Ni(NO_3)_2 + Mg(OH)_2 = Mg(NO_3)_2 + Ni(OH)_2 \quad \text{Rx. 2.16}$$

$$Co(NO_3)_2 + Mg(OH)_2 = Mg(NO_3)_2 + Co(OH)_2 \quad \text{Rx. 2.17}$$

The most critical part of the process is the thermal decomposition of the remaining magnesium nitrate solution, and the regeneration of the nitric acid from the NO_x gas. This technology employs the methods in DMI's patent, US 6264909 "Nitric Acid Production and Recycle". The remaining barren solution, which is 66-69% magnesium nitrate hexahydrate, is concentrated by evaporation at 200-215°C to form a magnesium nitrate melt. This molten salt is decomposed in a thermal decomposition unit to magnesium oxide powder, steam and NO_x (NO and NO_2) by heating to temperatures 300-500°C. Decomposition reaction of magnesium nitrate is as follows:

$$Mg(NO_3)_2.2H_2O = MgO + NO_2 + NO + O_2 + 2H_2O \qquad \text{Rx. 2.18}$$

NO_x vapor is retained in nitric acid regeneration system, which is a series of adsorbers and scrubbers, and was reacted with HNO_3. Afterwards it was allowed to oxidize with air and cooled to condense as nitric acid. Therefore, 99% of the NO_x was recovered to form a 55% nitric acid. A simplified flowsheet of MgO and NO_x recycle system is given in Figure 11. The nitric acid regeneration reaction sequence is as follows [72, 73]:

$$2NO + O_2 = 2NO_2 \qquad \text{Rx. 2.19}$$

$$3NO_2 + H_2O = 2HNO_3 + NO \qquad \text{Rx. 2.20}$$

$$4NO + 2HNO_3 = 2N_2O_3 + H_2O \qquad \text{Rx. 2.21}$$

$$N_2O_3 + O_2 + H_2O = 2HNO_3 \qquad \text{Rx. 2.22}$$

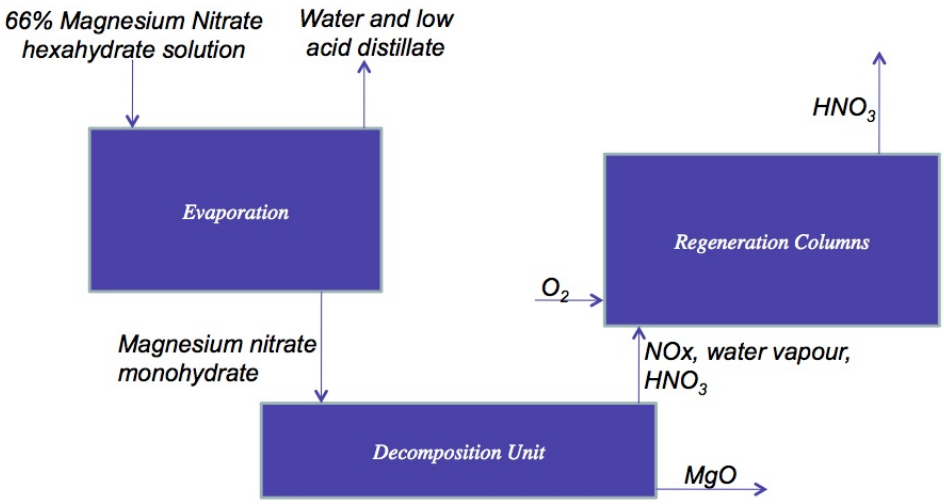

Figure 11: Reagent recycle flowsheet [72]

A test plant in Perth was operated throughout 2013. The ore feed used in the operation had concentrations of 1.6% Ni, 0.09% Co and 30.7% Fe. McCarthy and Brock, reported the extraction efficiencies as 95% Ni, 86% Co, and 89% Fe. Nickel and iron concentrations in the PLS was stated as 4277 mg/L and 745340 mg/L, respectively with a free acid of 292 g/L in the solution. An intermediate MHP product containing 32% Ni was produced, along with high quality hematite (59.8% Fe), alumina (31.3% Al) and magnesia (55.8% Mg) by-products. More than 95% of the nitric acid was reported to be recycled throughout the process. Direct Nickel is planning to build its first commercial plant at ANTAM's Buli operation in Halmahera, Indonesia [74].

On the review about technical and cost comparison of the laterite processes by Taylor, DNi and Neomet processes were presented as potentially competitive routes against established processes, and they are argued to be clearly superior if their produced by-products proved to be marketable for good prices [25].

2.4 Downstream Processes on Pregnant Leach Solutions

The resulting pregnant leach solution from HPAL or AL contains nickel and cobalt with several other contaminating metals such as iron, aluminum, chromium, magnesium, etc., which need to be discarded. The downstream processing route of leach liquors is generally independent from the upstream choice. The three main commercialized downstream recovery processes for laterites are Mixed Hydroxide Precipitation (MHP), Mixed Sulfide Precipitation (MSP) and Direct Solvent Extraction (DSX). There are also developing technologies such as; ion-exchange (IX), molecular recognition technology (MRT) and resin in pulp (RIP) apart from these primary processes. MSP and MHP flowsheets produces an intermediate product and can be practicable for smaller projects, however DSX process requires and integrated metal refinery [6]. Theoretically all the downstream recovery routes can be selected to AL leach liquors however; the economic feasibility may be an issue.

Mixed sulfide precipitation is the oldest method for downstream processing of laterites, which was firstly applied in Moa Bay. According to Willis, MSP process is applicable to any leach solution from any leaching method. It has high selectivity for nickel and cobalt over other impurity metals such as manganese and iron. There is no need for precipitation steps for removal of these impurities due to high selectivity of the process, prior the intermediate precipitation. MSP process is suitable for high iron containing low grade ores (limonites), since the nickel and cobalt losses are low because there is no precipitation step. It is also better suited to ores having high manganese content, which has Ni:Mg ratio less than 3:1, than MHP route due to its better selectivity. However, it has higher capital cost compared to MHP. The main steps in MSP flowsheet are: Pre-reduction, partial neutralization, nickel cobalt intermediate product precipitation and iron removal or final neutralization (if required) [6].

MHP is also a well-established process which was first applied in Cawse plant. META Nikel Kobalt A.Ş. is using the MHP process route. DNi process also employs the principles used in MHP process for downstream processing. It is a simpler and cheaper process compared to MSP and DSX. The process uses the pH increment for the production for an intermediate product, whereas the other processes use complex organic minerals (DSX) or risky sulfide gases (MSP) [29]. The downside of the process is that it lacks selectivity for nickel and cobalt over other impurities such as iron, aluminum. The stages of MHP process are: Recycle leach for the tailings of second stage of nickel-cobalt precipitation, single stage or two-stage iron removal, two-stage Ni-Co precipitation and manganese removal. A flowsheet of MHP can be seen in Figure 12. The iron removal step of MHP will only be summarized since the remaining steps are beyond the scope of this thesis.

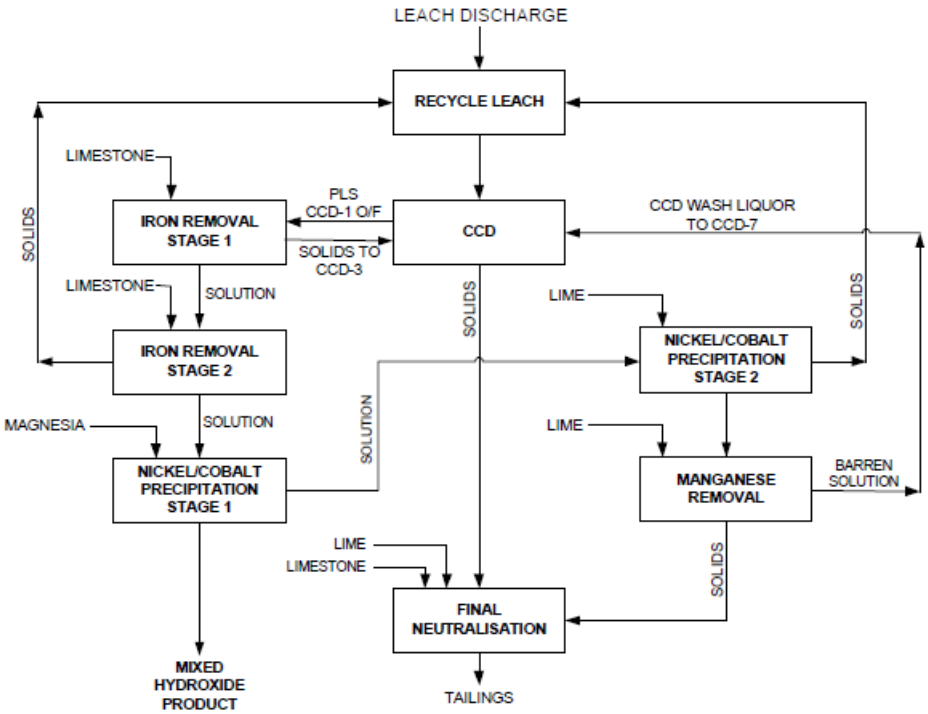

Figure 12: Typical MHP flowsheet [26]

2.4.1 Precipitation of Iron

As underlined previously, iron removal is the primary problem in the purification of pregnant leach solutions in AL, as re-precipitation does not occur during leaching. Iron may be precipitated as goethite, hematite or jarosite from the leach liquor. However hematite precipitation technique is generally applied for nitrate leach liquors. The only available choices for iron precipitation under atmospheric conditions are goethite and jarosite precipitations. Iron precipitation as iron hydroxide is also possible, but only small amount of iron (2 g/L) can be removed from the solution as a ferric hydroxide and nickel loss increases drastically at pH>2 [41].

Jarosite is a hydrous sulfate of iron, so jarosite precipitation is not an option for nitrate liquors. Jarosite precipitation occurs in the presence of sodium, potassium or ammonium ions. Controlled addition of limestone slurry also favors jarosite formation. Jarosite compounds are not stable on the long term and may decompose, and jarosite tailings possess a potential threat for the environment so iron disposal by jarosite is not generally permitted and jarosite precipitation is mostly avoided [8, 41].

2.4.1.1 Iron Precipitation as Goethite

Iron removal by hydrolytic precipitation as goethite (FeOOH) is a widely accepted process which separates the iron in high quantities. Several advantages of goethite precipitation compares to jarosite are that there is no need for alkali addition, and the production of a more stable and filterable leach residue having a lower volume [75]. There is also no need for special equipment since the iron is oxidized by oxygen, or hydrogen peroxide at 80-90°C. The goethite precipitation reaction is given in Rx. 23, and the overall

precipitation reaction when hydrogen peroxide used as an oxidant is given in Rx. 24 [7].

$$Fe^{3+} + 2H_2O = FeOOH + 3H^+ \qquad \text{Rx. 2.23}$$

$$2Fe^{2+} + H_2O_2 + 2H_2O = 2FeOOH + 4H^+ \qquad \text{Rx. 2.24}$$

Iron(III) concentration level can be decreased under 200 mg/L in leach liquors by keeping the pH in the range 2.5-3. The operation can be conducted between 70-90°C for 90-180 minutes. Precipitation of nickel and cobalt are very low at this pH range. The co-precipitation of aluminum and chromium along with goethite is also expected because the aqueous chemistry of trivalent states of iron, aluminum and chromium are similar [7]. The Monhemius Diagram given in Figure 13 shows the stability regions of several impurity elements versus pH. As can be seen from the diagram, trivalent ions of iron, chromium and aluminum are the first three lines, so they are aimed to be precipitated initially.

These co-precipitations are desired during iron removal process. The chromium is removed almost totally; however the aluminum concentration can generally be decreased to 2 g/L. Removal of this residual aluminum is important since it is a worrisome contaminant and undesired in the MHP product. To decrease the aluminum content to very low levels a pH range of 4.4-4.8 is required, but about 4-10% nickel and cobalt losses can be observed [6].

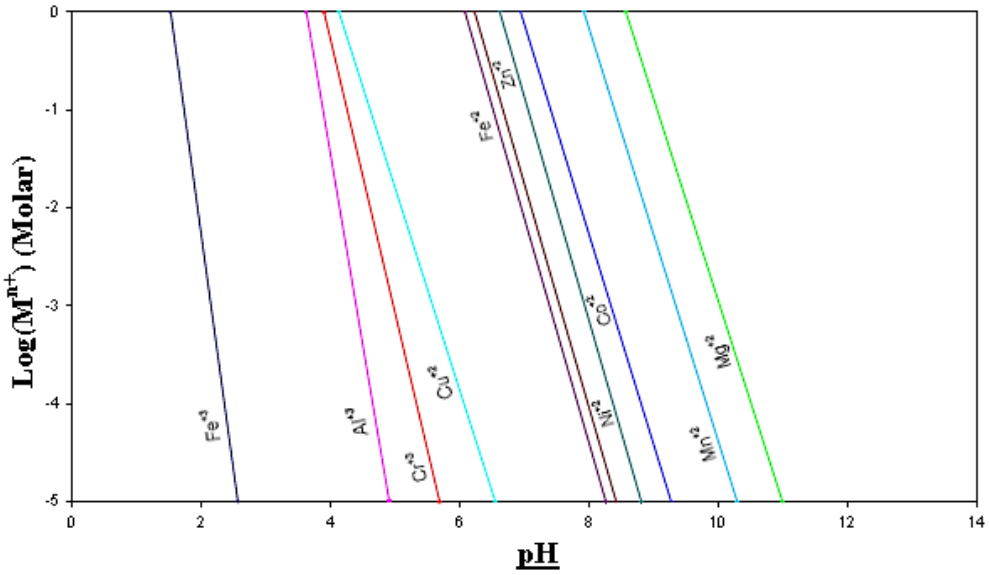

Figure 13: Stability curves of ions with respect to molarity and pH at ambient conditions [76]

The precipitation process generates acid, along with the high amount of residual free acid in the solution, so a neutralizing agent must be used to keep the reaction proceeding until completion. The pH value affects the oxidation rate of ferrous ions, but it is also a key parameter in nickel loss. The pH of the solution can be controlled via adjusting the addition rate of reagent. Several neutralizing agents can be used for this purpose. Generally, limestone is the preferred as a reagent in sulfate leach liquors due to its lower cost since high amounts of reagent is consumed for neutralization and precipitation. However in nitrate system, recycling of reagents plays a significant role, so MgO seems like a more suitable reagent even it is more expensive [29, 72].

2.4.1.2 Iron Precipitation as Hematite

Hematite is a desirable iron product since it is a stable, inert and marketable unlike jarosite or goethite. Also it need less water per ton of iron [8]. Hematite precipitation is achived by hydrolysis at temperatures higher than atmospheric

boiling point of the leach liquors (160-190°C), so special eqipment (autoclave) is needed since high pressure is needed to reach those temperatures. Atmospheric Nitric acid leaching processes like DNi employs the thermal hydrolysis method for the precipitation of iron as hematite.

Hydrolysis, which is the reaction of cations with water to give H^+ and OH^- is a good technique to remove cations from the pregnant leach solution allowing the regeneration of the acid without any foreign ion addition. The hydrolysis reaction of iron was previously given in Rx. 2.14.

The advantages of high temperature hydrolysis over the neutralization process are that the hydrolyzed product contains less impurities and the acid regeneration is possible without any foreign ions introduced into the system. Shang and Van Weert also stated the hydrolysis also produces an easily filterable precipitate, and the particle size increases with the increased hydrolysis temperature [8].

As can be seen from the Pourbaix diagram in Figure 14, the stability region of Fe^{3+} decreases with the increase in temperature. Consequently, the iron(III) will precipitate even when the acidity is high.

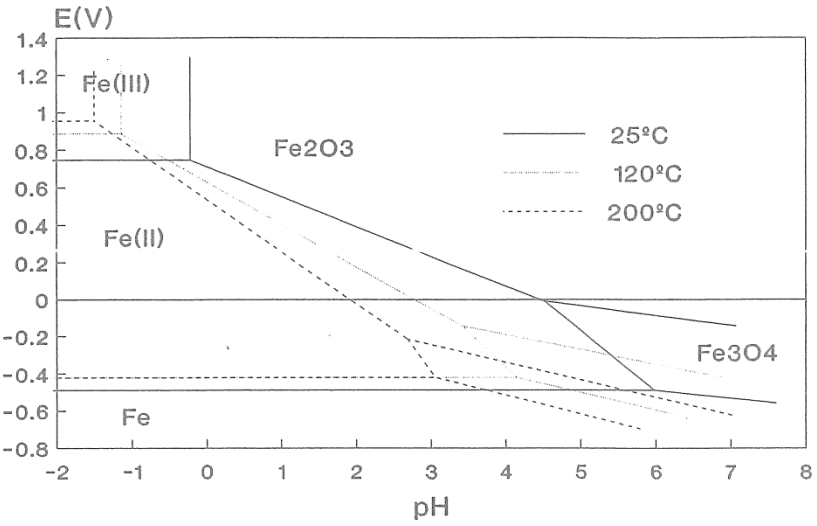

Figure 14: Pourbaix diagram of iron-water system at different temperatures [8]

According to Shang and Van Weert, the removal rate of iron is higher at the early stage of hydrolysis, although extended period of time is needed for complete hydrolysis of iron. Also the total amount of iron increases with the increasing initial iron concentration, however the precipitation percentage decreases. Shang and Van Weert also stated that the temperature has the highest effect on the hydrolysis process thus on the precipitation of hematite. The kinetics of the precipitation is accelerated and the degree of crystallization of the precipitate is thus increased. Starting iron concentration and level of agitation has only moderate effect on precipitation. Shang observed that the precipitation product is only hematite above 160°C, whereas between 140-160°C a mixture of goethite and hematite was formed.

It was stated that the HNO_3 concentration increases while iron concentration decrease with the increasing temperature which is given in Figure 15.

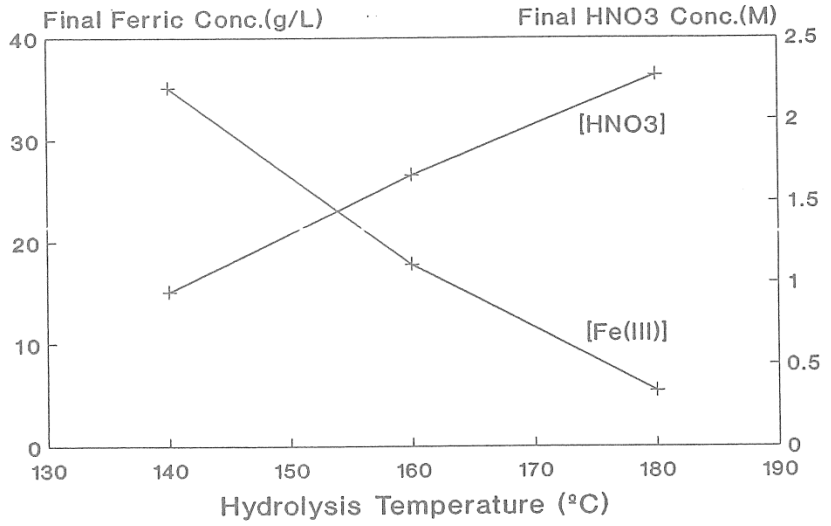

Figure 15 : Final nitric acid and iron concentration in liquor after 210 min hydrolysis at different temperatures [8]

Iron nitrate was reported to keep on decomposing at 180°C even when the acid concentration was as high as 2.6 M. However in sulphate system, sulphuric acid concentrations need to be less than 0.58 M at 185°C for iron oxide to precipitate. High acid recovery and efficient removal of iron as hematite can be possible with this phenomenon in nitrate system [8].

CHAPTER 3

EXPERIMENTAL PROCEDURE

3.1 Sample Description

Throughout this thesis study, two types of lateritic nickel ores namely limonite and nontronite from Gördes/Manisa were used for atmospheric nitric acid leaching experiments. The ore samples were obtained from META Nikel Kobalt A.Ş.

3.1.1 Sample Preparation and Physical Characterization of the Ore Sample

In order to determine the general characteristics of the ore sample, physical, chemical and mineralogical characterizations were performed, respectively. The representative ore samples supplied had as-received sizes of -20 mm. The limonitic sample had reddish dark brown color whereas the nontronite was dark yellow. Initially bulk and solid density measurements were done for both samples and results were evaluated according to the ore weight to ore volume ratio and the results are given in Table 2. The solid densities were measured with a helium pycnometer.

Table 2: Bulk and solid densities of limonitic and nontronitic ore samples (g/cm^3)

Representative ore sample	Limonite	Nontronite
Bulk Density (As-received)	1.04	0.93
True Density (-38 μm, dry)	3.26	2.64

The moisture contents of the ores were determined subsequently. Initially the particle size of each ore was reduced to -38 μm. To obtain such a fine ground ore, a series of crushing and grinding operations were conducted. Firstly a representative sample was obtained from as received ore via coning and quartering method and the particle size of this sample was reduced to under 850 μm for wet screen analysis with the help of jaw and roll crushers. Afterwards following sampling was done with the help of a riffle splitter and the ore was ground under 38 μm with a vibratory (ring) pulverizer. The ground sample was weighed and then dried at 105°C in a drying oven and reweighed. The measured moisture content for each ore sample is given in Table 3. These results show that the moisture content was too high, so it would not be feasible to apply pyrometallurgical methods on the ground that the removal of the physically held water would be too expensive.

Table 3: Moisture contents of the representative limonitic and nontronitic ore samples as wt. %

Representative Ore	Limonite	Nontronite
Moisture Content	27.8	39.4

The particle size distribution of each ore was determined by wet screen analyses. For these analyses five different sieves were placed on top of each other with a decreasing aperture size order from top to bottom in a vibrating

system. After screening was done, the ores accumulating on top of each sieve were collected and dried at 105°C and weighed afterwards. The results are given in Tables 4 and 5.

Table 4: Wet screen analysis for limonite

Size (μm)	Weight (%)	Cumulative wt. (%) Oversize	Cumulative wt. (%) Undersize
+600	7.59	7.59	92.41
+300	10.03	17.62	82.38
+150	12.58	30.20	69.80
+75	12.96	43.16	56.84
+38	13.94	57.10	42.90
-38	42.90		
Total	100		

Table 5: Wet screen analysis for nontronite

Size (μm)	Weight (%)	Cumulative wt. (%) Oversize	Cumulative wt. (%) Undersize
+600	9.73	9.73	90.27
+300	10.90	20.63	79.37
+150	12.11	32.74	67.26
+75	12.55	45.29	54.71
+38	14.48	59.77	40.23
-38	40.23		
Total	100		

The particle size distributions showed that almost half of the ore samples were consisted of very fine particles.

3.2 Chemical Characterization of the Ore Sample

Chemical characterization of the ore was done for many reasons. First of all, chemical analysis of the sample was used to determine the theoretical acid consumption prior to the experimental process and also to calculate the extraction percentages after leaching experiments. Furthermore; the lateritic ores contain various valuable elements which are critical due to their abundance, therefore the chemical characterization is important before the start of a study to set up objectives and priorities in terms of elements to be recovered. The chemistry of elements of critical importance has been already reported in the literature review section. The chemical analyses of samples were done with Inductively Coupled Plasma (ICP) method by ALS Analytical Chemistry and Testing Services, Canada. The results are given in Table 6.

Table 6: Chemical analyses of representative samples in wt.%

Element (%)	Limonite	Nontronite
Fe	28.70	15.95
Ni	1.28	1.20
Co	0.083	0.044
Sc	0.0055	0.0035
Cr	1.36	0.68
Mn	0.46	0.26
Al	3.09	2.80
Mg	1.36	4.15
Ca	0.91	1.54
K	0.10	0.10
Ti	0.07	0.05
Cu	0.03	0.007
Zn	0.03	0.02
As	0.680	0.020
S	0.43	0.01
Na	0.78	0.67
SiO_2	28.8	44.9

The analyses of metals and their distributions in each screen size stated by Büyükakıncı, on the same ore samples which had similar particle size distributions, showed that, finer sized particles contained more nickel and cobalt compared to coarser particles [59].

3.3 Mineralogical Characterization of Ore Sample

Leaching behaviors and extraction efficiencies of the laterite ores are heavily dependent on mineralogy of the ores. If the extraction efficiencies are low, the reasons behind can be identified by mineralogical characterization.

3.3.1 XRD Examinations

X-ray diffraction examination is done primarily for determining the phases present in the ores. A Rigaku D/MAX2200/PC model X-ray Diffractometer with a Cu-Kα X-ray tube working under 40 kV and 40 mA was used for this purpose. For analyses, ore samples ground to 100% -38 μm were used. The XRD patterns of limonitic and nontronitic samples are given in Figures 16 and 17.

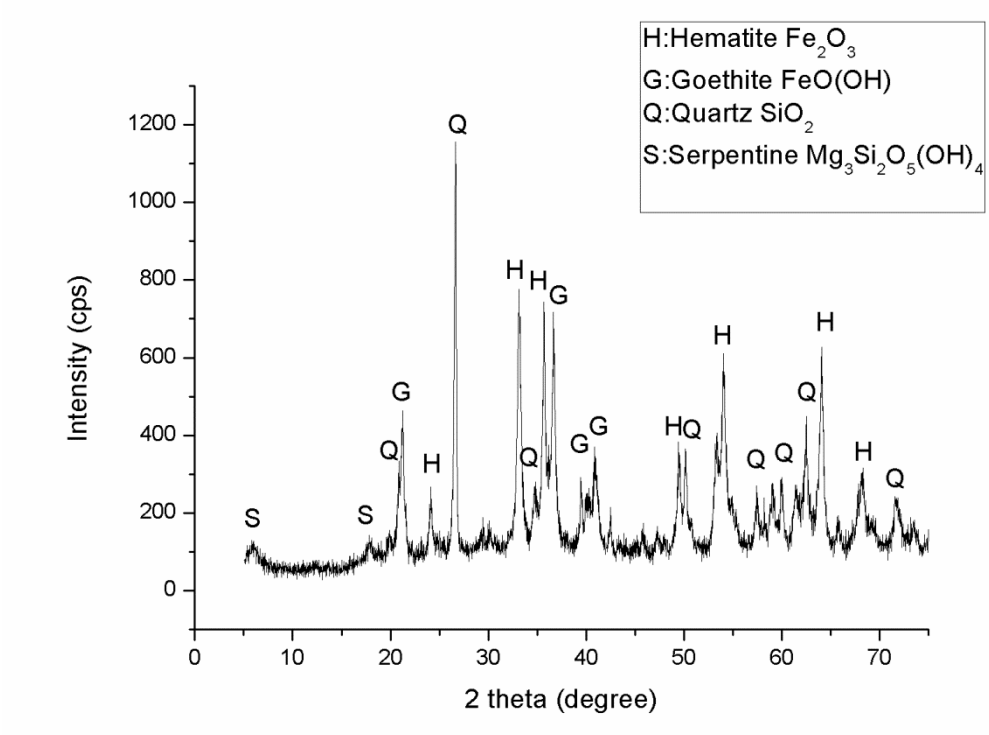

Figure 16: XRD pattern of limonite

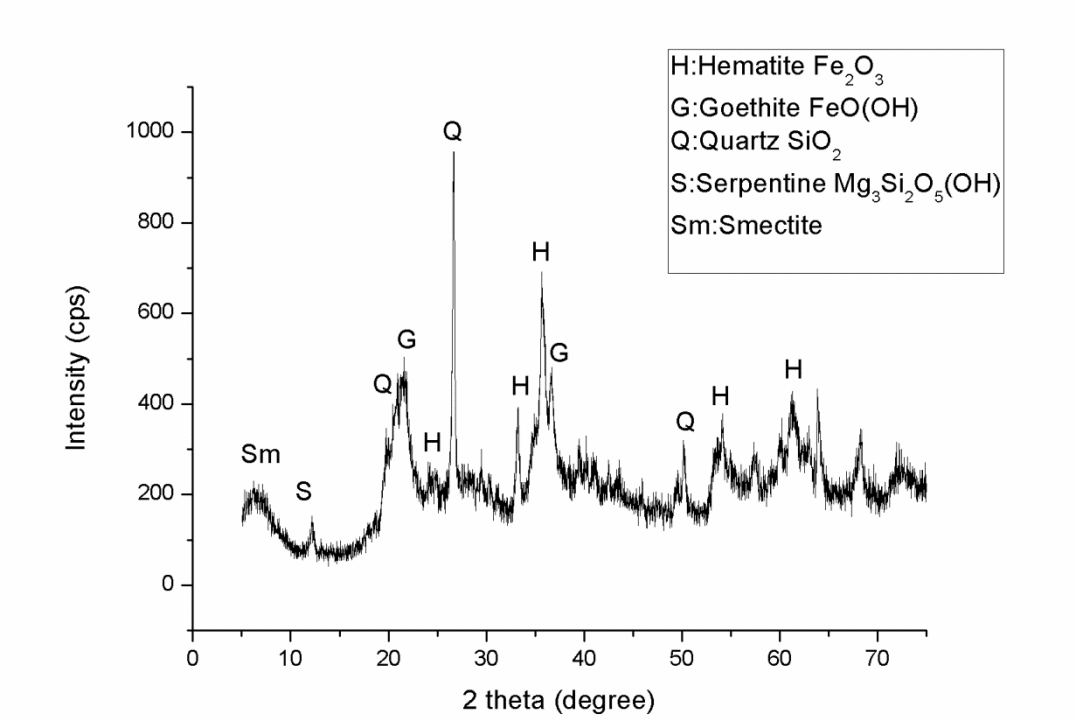

Figure 17 :XRD pattern of nontronite

The XRD patterns of limonite and nontronite suggested that the ores were mainly made up of hematite, goethite and quartz. These were the expected results since the chemical analyses showed that the ores were mostly consisted of iron and silica. Minor peaks of serpentine were also observed in both ore samples, whereas smectite was only found in nontronite. The XRD patterns of the two ores seemed rather similar, the only difference was the amounts of phases present. Chemical analysis showed that the iron content of limonitic sample was higher than that of nontronite which were also reflected in the intensities of hematite peaks in the XRD patterns.

3.3.2 DTA - TGA Examinations

The Differential Thermal Analysis (DTA) and Thermo Gravimetric Analysis (TGA) were done by the Central Laboratory in Middle East Technical

University. For these analyzes, ore samples 100% ground to -38 μm were used. Analyzes were done within 25-1000°C temperature range with a heating rate of 10°C per/minute in a nitrogen atmosphere. The diagrams showing the obtained results are given in Figures 18 and 19.

Examination of the DTA/TGA diagram of the limonitic sample showed that there was an endothermic peak at about 100°C on DTA curve which had occurred due to elimination of physically absorbed water. This vaporization could also be observed as a decrease on TGA curve, resulting from a weight loss. Another small endothermic peak could also be seen at about 290-300°C which was caused by the following chemical dehydration reaction [77]:

$$FeO(OH).xH_2O = FeO(OH) + xH_2O \qquad \text{Rx. 3.1}$$

A strong endothermic peak was clearly identified at about 310-330°C. According to previous studies, this peak most probably occurred due to transformation of goethite to hematite [78, 79]. Goethite naturally contains considerable amounts of substitutional or interstitial elements such as Al, Ni, Co, Cr, Mn, which may shift this dehydroxylation temperature. In consequence of this transformation a sharp decrease on the TGA curve was observed due to weight loss. Landers et al stated that the hematite is almost wholly transformed into goethite at about 320°C in a study with a lateritic ore [78]. Also in related studies with lateritic ores Lopez et al linked a peak corresponding to alteration of goethite to hematite at 305.5°C with a dehydroxylation reaction [79].

$$2\ FeO(OH) = Fe_2O_3 + H_2O \qquad \text{Rx. 3.2}$$

Another small peak was detected at about 550-580°C which may be due to the allotropic transformation of quartz from α-quartz to hexagonal β-quartz which normally occurs approximately at 573°C [80].

Although there are some variations on the DTA curve due to some smaller peaks, a high intensity peak was not observed between 580 to 1000°C, nevertheless a continuous weight loss was seen on the TGA curve. This was most likely caused by the dehydroxylation or decomposition of other hydroxyls such as serpentine. According to Földvári Mg-serpentine decomposition to forsterite occurs with two successive reactions. Firstly, between 640 to 820°C, an endothermic peak occurs due to dehydroxylation and this is followed by an exothermic peak in the temperature range of 800-840°C as a result of structural decomposition [81].

$$Mg_6[Si_4O_{10}].(OH)_8 = 2Mg_3[Si_2O_7] + 4H_2O \qquad \text{Rx. 3.3}$$

$$2Mg_3[Si_2O_7] = 3Mg_2[SiO_4] + SiO_2 + H_2O \qquad \text{Rx. 3.4}$$

Földvari also noted that the Curie-point of hematite is at about 675–680 °C so a small endothermic peak was also expected in that temperature range [81].

Similar conclusions were reached upon observations on the DTA/TGA graphs of the nontronitic sample. An endothermic peak corresponding to elimination of physical water could be seen between 100-130°C. A second endothermic peak at about 300°C which could be attributed to dehydroxylation reaction was not as sharp as it was in the DTA curve of the limonitic sample. The lower content of iron (hematite) in the nontronitic sample most likely has led to this output. The endothermic peak at about 600°C occurred presumably due to transformation of quartz. Two succeeding endothermic and exothermic peaks observed in the temperature range of 800-840°C could be linked to serpentine decomposition to forsterite.

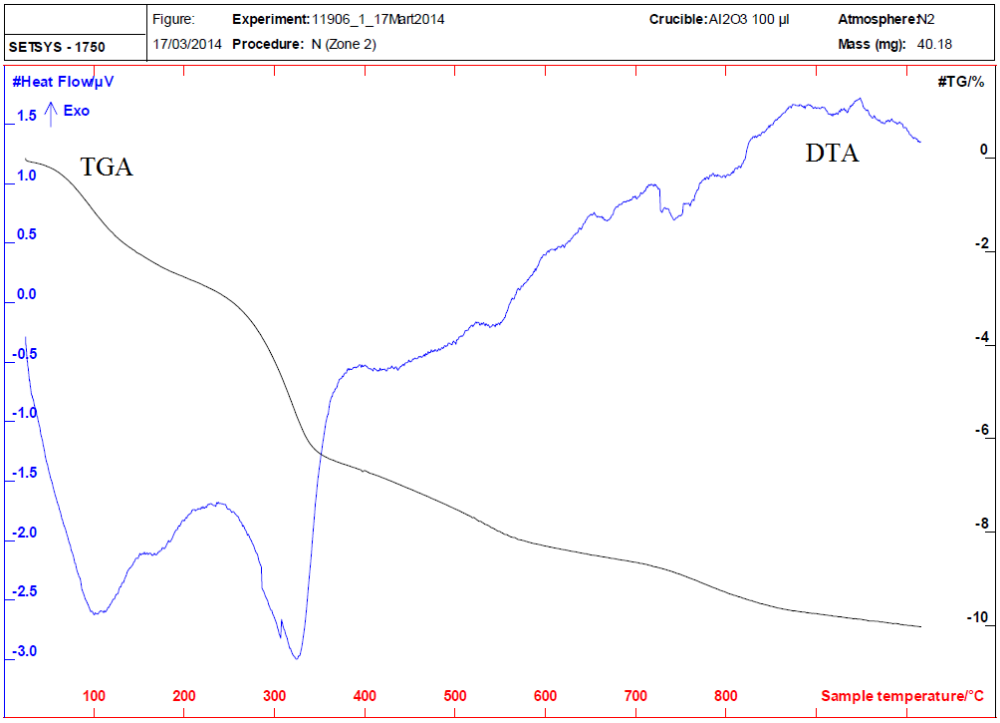

Figure 18 : DTA/TGA graph of limonite

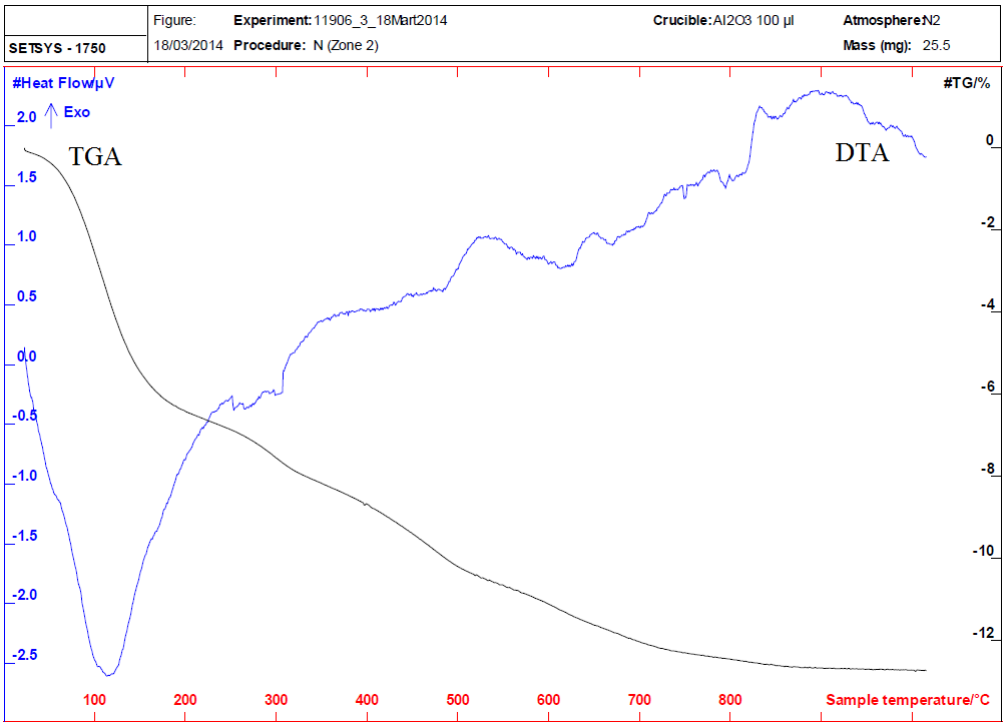

Figure 19 : DTA/TGA graph of nontronite

3.3.3 SEM Examinations

In order to support the results obtained by XRD and DTA/TGA, SEM examinations were done at the final step of mineralogical characterization. Both limonitic and nontronitic samples were studied with a Nova Nanosem 430 microscope provided by the Metallurgical and Materials Department in METU. Information obtained by SEM examinations may provide many noteworthy insights about the extraction characteristics of the sample. As noted previously in Chapter 2, nickel and cobalt elements exist as substitutional elements which are entrapped in iron mineral lattices. First of all, identification of the nickel and cobalt bearing minerals such as hematite and goethite, are important, as they may give presumption for probable insufficient extraction efficiencies. Secondly the presence of aluminum, magnesium or chromium containing minerals such as serpentine, affect leaching parameters as they are highly acid consuming. Quartz also affects leaching parameters as it is a gangue mineral in extraction process which cannot be dissolved substantially in an acid medium. Morphologies and particle sizes of minerals which affect the dissolution kinetics can also be revealed by SEM studies.

The examination by SEM gave coherent results about the existing minerals previously detected by XRD analyses. Goethite, hematite and quartz mineral particles were present within the ore samples.

Two different methods were used for preparation of the SEM samples. The first samples were prepared from very finely ground ore samples (-38 μm). These samples were put into alcohol and agitated for a couple of minutes, before a couple of drops of this mixture were dropped on the carbon tape covered sample holder, with the help of a pipette. For the second samples, the ores were screened and oversized particles were selected and washed. In order to select and inspect different type of minerals, different range of colored particles were selected via visual examination. These particles with different

appearances were placed on a carbon tape on a sample holder by the help of a tweezers. Both of these samples prepared with different methods were coated with platinum before analyses to prevent electrostatic charging of the specimen at the surface and to increase the signal/noise ratio. General view of finely ground ore samples can be seen in Figures 20 and 21.

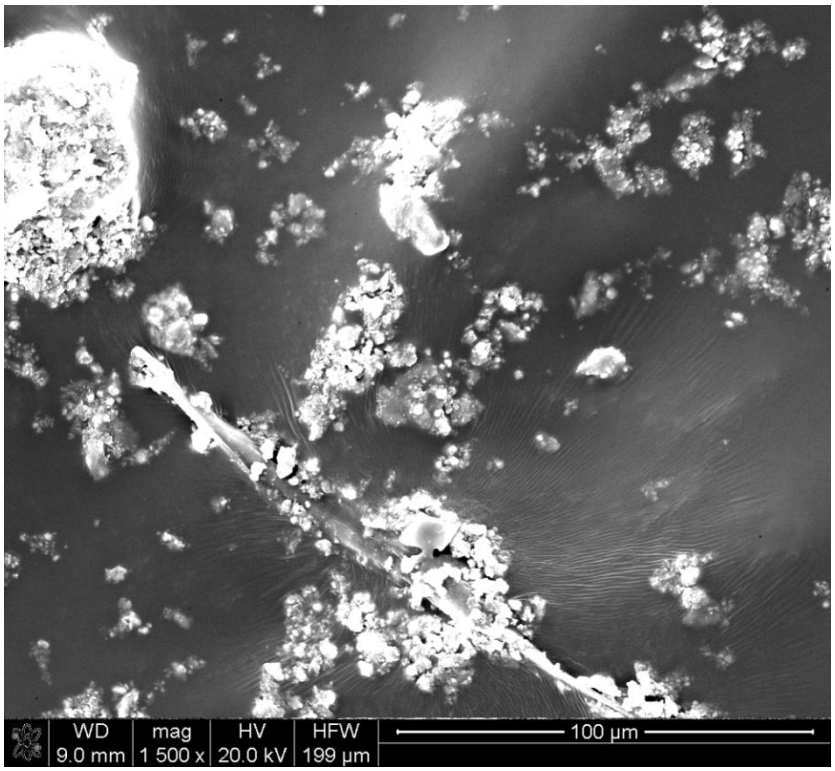

Figure 20: Overview of limonitic sample

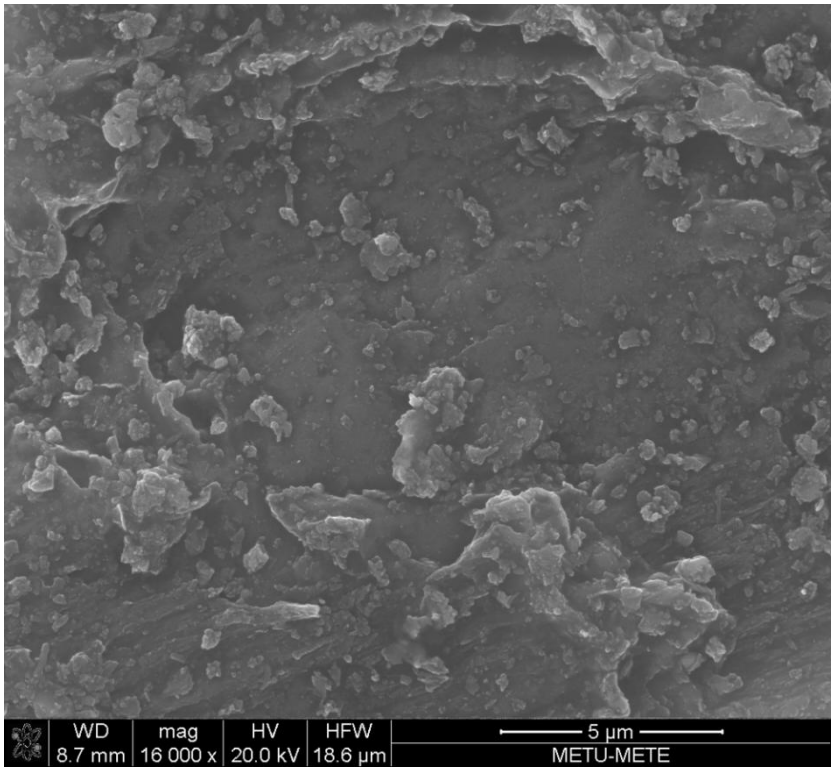

Figure 21: Overview of nontronitic sample

The finely ground samples did not provide much information because all the minerals were interlaced. It was decided to selectively pick different minerals from unground samples. Minerals were selected as different as possible from each other for the preparation of the second samples. Since these particles were selected form the unground ore samples, the particle sizes of the minerals were quite large. Images of some selected minerals from limonitic sample are shown in Figure 22. The EDS analyses associated with the images are included in Appendix C.

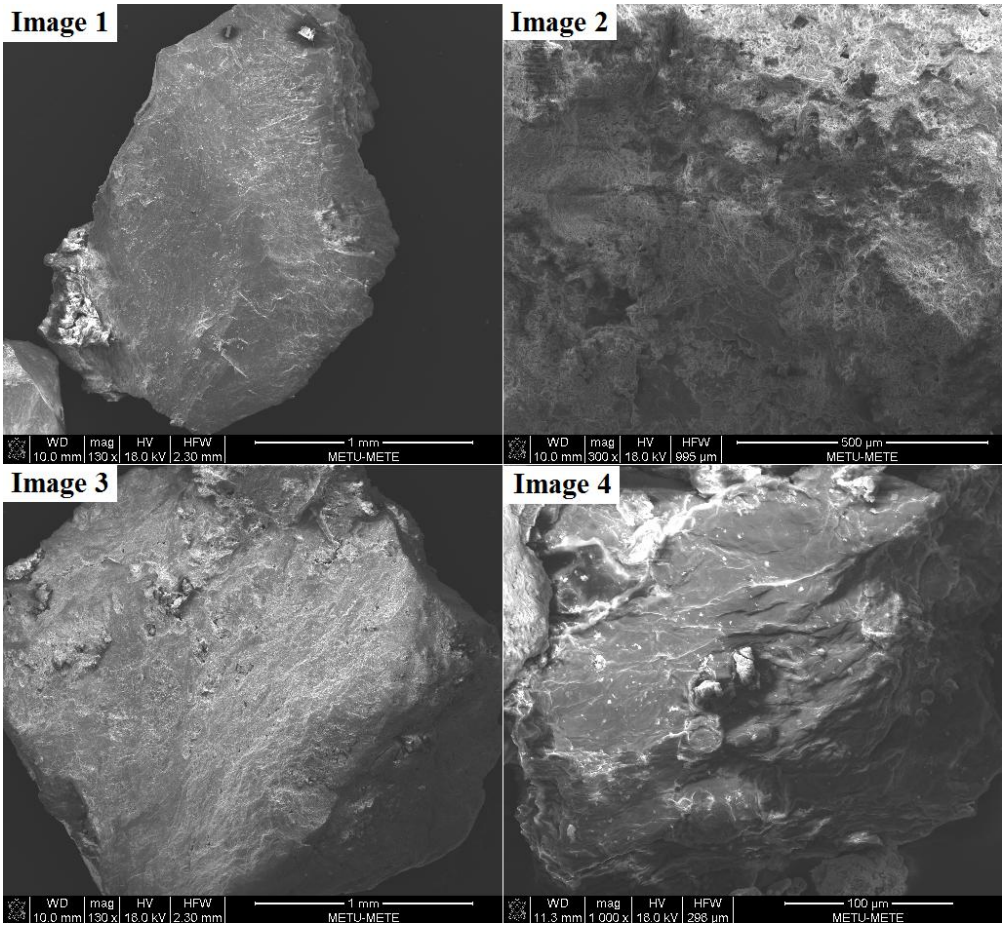

Figure 22: SEM images of selected particles from limonitic sample

In the first image of Figure 22, a large silica particle with distinct, sharp edges can be seen. This type of morphology is a typical characteristic of crystalline silica. The hematite particle in the second image is covered with silica. Aluminum and chromium are also present in this iron mineral. Chromite mineral could not be identified with the XRD analyses however the chromium present in this particle may belong to a chromite mineral. The third image belongs to a goethite particle which was confirmed by examining the EDS results. This particle is also covered with silica. In image 4, an aluminum silicate is observed. In literature, aluminum is generally linked with clay minerals such as smectite, and gibbsite which are said to be found in aluminum rich lateritic ores [20].

Images of some selected minerals from nontronitic sample are shown in Figure 23. The EDS analysis associated with the images are also included in Appendix C. In image 1 of Figure 23 a very large crystalline silica particle can be seen. It also shows the characteristics of a silica particle with clear cut edges. A serpentine mineral which was rich in magnesium content was found in image 2. In image 3 aluminum substituted goethite was observed. In image 4, hematite mineral can be observed as a bright part at the center section of a silicate particle. Nickel and magnesium is also present in this hematite mineral.

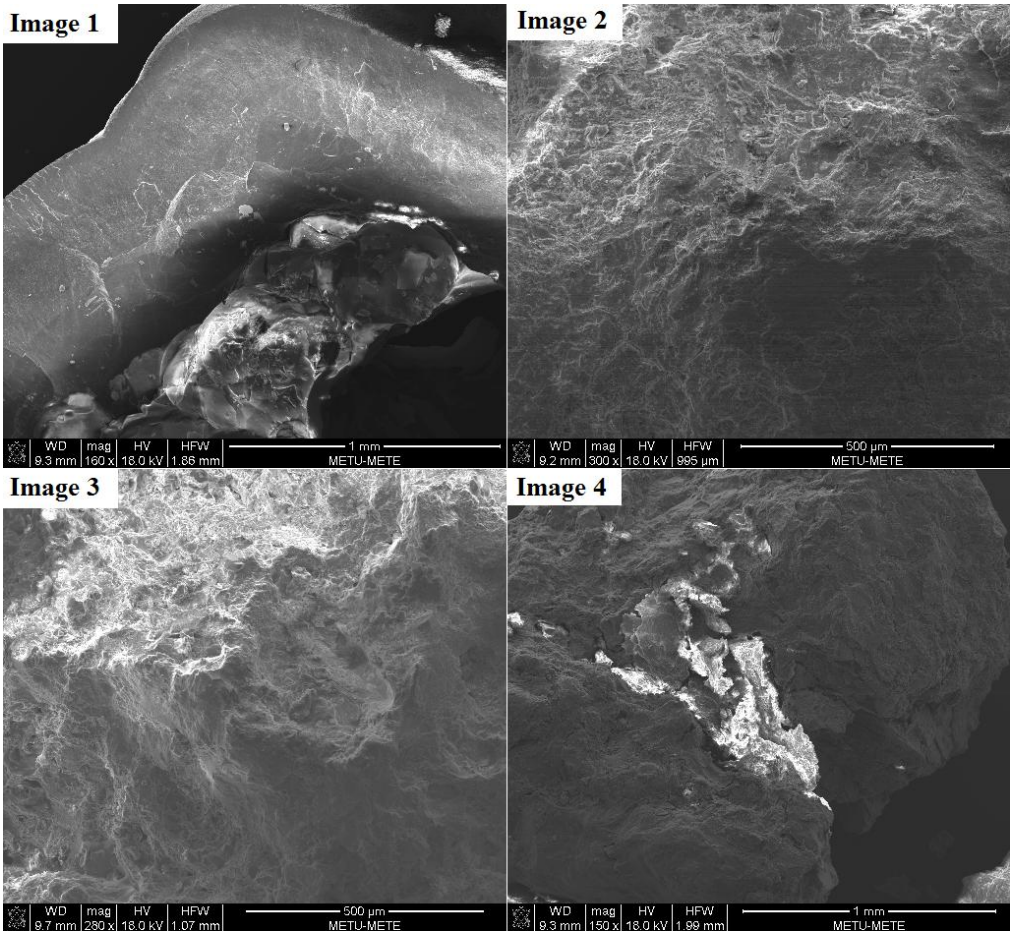

Figure 23: SEM images of selected particles from nontronitic sample

Detection of nickel and arsenic were possible with the EDS, although they could not be identified by XRD. This is due to nickel, cobalt and arsenic substitutions for iron in goethite and hematite structures. So these minerals should be almost completely dissolved upon leaching in order to liberate these substitution elements. Detection of cobalt was not possible with EDS due to its very low content 0.044-0.083%. The peaks of cobalt may also have been masked by other elements with higher intensities like of iron.

The substitution elements within the minerals, changes the crystal size and the texture which affects the rates and mechanisms of dissolution in hematite and goethite. Landers et al observed that the presence of structural aluminum and chromium instead of iron in goethite mineral reduces the dissolution rate of the mineral conceivably due to their greater bond strengths compared to iron [82].

3.4 Experimental Procedure

A simplified overview of the general process flowsheet is given in Figure 24. However, the scope of this thesis covers the steps until the end of iron precipitation.

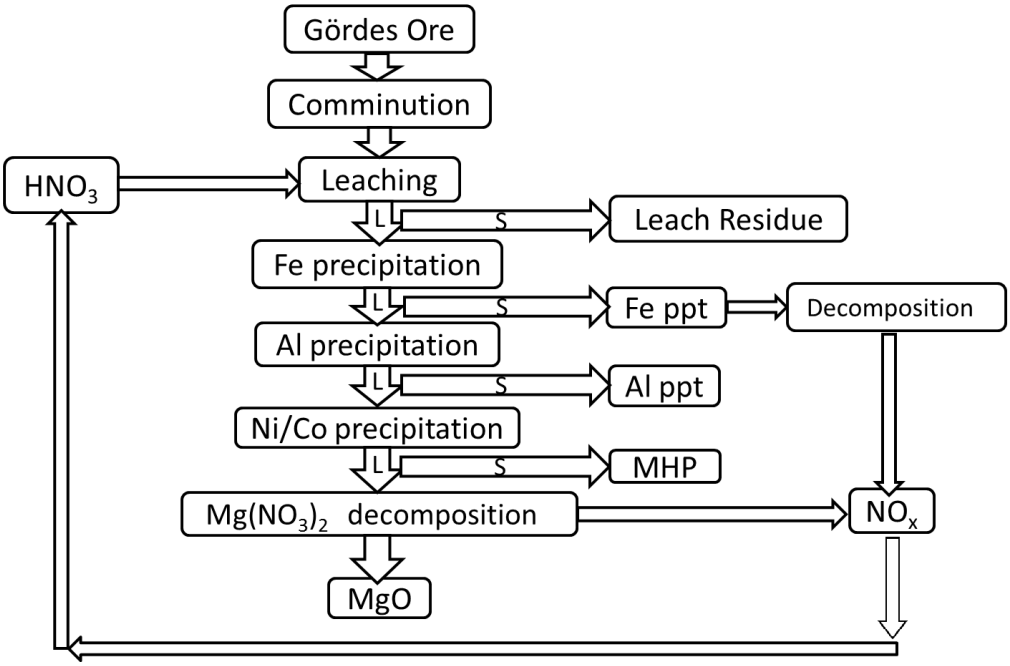

Figure 24: Simplified process flowsheet

3.4.1 Atmospheric Leaching Procedure

A representative sketch for the experimental set-up for atmospheric leaching experiments is shown in Figure 25. The set-up consisted of a 250 ml Pyrex glass balloon, a condenser column, a contact thermometer, a hot plate with magnetic stirrer and a Teflon® coated magnet for stirring.

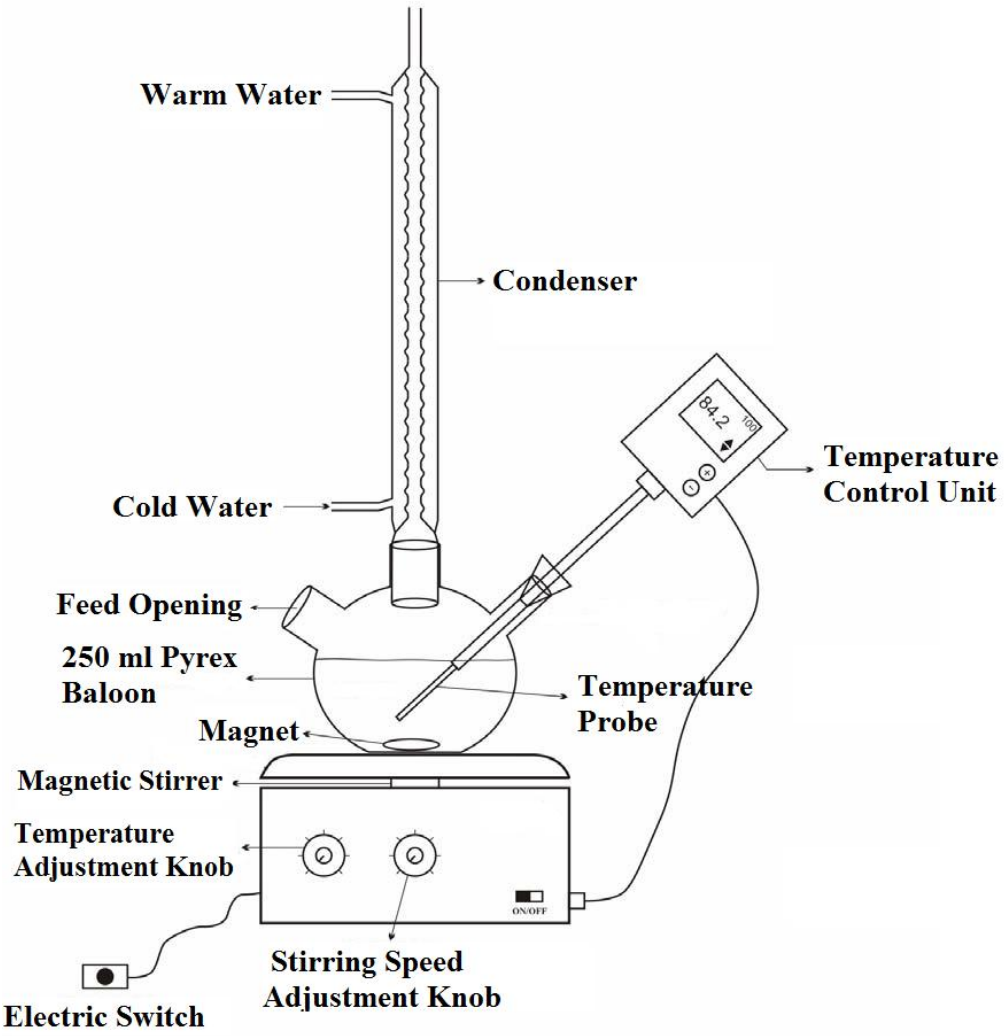

Figure 25: Sketch of atmospheric leaching system [83]

Initially, the balloon used in the experiment was weighed. Subsequently, the condenser column was connected to a tap, so that a cold water circulation was provided to avoid losses by evaporation, over the course of the experiment. Afterwards predetermined volumes of deionized water and nitric acid, along with the magnet were placed in the balloon. The contact thermometer was set to the desired temperature to keep it at that point; then connected and fixed to its place carefully by Parafilm®, so that it could measure the temperature of the leach solution effectively. Stirring speed and the heating knob temperature

were set to 500 rpm and 105°C, respectively. It should be noted that this temperature was the temperature of the heating plate, but the experiments were conducted at the temperature set by the contact thermometer. Ore sample mixture of measured weight was poured into the acidic solution once the boiling point was reached which set the starting point of the experiment. The water flow of the condenser and the temperature of the experiment were checked periodically, and in case of anything went wrong the experiment was cancelled. Once the leaching was over the balloon was cooled and the final weight of the experimental equipment was measured for future calculations. The pregnant leach solution and the solid leach residue were separated via a porcelain Buchner funnel and a filter paper, using a vacuum pump. The separated leach residue was rinsed with deionized water which was acidified to pH 2 with a few droplets of nitric acid. The pH of the water was adjusted to stop any further precipitation from the PLS remaining on the leach residue and to prevent any potential errors for future analysis. The leach residue was dried at 105°C and ground into fine powder form for analysis. For chemical analysis of the leach residues, Niton X-Met 820 X-ray Fluorescence (XRF) analyzer and Atomic Absorption Spectrophotometer (AAS) of META Nikel Kobalt A.Ş. were used. More detailed chemical analysis on the leach residue and PLS obtained under the selected conditions were done via inductively coupled plasma optical emission spectrometry (ICP-OES) and inductively coupled plasma mass spectrometry (ICP-MS) by METU Central Laboratory.

In atmospheric leaching experiments the studied parameters were:

1. Acid Concentration : 4 M, 5 M, 6 M, 8 M (1 M = 1 N for HNO_3)
2. Duration of the Experiment: 3 h, 6 h, 12 h, 24 h, 48h, 72 h
3. Particle Size of the Ore: -150 μm, -300 μm, -600 μm

Initially the effect of acid concentration was studied keeping the other parameters constant. Effect of the experiment duration on extraction values was investigated afterwards for different acid concentrations, and the optimum values for these parameters were determined for highest Ni and Co

extractions. Finally the effect of particle size was studied keeping the leaching temperature and duration constant at the optimum conditions. In all the experiments the temperature was kept at the boiling point, which varied between 99 - 104°C depending on the acid concentration. Liquid-to-solid ratio was also kept constant at 1/5 weight by volume, i,e., 15 grams of ore per 75 cc of leach solution. The ore mixture consisted of 70% limonite and 30% nontronite for all the experiments.

3.4.1.1 Free Acid and ORP Measurements

ORP values of the pregnant leach solutions were measured with a Pt-Ag electrode, saturated with 3M KCl solution.

For the free acid determination of the PLS, a set-up was prepared. A buffer solution of pH=7 was used for the calibration of the pH electrode. A 2M NaOH solution was prepared, for neutralization purpose. A reference solution was prepared by mixing 28 grams of di-potassium oxalate monohydrate ($K_2C_2O_4.H_2O$) in 100 cc deionized water, with magnetic stirring. This oxalic acid potassium salt was used for complexing the metal ions to prevent their intervention during the titration of the free acid. Then, 20 cc of reference solution and 5 cc of deionized water were put and mixed in a beaker and the pH electrode was placed into this solution. When the read pH value was fixed, it was noted as the target pH and 5 cc of PLS was added into this solution. The titration process started after the addition of NaOH solution. The amount of NaOH used to re-reach the target pH value, was used to calculate the free acid of the pregnant leach solution.

3.4.2 Procedure for Downstream Experiments

In high pressure acid leaching, which is generally used for extraction of lateritic ores, the dissolved iron re-precipitates as hematite at high temperatures. Since no such precipitation occurs in atmospheric leaching, the extraction of iron becomes very high compared to HPAL. As a result, the acid consumption would be also high and the produced leach liquor would be contaminated in atmospheric leaching. First of all, the iron should be precipitated in order to remove impurities and purify the pregnant leach solution. The iron precipitation process was carried out with two different methods: Addition of an alkali or by autoclave hydrolysis.

The main aim in these experiments was to precipitate the iron, aluminum and chromium as much as possible, while keeping the nickel and cobalt losses at minimum.

A real pregnant leach solution stock of 3 liters was produced initially in order to be used in the downstream experiments. This stock was produced by repeating the atmospheric leaching experiment under the determined optimum conditions (6 M, 600μm, 48h, at 104°C) for many times.

The chemical analysis of key elements, and other measured properties of the PLS stock are given in Tables 7 and 8, respectively.

Table 7: Some properties of PLS stock

Property of PLS Stock	Value
Density (g/L)	1.30
ORP (mV)	932
Free Nitric Acid (g/L)	193

Table 8: Chemical analysis of key elements in PLS

Element	Analysis (g/L)
Fe	61
Ni	2.88
Co	0.177
Al	5.34
Cr	1.66

3.4.2.1 Neutralization and Iron Precipitation with a reagent

The neutralization can be conducted and the pH of the solution can be increased, using different reagents. MgO was chosen as the neutralization agent. Although MgO is much more expensive compared to $CaCO_3$, it was chosen for this step as it is fully recovered, in downstream steps, and reused back as a reagent according to DNi process [72].

The initial free acid concentration was so high (193 g/L), that the pH meter could not give a healthy result for this initial pH, but it was expected to be very close to 0. Most of the MgO slurry prepared would be consumed by the neutralization of this free acid.

The experimental set-up for the neutralization and iron precipitation experiments is given in Figure 26.

Figure 26: Experimental set-up for neutralization and iron removal

Initially taking the properties of the PLS into consideration, and by calculating a theoretical MgO consumption for 100 ml PLS, a slurry containing 19,2 g MgO and 192 ml deionized water was prepared.

The experiments were conducted in a 250 ml Pyrex balloon with 4 necks, on a hot plate with magnetic stirrer. A contact thermometer, a pH electrode, and a condenser were inserted through these necks. The remaining neck was used for the feeding of reagent slurry. The pH electrode was calibrated using a pH=4 buffer solution at room temperature. The temperature of the contact thermometer was set at 95°C, and the cooling water flowing through the condenser was adjusted to obtain a sufficient flow rate at the beginning of each experiment to prevent evaporation losses.

When the PLS reached the target temperature of the experiment, the pH meter was recalibrated according to that temperature for accurate measurement. The slurry was added drop by drop by the help of a micropipette gradually until

the targeted pH of the experiment was reached. The addition of MgO should be slow, in order to keep the local MgO concentration low. A rapid addition could cause sharp increases in the local pH, resulting in undesired nickel and cobalt precipitations at that region. The experimental duration was started when the solution reached the desired pH value. During the experiment, pH meter was checked frequently and in the case of any decrease in pH value, a drop of MgO slurry was added to keep the pH constant at the desired level.

At the end of each experiment, the same procedures that were used for atmospheric leaching experiments were used for solid-liquid separations.

3.4.2.2 Autoclave Hydrolysis

In literature the thermal hydrolysis of iron was reported to be conducted between 140-180°C range. An autoclave was needed to reach these elevated temperatures, which was necessary for the thermal hydrolysis of iron. For this purpose a stainless steel autoclave purchased from the American Autoclave Company with a 1 liter capacity reaction vessel was used. A representative photograph of the autoclave used in iron hydrolysis is given in Figure 27.

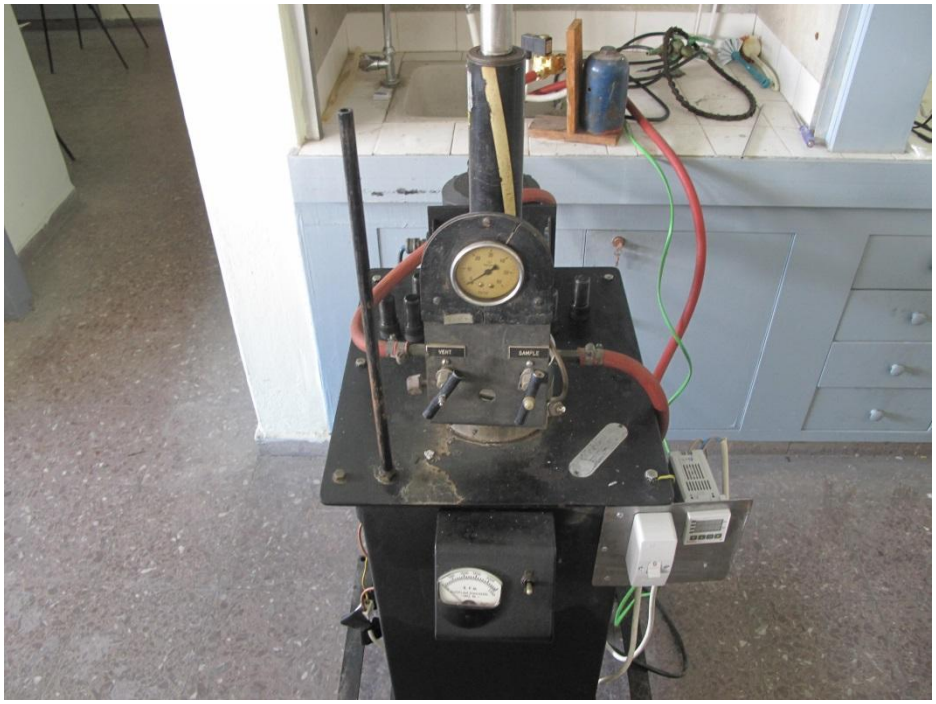

Figure 27: Stainless steel autoclave

Initially, the water hoses of the cooling coil were connected to a tap and the temperature controller was calibrated to keep the temperature of the PLS constant during the experiment duration.

Then, 250 ml of pregnant leach solution, or concentrated pregnant leach solution was put into the reaction vessel, and the system was closed. The screws were tightened to prevent any gas leakage. The temperature controller was set to the desired point. Heating of the autoclave took about 40 minutes. Experiment duration was started when the PLS reached the targeted temperature. Upon completion of the experiment, the temperature of the controller was set to room temperature and the water flow from the tap was increased to decrease the cooling duration. Since the reactor vessel of the autoclave was immovable, the autoclave was allowed to cool down, before opening the lid and taking the precipitates out. The solid precipitate and the remaining solution were then separated via filtering.

CHAPTER 4

RESULTS AND DISCUSSION

4.1 Atmospheric Leaching Experiments

For every single atmospheric leaching experiment, 15 g of dry limonitic and nontrontic ore mixture was used as a representative sample. The ore deposit of Manisa/Gördes comprises of 70% of limonite and 30% of nontronite. Ore mixture used in the atmospheric leaching studies also contained the same fractions of the deposit, for the experiments to be analogous with the industrial application.

In order to estimate the necessary acid input and set a starting point for the experiments a theoretical acid consumption calculation was done before the start of experimental stage. All the acid consuming elements assumed to be in their oxide form and they were assumed to be leached totally, so the calculations were done accordingly. The theoretical acid consumption of the ore mixture was calculated as 1282 kg of nitric acid per ton of ore. The major chemical reactions during leaching and theoretical acid consumption calculations are given in Appendix A.

Different parameters were studied throughout the course of the experimental stage, while some parameters were being kept constant. To be industrially applicable, solid/liquid ratio was kept constant at 1/5 wt/vol for all atmospheric leaching experiments. Temperature is another parameter which affects the dissolution kinetics directly, so it also has an important role for

leaching experiments. However it was decided not to study the effect of temperature, since the extraction efficiencies tend to rapidly increase with increasing temperature as indicated in previous studies in literature [60, 72]. McCarthy et al confirmed that the best leaching temperature would be over 100°C in direct nickel process [72]. Büyükakıncı showed that the temperature and extraction efficiencies of metals were directly proportional, so the highest metal extraction values were obtained at the highest temperature studied [60]. In the light of such information, the highest possible temperature was selected to be constant for all the experiments, which is the boiling point (100-104°C).

4.1.1 Effect of Acid Concentration and Leaching Duration

It was decided to start with a series of experiments to observe the effect of acid concentration on the extraction efficiencies. In order to examine the extraction efficiencies of atmospheric leaching experiments at different acid concentrations, the experiments were conducted at 4 M, 5 M, 6 M and 8 M acid concentrations.

Since the theoretical acid consumption of the ore was calculated approximately 1282 kg nitric acid per ton of ore, and a constant solid/liquid ratio of 1/5 g/cc was set for the experiments. It was determined that an acid concentration below 4 M would be insufficient for leaching experiments aiming maximum Ni and Co extractions. A set of experiments was carried out starting from a 4M (252 g/L) acid concentration. The experimental conditions for these set of experiments are given in Table 9.

Table 9: Parameters of acid concentration effect investigation at 3 h experiments.

Leaching Temperature	Boiling Point (100-104°C)
Stirring Speed	500 rpm
Liquid/Solid Ratio	5/1 vol/wt
Acid Concentrations	4 M (252 g/L), 5 M (315 g/L), 6 M (378 g/L), 8 M (504 g/L)
Leaching Duration	3 h
Particle Size	-150 μm

The experiments were all executed at the boiling temperatures. The boiling point varied slightly between 100-104°C depending upon the acid concentration. Extraction efficiencies were calculated using XRF and AAS analysis of the leach residues. The formula for the solid based extraction calculations are given in Appendix A. The graphical presentation of extraction values of Ni, Co, Fe, Cr, Mn, Cu, and As, with respect to different acid concentrations for 3 h experiments are given in Figure 28.

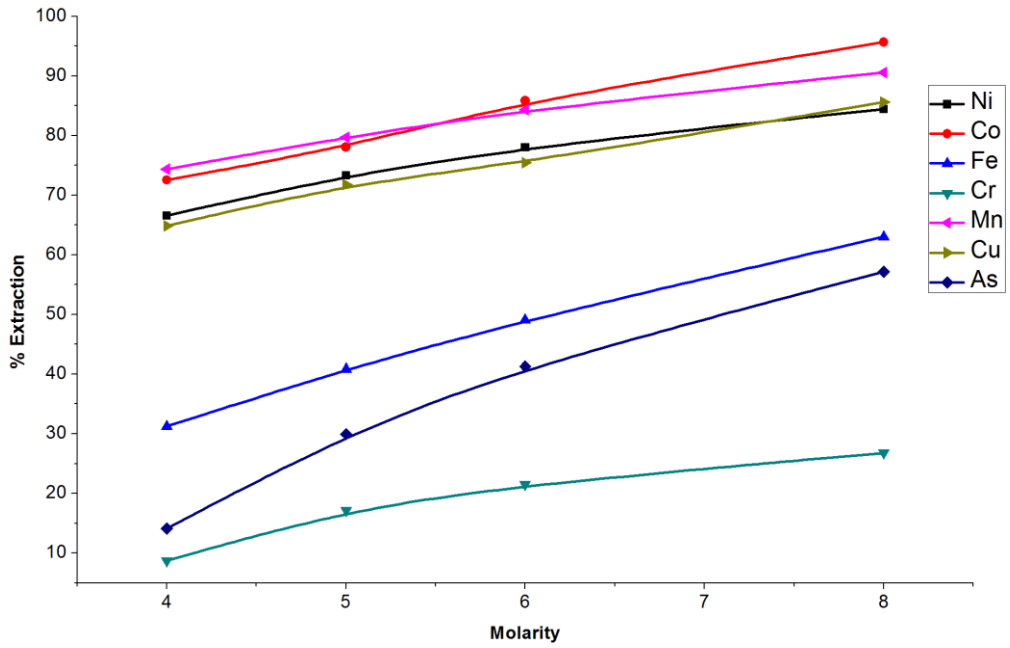

Figure 28: Extraction percentages of selected metals as a function of acid concentration at 3 h, for -150 µm particle size fixed conditions

Increasing acid concentration showed positive affect on both nickel and cobalt extraction efficiencies. Extraction values of nickel and cobalt showed similar dissolution characteristics. This was expected since both were mainly entrapped in hematite and goethite minerals. Highest extraction values were obtained at the highest acid concentration, but nickel and cobalt extraction values were still insufficient even at 8 M (504 g/L) acid concentration.

It was concluded that the extraction values could only be raised to a certain limit, with increasing acid concentration when the leaching duration was short. Higher dissolution of iron minerals were needed for complete leaching of nickel and cobalt, which could be obtained by more acid-ore interaction that needed more time. Another observation from the figure was that the slope of the trend line had dropped with the increasing acid concentration.

A second set of experiments were carried out to determine the effect of leaching duration. The experimental parameters were chosen based on the previous experiments. Since the extraction values were less than the

expectations, longer leaching durations were studied. A fixed acid concentration of 6 M was selected since the increase in the extraction values was not effective at higher acid concentration. The variables for this set of experiments are given in Table 10.

Table 10: Parameters of experiment duration effect investigation at 6 M experiments.

Leaching Temperature	Boiling Point (104°C)
Stirring Speed	500 rpm
Liquid/Solid Ratio	5/1 vol/wt
Acid Concentration	6 M (378 g/L)
Leaching Durations	3 h, 6 h, 12 h, 24 h, 48 h, 72 h
Particle Size	-150 μm

The graphical presentation of extraction values of Ni, Co, Fe, Cr, Mn, Cu, and As, for different leaching durations with 6 M acid concentration are given in Figure 29.

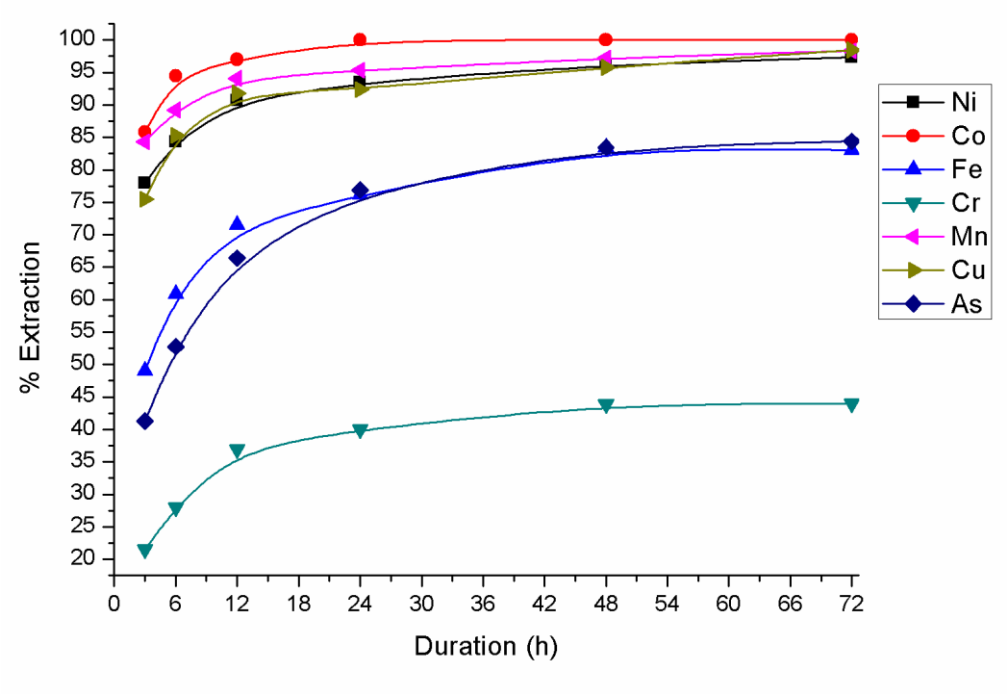

Figure 29: Extraction percentages of selected metals as a function of leaching duration at 6 M acid for -150 µm particle size fixed conditions.

As it is seen in Figure 29, the extraction percentages of nickel and cobalt improved with longer leaching durations. This trend was expected with the increasing acid-ore interaction duration. Cobalt was almost completely leached in the experiment carried out for 12 , but 48 h of leaching was necessary for the extraction of nickel to reach its maximum value. Although, 48 h of leaching duration appeared to be relatively long for a feasible application for industrial purposes, the extraction efficiencies showed a slump in shorter durations. Extraction efficiencies of almost all elements, except iron, stayed at the same levels for 48 h and 72 h experiments. Iron extraction value peaked at 72 h experiment. Iron is the primary undesired impurity element in the PLS, so 72 h of leaching was not chosen for the remaining experiments.

Dissolution values of elements had shown that the leaching experiments were successful at long leaching durations for high acid concentrations. Higher acid

concentrations were expected to increase the dissolution rate, but since there was enough time for acid-ore surface interaction, the effect of lesser acid concentration for 48 h and 72 h experiments were carried out. It was done in order to find out whether the acid consumption could be decreased if longer leaching durations were utilized.

Experimental parameters for 48 h and 72 h experiments at different acid concentrations are given in Table 11.

Table 11: Parameters of acid concentration effect investigation at 48 and 72 h experiments.

Leaching Temperature	Boiling Point (100-104°C)
Stirring Speed	500 rpm
Liquid/Solid Ratio	5/1 vol/wt
Acid Concentrations	4 M (252 g/L), 5 M (315 g/L), 6 M (378 g/L)
Leaching Durations	48 h, 72 h
Particle Size	-150 μm

In Figures 30 and 31, the extraction rates of important metals against different acid concentrations for 48 h and 72 h experiments are given.

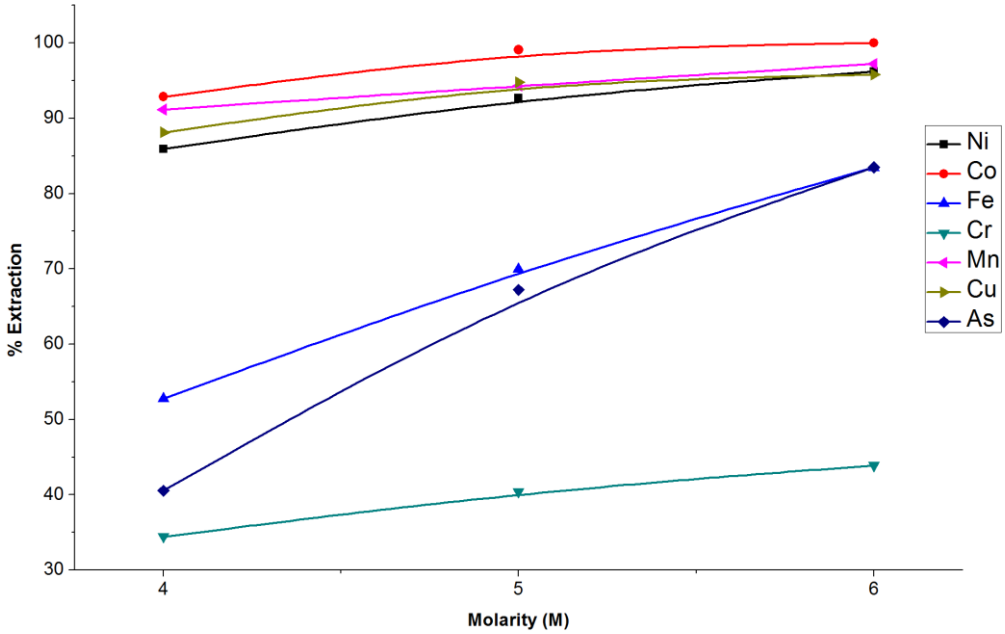

Figure 30: Extraction percentages of selected metals as a function of acid concentration, 48 h for -150 µm particle size fixed conditions

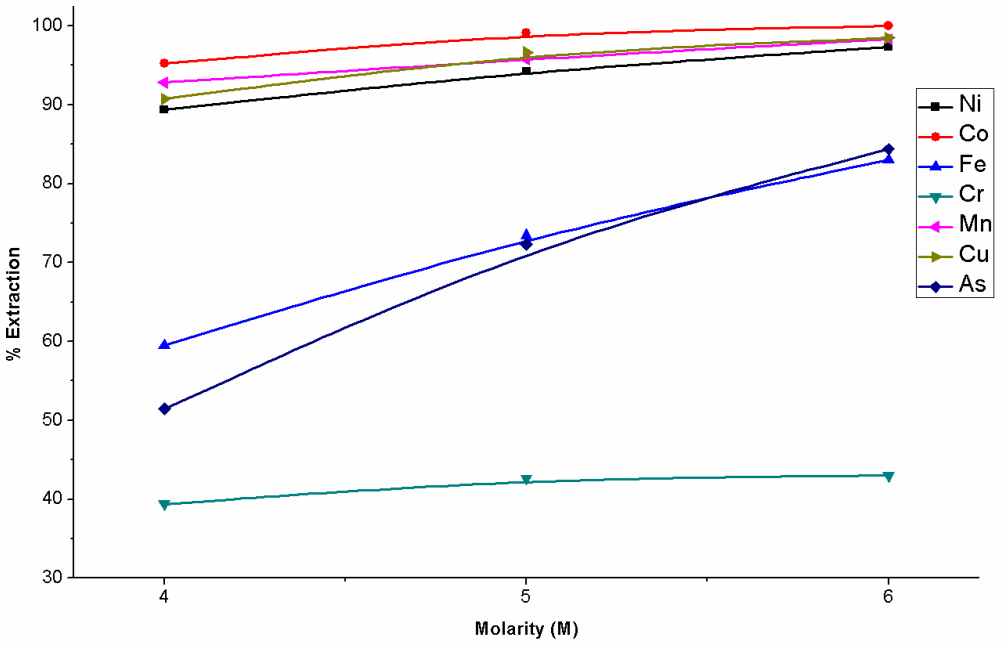

Figure 31: Extraction percentages of selected metals as a function of acid concentration, 72 h for -150 µm particle size fixed conditions

From the mentioned figures, it is clear that the nickel and cobalt extractions decreased gradually with decreasing nitric acid concentration. The extraction efficiencies of other elements showed similar trends when the results from Figures 30 and 31 were cross-checked. The extraction values of cobalt and manganese shown in Figures 30 and 31 are in accord with Canterford's statement that the dissolution kinetics of manganese and cobalt are similar to each other and they are extracted at a faster rate than nickel [84].

Comparison of extraction values of Ni, Co, Fe, Cr and As for 48 h and 72 h experiments are illustrated in Figures 32-36.

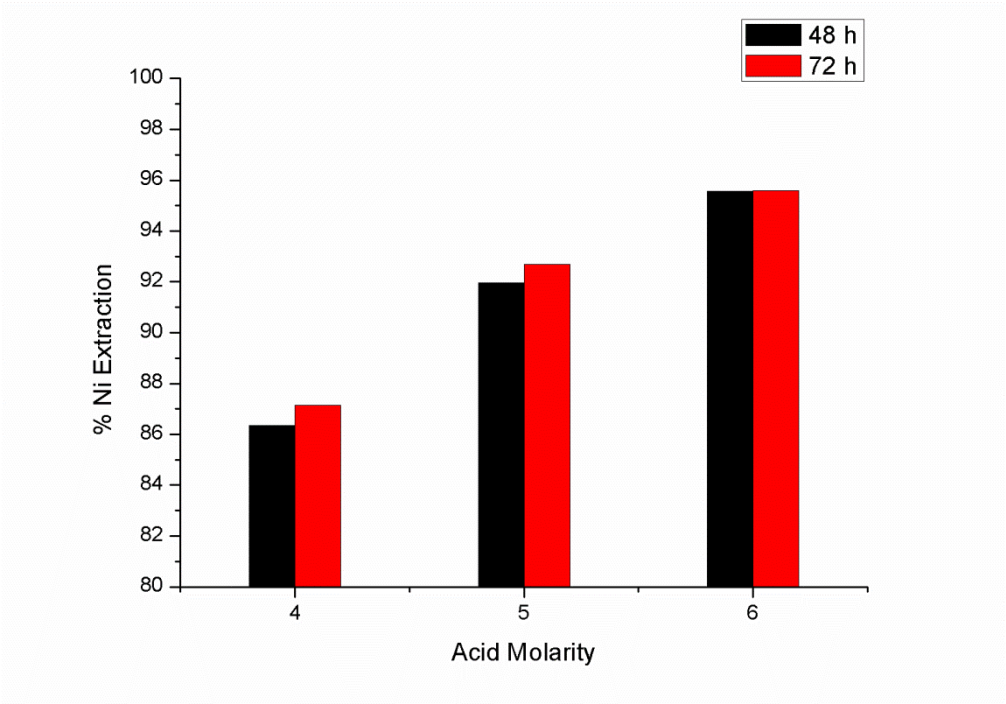

Figure 32: Effect of leaching duration on nickel extraction efficiency at 4 M, 5 M and 6 M acid concentrations

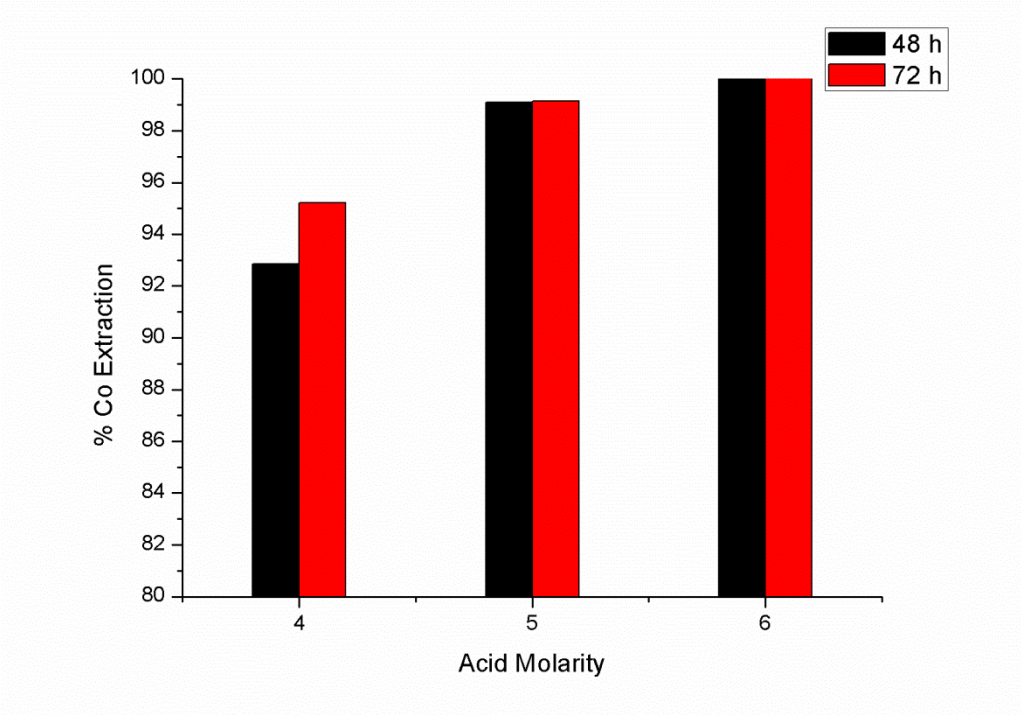

Figure 33: Effect of leaching duration on cobalt extraction efficiency at 4 M, 5 M and 6 M acid concentrations

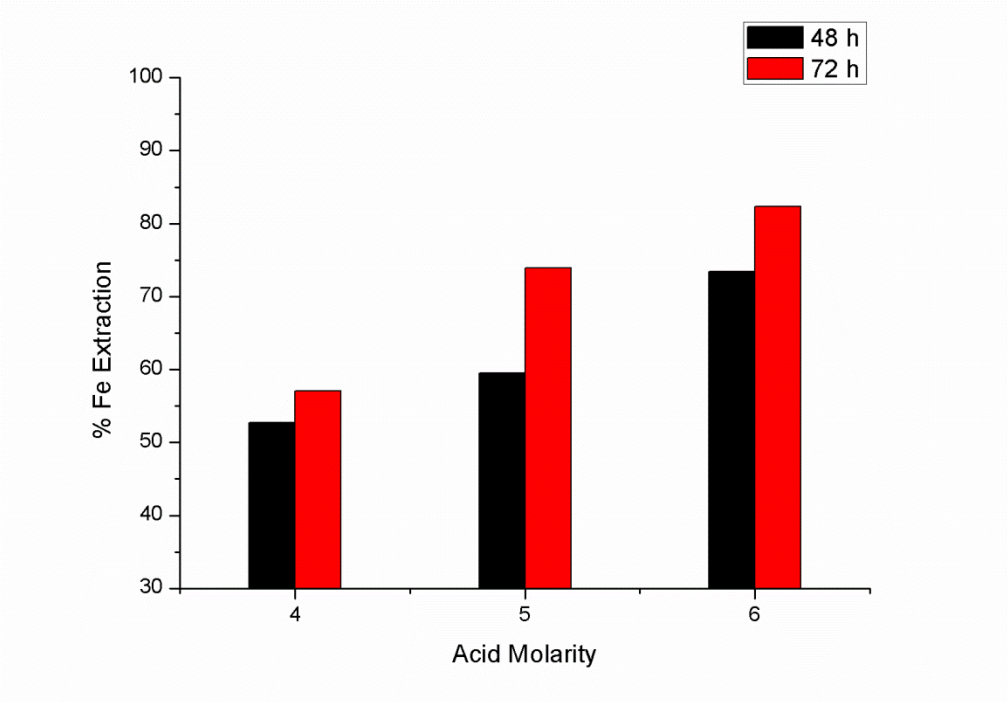

Figure 34: Effect of leaching duration on iron extraction efficiency at 4 M, 5 M and 6 M acid concentrations

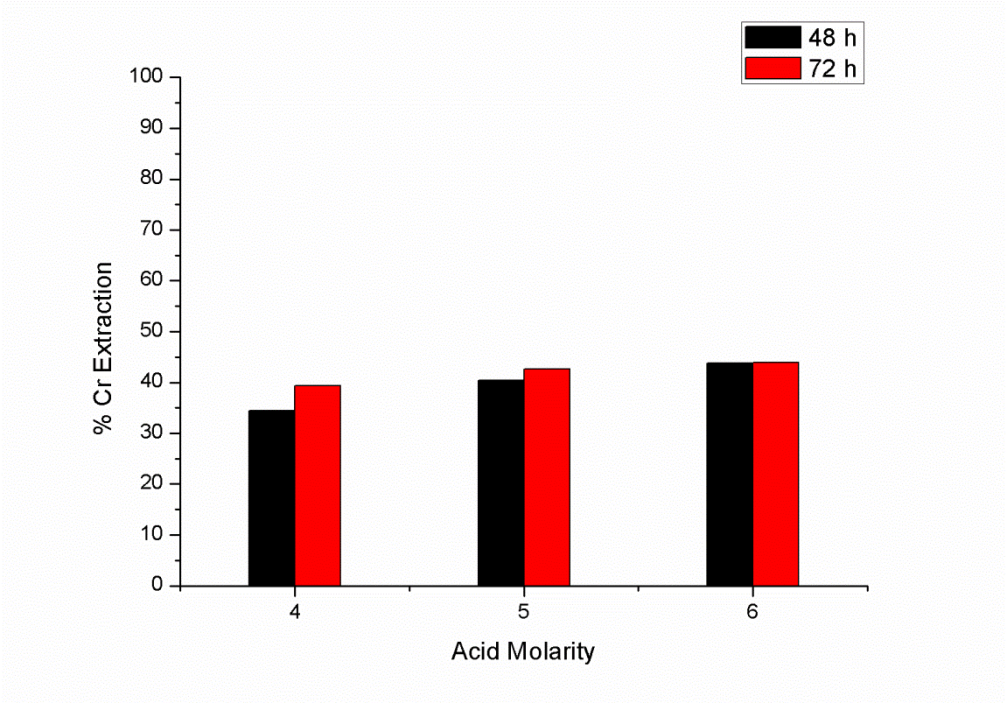

Figure 35: Effect of leaching duration on chromium extraction efficiency at 4 M, 5 M and 6 M acid concentrations

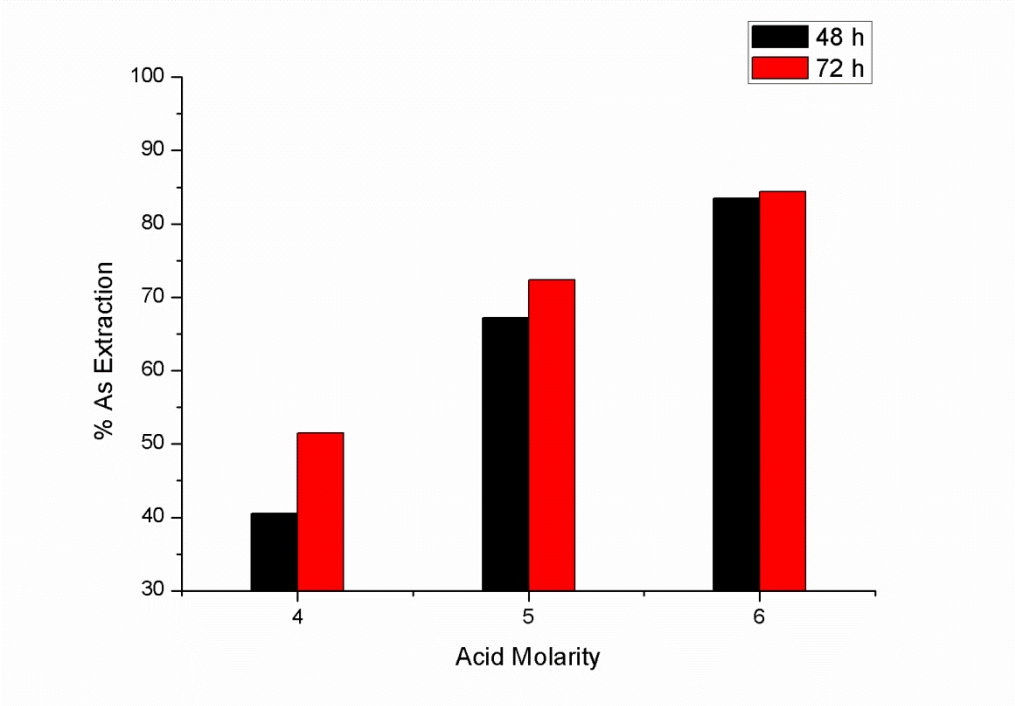

Figure 36: Effect of leaching duration on arsenic extraction efficiency at 4 M, 5 M and 6 M acid concentrations

Extraction efficiencies of the elements calculated at the end 72 h durations were higher than those of 48 h durations for 4 M acid concentration. When the acid concentration is increased, the difference between the leaching efficiencies of the elements got lower for 48 and 72 h experiments. When the nitric acid concentration was 5 M, only a minor difference was seen between extractions of elements for 48 and 72 h experiments. No significant difference was observed on the nickel, cobalt, chromium and arsenic extractions between 48 and 72 h experiments when the acid concentration was 6 M. Iron was the only element that seemed to be extracted more at 72 h leaching duration when the acid concentration was 6 M, but this increase in its dissolution rate did not lead up to an increase in nickel extractions. Korkmaz stated that undissolved iron might be present in silica or chromite particles, which may be the reason behind that the extraction values of iron not reaching to high percentages as Ni and Co [32]. In the present study, the entrapment of iron in other minerals also might be responsible for lower extraction values at 48 h.

Summary of extraction values obtained for the experimental data from studies of the effect of acid and temperature experiments are given in Table 12.

Table 12: Extraction values of atmospheric leaching experiments for different durations and acid concentrations.

Leaching Duration, (h)	Nitric Acid Concentration, (M)	Ni (%)	Co (%)	Fe (%)	Cr (%)	As (%)
3	4	64.6	72.6	31.2	8.7	14.1
	5	72.4	78.0	40.8	17.2	29.9
	6	76.4	85.8	49.1	21.5	41.3
	8	82.3	95.7	58.9	26.8	57.2
6	6	81.4	94.4	56.4	28.0	52.7
12	6	89.5	100	69.8	38.9	66.4
24	6	93.4	100	76.3	40.0	76.9
48	4	86.4	92.8	52.8	34.4	40.5
	5	92.0	99.1	59.5	40.4	67.2
	6	95.6	100	73.4	43.5	83.5
72	4	87.1	95.2	57.1	39.4	51.5
	5	92.7	99.1	73.9	42.6	72.3
	6	95.7	100	82.3	43.9	84.4

In order to study the effect of particle size in AL, the optimum nitric acid concentration and duration combination were needed to be determined. The acid concentration and leaching duration were selected as 6 M and 48 h, respectively before carrying out further experiments.

4.1.2 Effect of Particle Size

Upon determinations of the optimum acid concentration and the duration of the experiments, the effect of particle size was studied with a set of experiments using the ground ores with varying particle sizes. The experiment

duration, acid concentration, and the temperature were kept constant at 48 h, 6 M (378 g/L), and 104°C (boiling point), respectively. Parameters of particle size effect investigation experiments are given in Table 13:

Table 13: Parameters of particle size effect investigation experiments

Leaching Temperature	Boiling Point (104°C)
Stirring Speed	500 rpm
Liquid/Solid Ratio	5/1 vol/wt
Acid Concentration	6 M (378 g/L)
Leaching Duration	48 h
Particle Sizes	-600 µm, -300 µm, -150 µm,

Graphical illustration of the effect of particle size on the extraction values of selected elements are given in Figure 37.

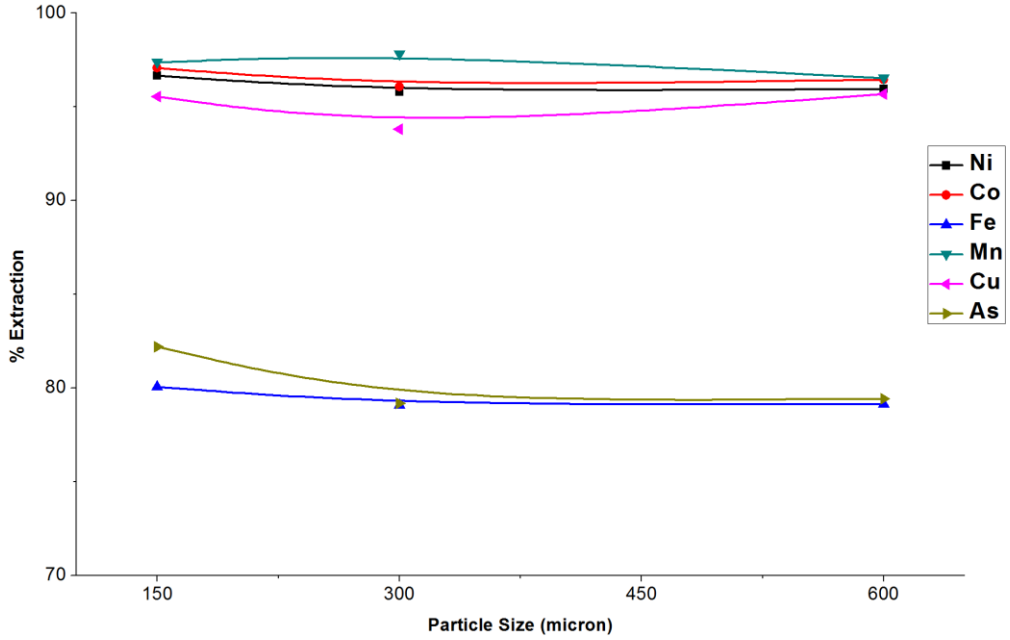

Figure 37: % Extraction vs particle size for 48 h, at 6 M acid fixed conditions

It was predicted prior to the experiments, was that the extraction efficiencies would increase with the decreasing particle size of the ore. However, the results have shown that particle size had a minor effect on the extraction efficiencies. A reason that the extraction efficiencies were not different from each other could be attributed to particle size distribution of the ore samples and their porous structure. As given in Tables 4 and 5, more than 40 wt.% of the particles were below 38 μm even in the unground ore (-850 μm), so it can be expected that this proportion would be even higher for the ground ores (-600 μm, -300 μm, -150 μm).

The similar extraction efficiencies confirmed that no matter how big the particle size was the concentrated nitric acid medium easily dissolved the particles with the help of magnetic agitation. Wet screen analysis was performed on both the -600 μm ground ore sample prior to the experiment, and on the leach residue afterwards to justify this conclusion. The particle distributions of the ore sample and the leach residue are given in Tables 14 and 15, respectively.

Table 14: Particle size distribution of -600 μm ore mixture

Size (μm)	**Weight (%)**	**Cumulative wt. (%) Oversize**	**Cumulative wt. (%) Undersize**
+300	12.06	12.06	87.94
+150	13.40	25.46	74.54
+75	14.50	39.96	60.04
+38	16.64	56.60	43.40
-38	43.40		
Total	100		

Table 15: Particle size distribution of leach residue

Size (µm)	Weight (%)	Cumulative wt. (%) Oversize	Cumulative wt. (%) Undersize
+300	2.24	2.24	97.76
+150	4.14	6.38	93.62
+75	5.92	13.30	87.70
+38	7.84	20.14	79.86
-38	79.86		
Total	100		

In the ore sample 43.4 wt.% of the particles were under the size of 38 µm, whereas in the leach residue, this value increased up to nearly 80% as seen in Tables 14 and 15. The sharp decrease in the particle size strengthens the claim that the large particles were easily leached in the nitric acid.

The measured ORP values and calculated free acidity of pregnant leach liquors are given in Table 16.

Table 16: Oxidation reduction potentials (ORP) and free acidity of PLS from atmospheric leaching experiments

Leaching Duration (h)	Nitric Acid Concentration (M)	Particle Size (μm)	Free Acid (g/L)	ORP (mV)
3	4	-150	178	941
	5	-150	215	861
	6	-150	289	854
	8	-150	364	832
6	6	-150	248	861
12	6	-150	228	877
24	6	-150	217	883
48	4	-150	102	989
	5	-150	155	954
	6	-150	205	864
72	4	-150	91	1002
	5	-150	138	948
	6	-150	184	939
48	6	-300	195	930
		-600	192	932

Oxidation reduction potential values were very high as seen in Table 16, as the result of rich Fe^{3+} ion concentration in the PLS. The very high values of free acid and ORP values indicated that the reagent consumption would be very high for the neutralization and precipitation steps.

4.1.3 Optimum Conditions for Atmospheric Leaching Experiments

After studying the effect of acid concentration, leaching duration and the particle size, the optimum experimental parameters for highest Ni and Co

extractions were selected as 48 h of leaching duration, 6 M of nitric acid, and -600 μm particle size. The optimum experimental parameters determined for the atmospheric leaching experiments are given in Table 17. Chemical composition of the PLS is given in Table 18. Oxidation reduction potential and the free acidity of the PLS solution is given in Table 19.

Table 17 : Optimum parameters for AL experiments

Leaching Temperature	Boiling Point (104°C)
Stirring Speed	500 rpm
Liquid/Solid Ratio	5/1 vol/wt
Acid Concentration	6 M (378 gr/L)
Leaching Duration	48 h
Particle Size	-600 μm

The extraction efficiencies were calculated via solid based calculations from the obtained chemical analysis of the leach residue by ICP-MS analysis. Extraction values were double checked also by liquid based calculations from PLS concentrations.

Table 18: Extraction efficiencies and the composition of the pregnant leach solution obtained at the optimum conditions

Element	**Extraction %**	**Pregnant Leach Solution (g/L)**
Ni	95.4	2.88
Co	96.6	0.177
Sc	99.8	0.0123
Fe	78.8	61.0
Al	89.4	5.34
Cr	26.1	1.66
Mn	95.9	1.06
As	79.4	1.45
Mg	96.3	2.89
Ca	96.7	1.09
Na	47.8	0.117
Cu	92.4	0.053
Zn	99.8	0.035

Table 19: Properties of the pregnant leach solution obtained at the optimum conditions

Oxidation Reduction Potential (ORP)	932 mV
Free acid	192 g/L

Amount of nitric acid consumed during the leaching process was found out as 1079 kg HNO_3/ton of ore. It was calculated from the difference between the initial acid concentration and the free acid in the PLS. Since the acid consuming elements, especially the most acid consuming element, which was iron, were not totally extracted. This value came out to be lower than the

theoretical acid calculated as 1282 kg HNO_3/ton of ore as given in Appendix A. The amount of free acid in the PLS solution was high for the same reason.

4.1.4 Leach Residue Characterization

4.1.4.1 XRD Examination of Leach Residue

Comparison of the XRD patterns of the ore mixture which was used in experiments with the leach residue of the experiment under the optimum conditions are given in Figure 38.

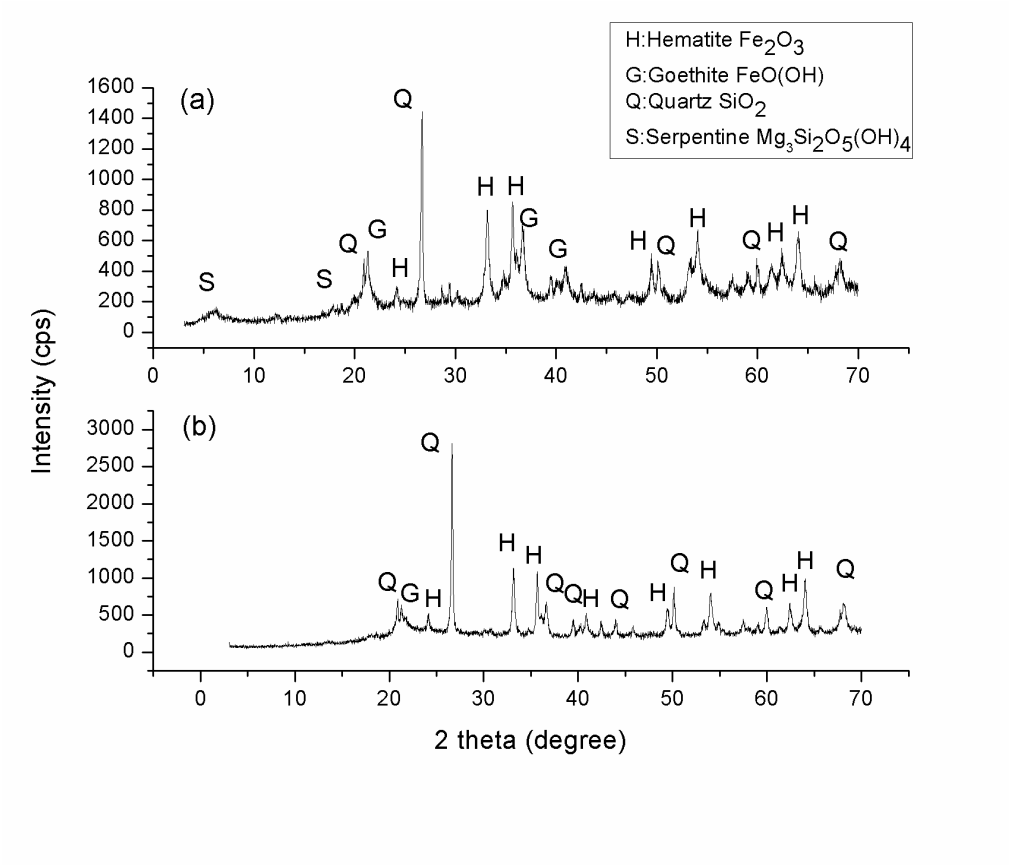

Figure 38: Comparison of XRD patterns of leach residue of experiment conducted under the optimum conditions (b) and its unleached mixed ore sample (a)

The XRD pattern of leach residue suggested that the remaining major phases were quartz and hematite, and the minor phase was goethite. Serpentine peaks could not be identified after leaching, so it can be said that all serpentine mineral existed in the ore had been dissolved. Complete dissolution of serpentine was a foreseen result since clay silicates and clay-like minerals are expected to be leached more easily than limonites. According to Canterford [50] and Griffin et al [66]. smectites, serpentines and saprolites are more easily leached at atmospheric leaching conditions and their complete dissolution is important for many elements forming their structure.

Only one goethite peak was identified in the pattern of the leach residue. This showed that most of the goethite mineral were dissolved during leaching. High extraction values of nickel could be attributed to this. According to Chander [67], and Senanayake and Das [54], the complete dissolution of the goethite grains is needed for nickel extraction.

An increase in the intensity of quartz peaks was observed in the pattern of leach residue. Since the quantities of other minerals decreased in the leach residue compared to original ore, the intensity of quartz was expected to be higher as it is very acid resistant and almost insoluble. The increased intensities in the quartz peaks also indicated that the transformation of quartz to amorphous silica gel did not occur much. Transformation of quartz to gel-like silica is an undesired phenomenon since nickel and cobalt losses may be encountered due to entrapment in it.

Hematite was another mineral which was observed in the leach residue. Since the extraction values of Ni and Co were very high, the nickel and cobalt might be nonexistent in the structure of remaining hematite. The relative intensity of hematite peaks stayed about the same level. This did not mean that hematite wasn’t leached completely, but leaching efficiency of hematite was lower compared to other minerals. Liu et al stated that hematite is one of the harder leached minerals in laterites, and has a slower dissolution rate compared to goethite in sulfuric acid [85].

4.1.4.2 SEM Examination of Leach Residue

Identification of phases by morphological investigation and chemical structure analyses by EDS were done by SEM examinations on the leach residue. Nickel and cobalt losses were minimal, so they were not expected to be seen in Figure 39. Since the particle size was much finer in leach residue, due to strong acid attack and agitation, compared to original ore sample, and the particles could not be selected one by one, so the particle surfaces were not clear, and mixed and agglomerated particles were observed in most of the images.

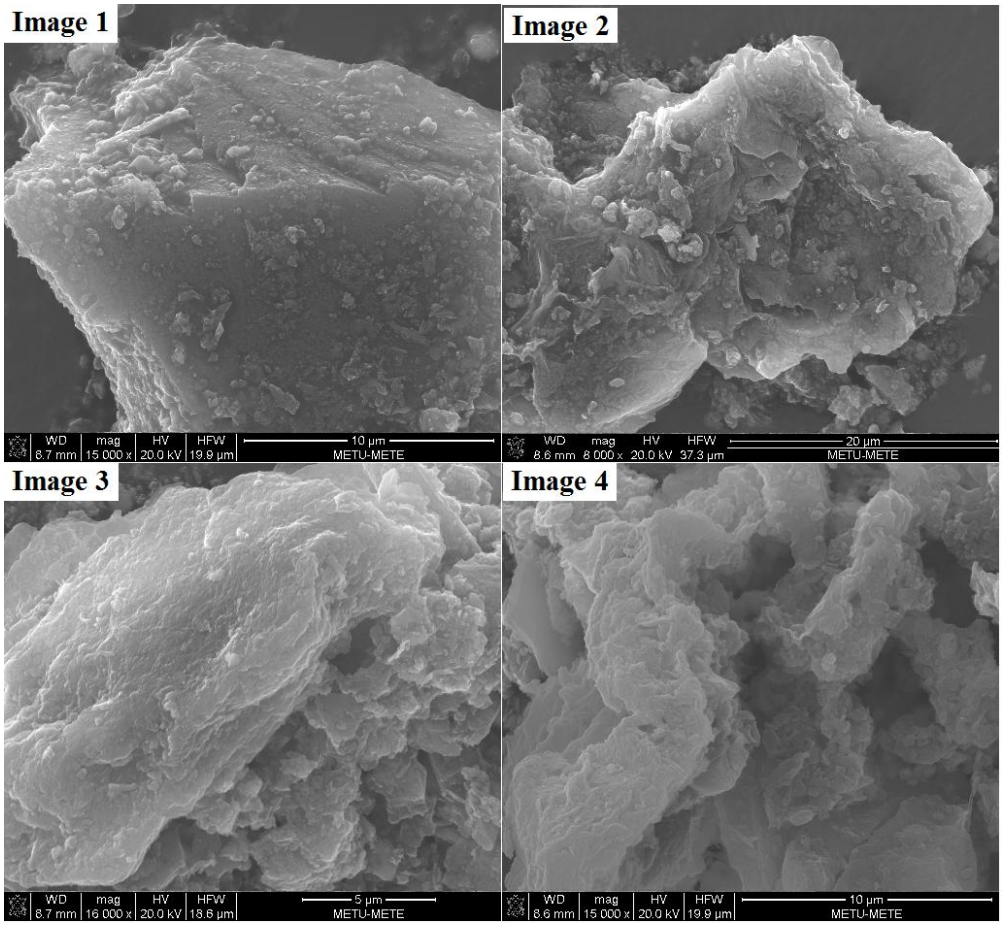

Figure 39: Several SEM images taken from the leach residue obtained from the experiment conducted at the optimum conditions

The major phases found in the X-ray analysis were quartz and hematite which were also identified in SEM by EDS analysis. However the quartz phase was so dominant in the leach residue that all the hematite phases found were covered with silica.

In images 1 and 2 pure silica particles are seen in Figure 39. The particle on image 1 has distinct cut edges; however the surface was not very smooth due to the agglomerations on it. Hematite mineral with aluminum was identified in image 3. Hematite was also identified in image 4 with arsenic and aluminum contents. Although the extraction efficiencies of chromium were not very high no trace of chromium could be found. Nickel and cobalt could not be detected in the leach residue which was expected. EDS results of corresponding images are given in Appendix C.

4.2 Downstream Experiments

4.2.1 Iron Removal by MgO

The main aim in these experiments was to determine the optimum pH level to precipitate the iron as much as possible, since it was the main impurity with the highest quantity in the PLS. Aluminum and chromium precipitation values were also tried to be maximized, while keeping the nickel and cobalt losses at minimum. MgO was used as a neutralizing and precipitating agent. The stock of prepared PLS obtained at the optimum conditions were used in iron removal experiments. The experiments were conducted at 95°C, and 2 h fixed conditions. The stirring speed was also fixed at 650 rpm to obtain a fast agitation to decrease the Ni and Co losses due to increase in local pH upon MgO addition as slurry.

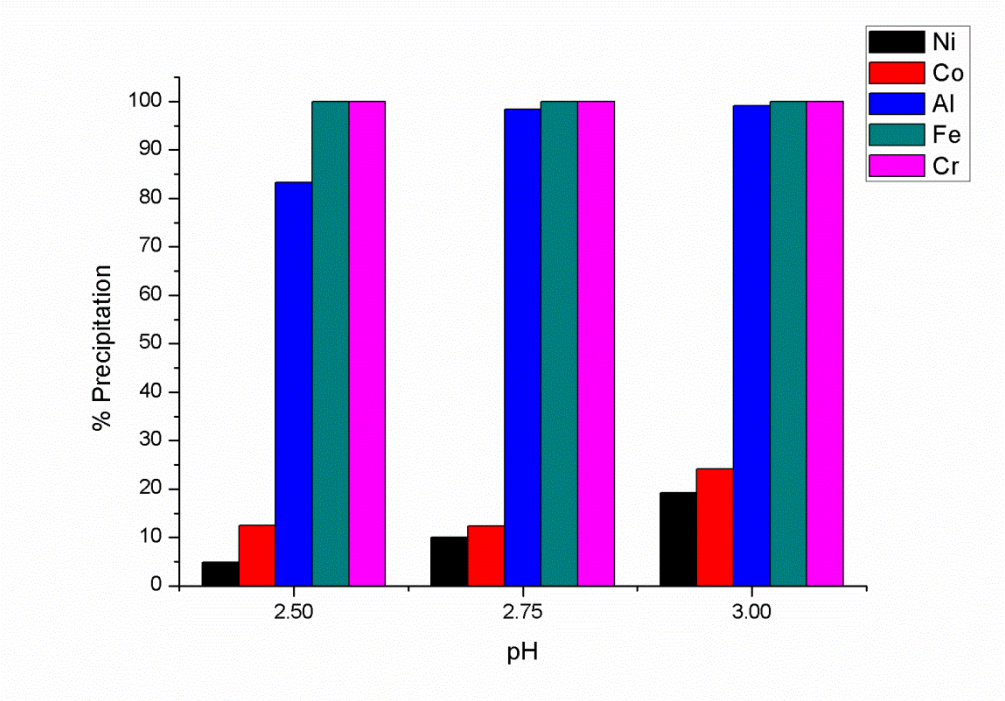

Figure 40: Precipitation of important metals versus equilibrium pH at 95°C and 120 minutes fixed conditions

Precipitation percentages were calculated using the analyses of PLS and solid precipitation product. The results were double checked by calculations from the ICP results of the purified solution. As seen from Figure 40, regardless of the pH used all the iron and chromium were precipitated in all three of the experiments. However, there was an increasing trend in Ni, Co and Al precipitations with the increasing pH. Nickel and cobalt losses were at minimum at pH=2.50, where only 4.8% of Ni and 12.5% of Co were precipitated. While the Al precipitation became higher at pH=2.75, much more nickel was also lost. Since the recovery of precipitated nickel and cobalt at this stage is not possible, the optimum pH was determined as 2.50 for the iron precipitation experiments. Nickel and cobalt losses most likely have occurred due to sharp regional increase in the pH where the MgO slurry was dripped.

Precipitation percentages of some elements are given in Table 20.

Table 20: Precipitation values of important elements in the iron removal

Element	Precipitation %	Element	Precipitation %
Ni	4.8	As	71.1
Co	12.5	Cu	44.9
Fe	100	Mn	26.4
Al	83.4	Sc	100
Cr	100		

Scandium was also precipitated totally and lost in this iron removal step. A by-product scandium recovery step was needed before iron removal experiments to recover the scandium present in the PLS.

4.2.1.1 XRD Examination of Iron Removal Precipitate

XRD patterns of precipitates obtained from the iron precipitation experiments conducted at pH=2.50, pH=2.75 and pH=3.00 are given in Figure 41.

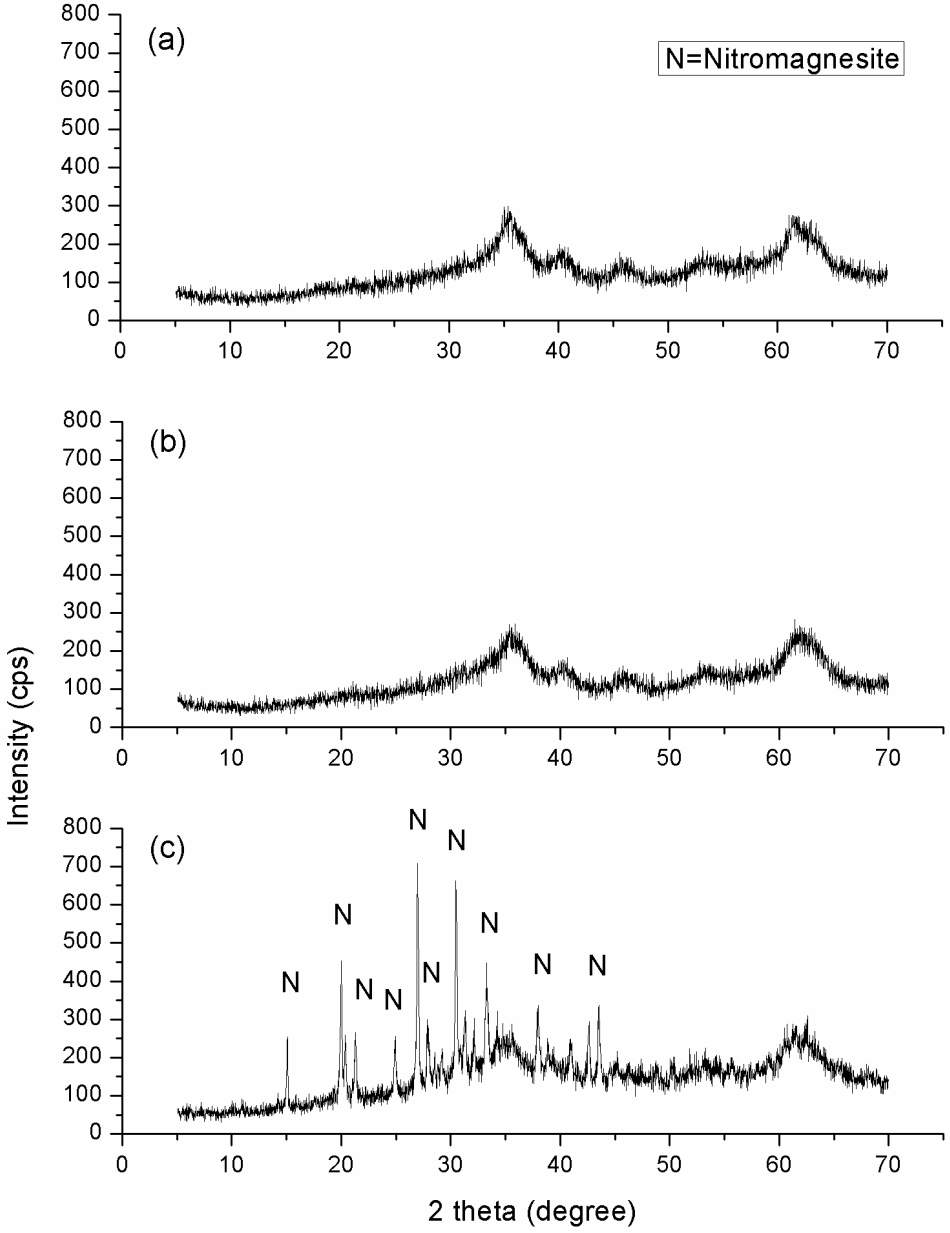

Figure 41: XRD patterns of solid precipitates at pH=2.50 (a), pH=2.75 (b), pH=3 (c)

The intensities of the peaks were small and the peak widths were very large, so no distinct peak could be identified from the XRD patterns of the solid residues of iron precipitation experiments conducted at pH=2.50 and pH=2.75. The crystalline structure of the phases might not have been well developed, or the grain size of the precipitates might have caused this broadening of the peaks.

Nitromagnesite was the only crystalline phase which could be identified within the residue of iron precipitation experiment conducted at pH=3.00. Nitromagnesite has a formula of $Mg(NO_3)_2.6H_2O$. The solubility of magnesium nitrate is very high in water, which was probably the main reason that it was not detected in the residues obtained at pH=2.5 and pH=2.75. The precipitation of nitromagnesite at pH=3.00 most probably occurred due to its oversaturation in the solution [86].

Since not much information could be obtained from the XRD patterns of the precipitates, it was decided to further analyze the precipitates under SEM to obtain better results.

4.2.1.2 SEM Examination of Iron Removal Precipitate

Goethite is the mineral that was expected to precipitate at 95°C, according to the literature. The expected equation for iron precipitation is given below:

$$2Fe(NO_3)_3 + 3MgO + H_2O = 2FeO(OH) + 3Mg(NO_3)_2 \qquad \text{Rx. 4.1}$$

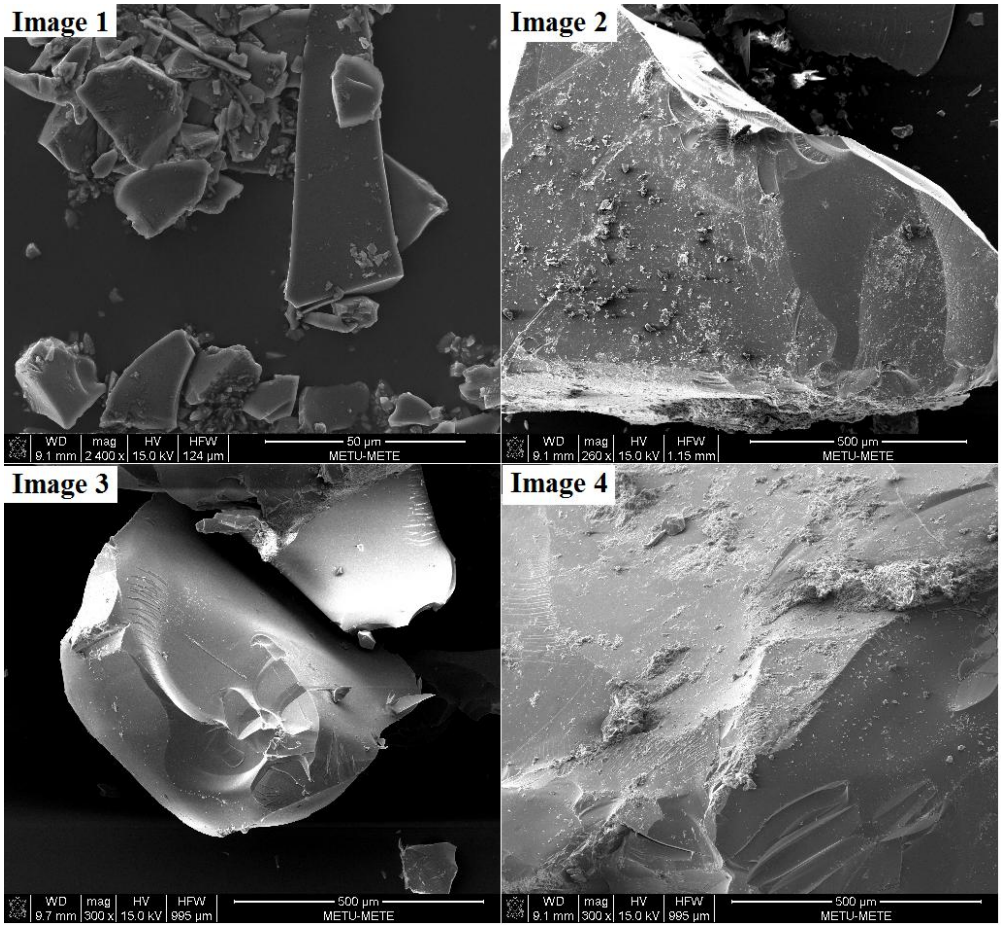

Figure 42: SEM images from iron precipitation experiment with pH= 2.50

All of the particles are iron precipitates which can also be characterized by their sharp and clear cut edges in the general view given in image 1 in Figure 44. In image 2, a goethite particle with aluminum, chromium and arsenic content was observed. In image 3, another goethite particle with a shiny surface was seen. Chromium, aluminum and arsenic were also found in the EDS results of this particle. Another goethite particle was found in image 4. EDS results of the corresponding images are given in Appendix C.

4.2.2 Autoclave Hydrolysis of Iron

It was decided to start the autoclave hydrolysis of iron at 180°C with 3 h of duration experiments. The first experiment was with original PLS from the stock with δ=1.3 g/cc. The experiment was initiated with 250 cc PLS and the reasonable precipitation of iron was not achieved.

PLS of the second experiment was concentrated by evaporation at its boiling point and density of the solution was increased up to 1.6 g/cc. To obtain a 250 cc PLS with δ=1.6 g/cc, 700 cc of PLS from the stock was used. Since the PLS stock contained 61 g/L of iron, its 250 cc of concentrated PLS was expected to embody 43 grams of iron.

The same experiment was repeated with the concentrated PLS and the iron precipitated was found to be 56.3 wt% of the precipitate. Assuming that it precipitated as hematite, therefore 80.4 wt% of the precipitate consisted of iron oxide. Nickel was found to be 0.069% in the precipitate. Although the compositions of the iron and nickel in the precipitate were at the desired levels, the amount of solid precipitate was less than 15 grams. Knowing that the PLS initially contained 43 grams of iron, the resulting iron precipitation values were much lower than the desired levels. A possible reason behind this unsatisfactory precipitation levels might be due to the equipment used. The cooling rate of the stainless steel autoclave was very slow and the reaction vessel was immovable, therefore the cooling of the PLS took up to 12 h after the experiment.

CHAPTER 5

CONCLUSIONS

Throughout the course of this study, the leachability of lateritic nickel ores from Gördes/Manisa open pit mine was studied with atmospheric nitric acid leaching. The optimum conditions for highest nickel and cobalt extractions were determined and purification of the PLS by iron precipitation was practiced. Several characterization methods were used on the ore to determine its characteristics and to predict its leaching behavior. Throughout the experimental examinations, various process parameters were tested with the intention of getting the best extraction percentages. The summary of the obtained results are below:

- Chemical characterization of Gördes ore samples showed that the limonite had 1.28% nickel and 0.083% cobalt together with 28.70% iron, 0.68% arsenic, 3.09% aluminum, 1.36% magnesium, 1.36% chromium and 28.80% SiO_2. On the other hand, the nontronite had 1.20% nickel and 0.068% cobalt together with 15.95% iron, 0.02% arsenic, 2.80% aluminum, 4.15% magnesium 0.36% chromium and 44.90% SiO_2.
- Particle size analysis of limonite showed that 42.9% of this ore sample was below 38 μm. Particle size analysis of nontronite showed that 40.2% of this ore sample was below 38 μm.

- XRD and DTA-TGA examinations of the original run-of-mine ores revealed that the major minerals present were goethite, quartz, hematite and minor mineral was serpentine. SEM-EDS examinations have shown that the nickel was found within mainly in the crystal structures of goethite and hematite.

- The theoretical nitric acid consumption calculations based on the chemical ore compositions indicated that 1282 kg/ton of dry ore was needed for AL experiments for an ore mixture of 70% limonite and 30% nontronite.

- The optimum conditions for atmospheric leaching experiments were 104 ^{o}C leaching temperature, 48 h leaching duration, 378 g/L of nitric acid concentration, 100% -600 μm particle size, 1/5 wt/vol solid/liquid ratio and 500 rpm stirring speed.

- At the optimum conditions, the average extraction efficiencies were; 95.4% Ni, 96.6% Co, 78.8 % Fe, and 89.4% Al.

- In the XRD examinations of leach residues of agitated leaching experiments quartz and hematite were identified as the major phases and goethite was found as a minor phase.

- According to the SEM investigations, all of the major phases determined by XRD were found in the images and confirmed by EDS analyses which were found in atmospheric HNO_3 leach residues.

- The optimum conditions for the iron removal experiments by MgO was found as 95°C, 120 minutes of experimental duration, and pH=2.50. Under these selected conditions, 100% Fe, 83.4% Al, 100% Cr, 4.8% Ni, 12.5% Co were precipitated from the pregnant leach solution. The experiments for iron precipitation by thermal hydrolysis were unsuccessful. Expected amount of iron could not be precipitated.

Recommendations for Future Studies

Although lower pH values than 2.50 were not seen sufficient by the literature, lower pH can also be studied by increasing the duration time of iron precipitation experiments by using a reagent, to decrease the nickel and cobalt losses.

Thermal hydrolysis can be studied in an autoclave with a faster cooling rate. Reagents can be added to increase precipitation values.

REFERENCES

1. *International Nickel Study Group, "Production, Usage and Prices*. [cited 2014 15.08]; Available from: http://www.insg.org/prodnickel.aspx.

2. *London Metal Exchange, Nickel.* [cited 2014 15.08]; Available from: http://www.lme.com/en-gb/metals/non-ferrous/nickel/.

3. Dalvi, A.D., Bacon, W.G., Osborne, R.C., *The Past and the Future of Nickel Laterites*, in *PDAC International Convention*. 2004: Ontario, Canada. p. 1-27.

4. McDonald, R.G. and B.I. Whittington, *Atmospheric acid leaching of nickel laterites review: Part I. Sulphuric acid technologies.* Hydrometallurgy, 2008. 91(1–4): p. 35-55.

5. Piret, N.L., *Enhancing cobalt recovery from primary and secondary resources.* JOM, 1998. 50(10): p. 42-43.

6. Willis, B., *Downstream Processing Options for Nickel Laterite Heap Leach Liquors*, in *ALTA*. 2007: Perth, Australia.

7. Guise L., Castro, F., *Iron, aluminum and chromium co-elimination by hydrolytic precipitation from nickel and cobalt containing sulfuric acid solutions*. Iron Control and Disposal, ed. H.G.B. Dutrizac J. E. 1996: The Canadian Institute of Mining.

8. Shang, Y. and van Weert, G., *Iron control in nitrate hydrometallurgy by autoclave hydrolysis of iron(III) nitrate.* Hydrometallurgy, 1993. 33(3): p. 273-290.

9. *International Nickel Study Group, "What is Nickel"*. Available from: http://www.insg.org/whatnickel.aspx.

10. Kerfoot, D.G.E., *Nickel:*, in *Ullmann's Encyclopedia of Industrial Chemistry*. 2005, Wiley Interscience. p. 1-63.

11. Boldt, J.R., *The Winning of Nickel*. 1967, London: Methuen & Co. Ltd. E.C.4.

12. *Mineral Commodity Summaries*. 2014, U.S. Geological Survey.

13. Canterford, J.H., *Mineralogical aspects of the extractive metallurgy of nickeliferous laterites*, in *Proceedings of the Australasian Institute of Mining and Metallurgy Conference. Australasian Institute of Mining and Metallurgy*. 1978: Melbourne. p. 361–370.

14. *The map showing major Nickel Producing Countries in World*. [cited 2014 07.08]; Available from: www.mapsofworld.com.

15. Mudd, G.M., *Nickel Sulfide Versus Laterite: The Hard Sustainability Challenge Remains*. in *48th Annual Conference of Metallurgists - Pyrometallurgy of Nickel and Cobalt*. 2009. Sudbury, Ontario, Canada: Canadian Metallurgical Society.

16. Mudd, G.M., *Global trends and environmental issues in nickel mining: Sulfides versus laterites.* Ore Geology Reviews, 2010. **38**(1–2): p. 9-26.

17. *Nikel Raporu*. 2012, TMMOB Maden Mühendisleri Odası.

18. *Meta Nikel [Online]*. [cited 2014 11.08]; Available from: http://www.metanikel.com.tr/tr/gordes-nikel-isletmesi.

19. Bide T., Hetherington, L., Gunn G., *Definition, Mineralogy and Deposits*, in *British Geological Survey*. 2008.

20. Whittington, B.I. and D. Muir, *Pressure Acid Leaching of Nickel Laterites: A Review.* Mineral Processing and Extractive Metallurgy Review, 2000. 21(6): p. 527-599.

21. Marsh, E., Anderson, E., Gray, F.,, *Nickel-cobalt laterites—A deposit model*, in *U.S. Geological Survey Scientific Investigations Report*. 2013.

22. Brand, N.W., Butt, C.R.M., and Elias, M., *Nickel laterites: Classification and features.* AGSO Journal of Australian Geology and Geophysics, 1998. **17**(4): p. 81-88.

23. *Direct Nickel Process*. 10.08.2014]; Available from: http://www.directnickel.com/category/process/.

24. Kyle, J., *Nickel Laterite Processing Technologies: Where to Next?*, in *ALTA*. 2010: Perth, Australia.

25. Taylor, A., *Technical & Cost Comparison of Laterite Treatment Processes*, in *ALTA*. 2014: Perth, Australia.

26. Willis, B., *Developments And Trends in Hydrometallurgical Processing of Nickel Laterites*, in *ALTA*. 2012: Perth, Australia.

27. John Reid, S.B., *Nickel Laterite Hydrometallurgical Processing Update*, in *ALTA*. 2002, BHP Billiton, Stainless Steel Materials.

28. Georgiou, D. and Papangelakis, V.G., *Sulphuric acid pressure leaching of a limonitic laterite: chemistry and kinetics.* Hydrometallurgy, 1998. 49(1–2): p. 23-46.

29. Önal, M.A.R., *Pressure Leaching Of Çaldağ Lateritic Nickel Ore*. 2013, MIDDLE EAST TECHNICAL UNIVERSITY: Ankara.

30. Balıklı, İ., *Gördes Nikel Madeni Projesi*.

31. *Mining Journal, Turkey Supplement*. 2013.

32. Korkmaz, K., *Comparative Study of High Pressure and Atmospheric Acid Leaching for the Extraction of Nickel and Cobalt from Refractory Nickel Laterite Ores*. 2014, Middle East Technical University: Ankara.

33. Queneau, P.B. and Chou, E.C., *Sulfuric acid leaching of nickeliferous laterite*. 1977, Google Patents.

34. Ma, B., et al., *Selective pressure leaching of Fe (II)-rich limonitic laterite ores from Indonesia using nitric acid.* Minerals Engineering, 2013. 45(0): p. 151-158.

35. Ma, B., Wang. C., Yang, W., Yang, B., Yin, F., Chen, Y., Yang. Y., *Pilot Plant Study on the Nitric Acid Pressure Leaching Technology for Limonitic Laterite Ores*. in *Ni-Co 2013*. 2013. 2013 TMS Annual Meeting & Exhibition.

36. Agatzini-Leonardou, S., Tsakiridis, P. E., Oustadakis, P., Karidakis, T., Katsiapi, A., *Hydrometallurgical process for the separation and recovery of nickel from sulphate heap leach liquor of nickeliferrous laterite ores.* Minerals Engineering, 2009. **22**(14): p. 1181-1192.

37. Queneau, P.B., et al., *Easy descaling of water-soluble magnesium sulfate-hematite*. 1983, Google Patents.

38. Agatzini, S. and Dimaki, D., *Recovery of nickel and cobalt from low-grade nickel oxide ores by heap leaching with dilute sulphuric acid at room temperature.* Greek patent, 1991. 910100234: p. 31.

39. Oxley A., Sırvancı N., Purkiss S., *Çaldağ Nickel Laterite Atmospheric Heap Leach Project.* Association of Metallurgical Engineers of Serbia, 2007.

40. Agatzini-Leonardou, S., Dimaki, D.,, *Recovery of Nickel and Cobalt from Lowgrade Nickel Oxide Ores by the Technique of Extraction in Heaps Using Dilute Sulphuric Acid at Ambient Temperature*. 1994: Greek Patent.

41. Willis, B., *Atmospheric Tank Leach Flowsheet Development for the Çaldağ Nickel Project in Western Turkey*, in *ALTA*. 2014: Perth, Australia.

42. Liu, H. and Miller, G.W., *Process for recovery of nickel and cobalt by heap leaching of low grade nickel or cobalt containing material*. 2005, Google Patents.

43. Duyvesteyn, W.P.C., Liu, H., Davis, M.J., *Heap leaching of nickel containing ore*. 2001, Google Patents.

44. Liu, H., *An improved process for heap leaching of nickeliferous oxidic ores*. 2006, Google Patents.

45. Purkiss, S.A.R., *Heap leaching base metals from oxide ores*. 2005, Google Patents.

46. Panagiotopoulos N., Agatzini, S., Kontopoulos A., *Extraction of nickel and cobalt from serpentinic type laterites by atmospheric pressure sulfuric acid leaching*, in *115th TMS-AIME Annual Meeting*. 1986: New Orleans.

47. Pereira, G., Gobbo, O., *Process for extraction of nickel, cobalt, and other base metals from laterite ores by using heap leaching and product containing nickel, cobalt, and other metals from laterite ores*. 2007, Google Patents.

48. Readett, D.J., Fox, J., *Development of Heap Leaching and Its Integration into the Murrin Murrin Operations*, in *ALTA*. 2009: Perth, Australia.

49. Apostolidis, C.I. and Distin, P.A., *The kinetics of the sulphuric acid leaching of nickel and magnesium from reduction roasted serpentine*. Hydrometallurgy, 1978. 3(2): p. 181-196.

50. Canterford, J.H., *Leaching of some Australian nickeliferous laterites with sulphuric acid at atmospheric pressure*, in *Proceedings of the Australasian Institute ofMining andMetallurgy*. 1978. p. 19–26.

51. Panagiotopoulos N., Kontopoulos, A., *Atmospheric Pressure Sulfuric Acid Leaching of Low–Grade Hematitic Laterites*. Extractive Metallurgy of Nickel & Cobalt, ed. L.C.A. Tyroler G.P. 1988.

52. Curlook, W., *Direct atmospheric leaching of highly-serpentinized saprolitic nickel laterite ores with sulphuric acid*. 2002, Google Patents.

53. Das, G.K., Anand, S., Das, R.P., Muir, D.M., Senanayake, G., Singh, P., Hefter, G.,, *Acid leaching of nickel laterites in the presence of sulphur dioxide at atmospheric pressure.* Hydrometallurgy and Refining of Nickel and Cobalt, 1997. 1: p. 471-488.

54. Senanayake, G. and Das, G.K., *A comparative study of leaching kinetics of limonitic laterite and synthetic iron oxides in sulfuric acid containing sulfur dioxide.* Hydrometallurgy, 2004. **72**(1–2): p. 59-72.

55. Das, G.K., Lange, A., Li, J.I., Robinson, D.J., *Superior Atmospheric Leaching of Various West Australian Laterites in The Presence of Sulphur Dioxide*, in *ALTA*. 2010: Perth, Australia.

56. Verbaan, N., Sist, F., Mackie, S., Todd, I., *Development and piloting of Skye Resources atmospheric leach (SAL) process at SGS Minerals*, in *ALTA Nickel/Cobalt*. 2007.

57. O'Neill, C.E., *Leaching nickeliferous silicate ores with hydrochloric acid*. 1978.

58. Girgin, İ., Obut, A., and Üçyildiz, A., *Dissolution behaviour of a Turkish lateritic nickel ore.* Minerals Engineering, 2011. **24**(7): p. 603-609.

59. Büyükakinci, E., *Extraction of Nickel from Lateritic Ores*. 2008, Middle East Technical University.

60. Büyükakinci, E. and Topkaya, Y.A., *Extraction of nickel from lateritic ores at atmospheric pressure with agitation leaching.* Hydrometallurgy, 2009. 97(1–2): p. 33-38.

61. Taylor, A., *Future Trends in PAL Plant Design for Ni/Co Laterites*, in *ALTA*. 2000: Perth, Australia.

62. Arroyo, J.C., et al., *Method for leaching nickeliferous laterite ores*. 2002, Google Patents.

63. Norgate, T. and Jahanshahi, S., *Reducing the greenhouse gas footprint of primary metal production: Where should the focus be?* Minerals Engineering, 2011. 24(14): p. 1563-1570.

64. McDonald, R.G. and Whittington, B.I., *Atmospheric acid leaching of nickel laterites review. Part II. Chloride and bio-technologies.* Hydrometallurgy, 2008. 91(1–4): p. 56-69.

65. Li, J., et al., *Physicochemical factors affecting leaching of laterite ore in hydrochloric acid.* Hydrometallurgy, 2012. 129–130(0): p. 14-18.

66. Griffin A., Nofal P., Johnson G., Evans H., *Laterites – Squeeze or Ease?*, in *ALTA Nickel/Cobalt*. 2002.

67. Chander, S., *Atmospheric Pressure Leaching of Nickeliferous Laterites in Acidic Media.* Transactions of the Indian Institute of Metals, 1982. 35,(4): p. 366–371.

68. Harris, B., White, C., *Recent Developments in the Chloride Processing of Nickel Laterites*, in *ALTA Ni-Co*. 2011: Perth, Australia.

69. Drinkard, W.F., *Nickel-laterite process*. 2011, Google Patents.

70. Drinkard, W.F., *Nitric acid production and recycle*. 2001, Google Patents.

71. McCarthy, F., G.B. *Breaking New Ground*. in *ALTA*. 2013. Perth, Australia.

72. McCarthy, F., Brock, G., *The Direct Nickel Process Continued Progress on the Pathway to Commercialisation*, in *ALTA*. 2011: Perth, Australia.

73. Dry M., Harris, B., *Nickel Laterite and the Three Mineral Acids*, in *ALTA*. 2012: Perth, Australia.

74. McCarthy, F., Brock,G., *Test Plant Program 2013 in Review*. in *ALTA*. 2014. Perth, Australia.

75. Chang, Y., Zhai. X., Li, B., Fu, Y., *Removal of iron from acidic leach liquor of lateritic nickel ore by goethite precipitate.* 2010(101): p. 84–87.

76. Willis, B., *Trends in PAL Downstream Recovery Options*, in *ALTA*. 2008: Perth, Australia.

77. Kaya, Ş., *High Pressure Acid Leaching Of Turkish Laterites*. 2011, Middle East Technical University: Ankara.

78. Landers, M. and Gilkes, R.J., *Dehydroxylation and dissolution of nickeliferous goethite in New Caledonian lateritic Ni ore.* Applied Clay Science, 2007. 35(3–4): p. 162-172.

79. López, F.A., et al., *Kinetic study of the thermal decomposition of low-grade nickeliferous laterite ores.* Journal of Thermal Analysis and Calorimetry, 2008. 94(2): p. 517-522.

80. Kowalski, J.S., *Thermal aspects of temperature transformations in silica sand.* Archives of Foundry Engineering, 2010: p. 111-114.

81. Földvári, M., *Handbook of Thermogravimetric System of Minerals and Its Use in Geological Practice*. 2011: Geological Institute of Hungary.

82. Landers, M., R.J. Gilkes, and M. Wells, *Dissolution kinetics of dehydroxylated nickeliferous goethite from limonitic lateritic nickel ore.* Applied Clay Science, 2009. 42(3–4): p. 615-624.

83. Göveli, A., *Nickel Extraction from Gördes Laterites by Hydrocloric Acid Leaching*. 2006, M.Sc Thesis in Department of Mining Engineering, Middle East Technical University: Ankara.

84. Canterford, J.H., *Acid leaching of chromite-bearing nickeliferous laterite from Rockhampton, Queensland.* . Proceedings of the Australasian Institute of Mining and Metallurgy, 1986: p. 51-56.

85. Liu, K., Chen, Q., Hu, H., *Comparative leaching of minerals by sulphuric acid in a Chinese ferruginous nickel.* Hydrometallurgy, 2009: p. 281-286.

86. *Magnesium nitrate*. [cited 2014 10.08]; Available from: ttp://en.wikipedia.org/wiki/Magnesium_nitrate.

APPENDIX A

The thoretical nitric acid consumption of metals present in the lateritic ore was calculated by assuming as if all the metals were present in their oxide form and 100% of them were extracted into the pregnant leach solution. Corresponding chemical reactions between the ideal metal oxides and HNO_3 are given in Reaction A.1, where M denotes the metals present in the lateritic nickel ore, x and y denote their corresponding stoichiometric coefficints. The theoretical amount of HNO_3 required for the reaction is given in Equation A.2. It is assumed that 0.7 and 0.3 are the fractions of the limonite and the nontronite in the ore mixture, respectively.

$$M_xO_y + 2yHNO_3 = xM(NO_3)_y + yH_2O \quad \text{(A.1)}$$

HNO_3 consumed by a metal oxide (kg/ ton of ore) =

$$\left[\frac{(\text{MxOy \% in limonite} \times 0.7)+(\text{MxOy \% in nontronite} \times 0.3)}{100} \times \frac{2y \times MW\text{HNO3}}{MWMxOy} \times 1000\right] \quad \text{(A.2)}$$

Theoretical HNO_3 consumption of iron oxide per ton of 70% limonitic and 30% nontronitic ore mixture:

$$Fe_2O_3 + 6HNO_3 = 2Fe(NO_3)_3 + 3H_2O \quad \text{(A.3)}$$

$$\left[\frac{(41.03 \times 0.7)+(22.80 \times 0.3)}{100} \times \frac{6 \times 63}{159.7} \times 1000\right] = 841.71 \quad \text{(A.4)}$$

Theoretical HNO_3 consumption of aluminum oxide per ton of 70% limonitic and 30% nontronitic ore mixture:

$$Al_2O_3 + 6HNO_3 = 2Al(NO_3)_3 + 3H_2O \quad \text{(A.5)}$$

$$\left[\frac{(5.83\times0.7)+(4.17\times0.3)}{100}\times\frac{6\times63}{101.96}\times 1000\right] = 197.68 \quad \text{(A.6)}$$

Theoretical HNO_3 consumption of nickel oxide per ton of 70% limonitic and 30% nontronitic ore mixture:

$$NiO + 2HNO_3 = Ni(NO_3)_2 + H_2O \quad \text{(A.7)}$$

$$\left[\frac{(1.63\times0.7)+(1.53\times0.3)}{100}\times\frac{2\times63}{74.69}\times 1000\right] = 26.99 \quad \text{(A.8)}$$

Theoretical HNO_3 consumption of cobalt oxide per ton of 70% limonitic and 30% nontronitic ore mixture:

$$CoO + 2HNO_3 = Co(NO_3)_2 + H_2O \quad \text{(A.9)}$$

$$\left[\frac{(0.11\times0.7)+(0.06\times0.3)}{100}\times\frac{2\times63}{74.93}\times 1000\right] = 1.60 \quad \text{(A.10)}$$

Theoretical HNO_3 consumption of chromium oxide per ton of 70% limonitic and 30% nontronitic ore mixture:

$$Cr_2O_3 + 6HNO_3 = 2Cr(NO_3)_3 + 3H_2O \quad \text{(A.11)}$$

$$\left[\frac{(1.99\times0.7)+(0.99\times0.3)}{100} \times \frac{6\times63}{152} \times 1000\right] = 42.03 \quad \text{(A.12)}$$

Theoretical HNO_3 consumption of manganese oxide per ton 70% limonitic and 30% nontronitic ore mixture:

$$MnO + 2HNO_3 = Mn(NO_3)_2 + H_2O \quad \text{(A.13)}$$

$$\left[\frac{(0.59\times0.7)+(0.34\times0.3)}{100} \times \frac{2\times63}{70.94} \times 1000\right] = 9.15 \quad \text{(A.14)}$$

Theoretical HNO_3 consumption of magnesium oxide per ton of 70% limonitic and 30% nontronitic ore mixture:

$$MgO + 2HNO_3 = Mg(NO_3)_2 + H_2O \quad \text{(A.15)}$$

$$\left[\frac{(2.25\times0.7)+(6.88\times0.3)}{100} \times \frac{2\times63}{40.30} \times 1000\right] = 113.78 \quad \text{(A.16)}$$

Theoretical HNO_3 consumption of calcium oxide per ton of 70% limonitic and 30% nontronitic ore mixture:

$$CaO + 2HNO_3 = Ca(NO_3)_2 + H_2O \text{ (A.17)} \qquad \text{(A.17)}$$

$$\left[\frac{(1.27\times0.7)+(2.15\times0.3)}{100}\times\frac{2\times63}{56.08}\times1000\right] = 34.47 \qquad \text{(A.18)}$$

Theoretical HNO_3 consumption of potassium oxide per ton of 70% limonitic and 30% nontronitic ore mixture:

$$K_2O + 2HNO_3 = 2KNO_3 + H_2O \qquad \text{(A.19)}$$

$$\left[\frac{(0.12\times0.7)+(0.12\times0.3)}{100}\times\frac{2\times63}{94.20}\times1000\right] = 1.61 \qquad \text{(A.20)}$$

Theoretical HNO_3 consumption of copper oxide per ton of 70% limonitic and 30% nontronitic ore mixture:

$$CuO + 2HNO_3 = Cu(NO_3)_2 + H_2O \qquad \text{(A.21)}$$

$$\left[\frac{(0.04\times0.7)+(0.01\times0.3)}{100}\times\frac{2\times63}{79.55}\times1000\right] = 0.49 \qquad \text{(A.22)}$$

Theoretical HNO_3 consumption of zinc oxide per ton of 70% limonitic and 30% nontronitic ore mixture:

$$ZnO + 2HNO_3 = Zn(NO_3)_2 + H_2O \quad \text{(A.23)}$$

$$\left[\frac{(0.04\times0.7)+(0.03\times0.3)}{100}\times\frac{2\times63}{81.41}\times 1000\right] = 0.57 \quad \text{(A.24)}$$

Theoretical HNO_3 consumption of arsenic oxide per ton of 70% limonitic and 30% nontronitic ore mixture:

$$As_2O_3 + 6HNO_3 = 2As(NO_3)_3 + 3H_2O \quad \text{(A.25)}$$

$$\left[\frac{(0.90\times0.7)+(0.03\times0.3)}{100}\times\frac{6\times63}{197.84}\times 1000\right] = 12.21 \quad \text{(A.26)}$$

Total=1282.29 kg nitric acid / ton of dry ore

APPENDIX B

Metal extraction values based on the solid based calculations were obtained using the equation below:

$$\text{Extraction\% of M} = \left[1 - \frac{Leach\ Residue\ Weight \times \%\ M\ in\ Leach\ Residue}{Ore\ Feed\ Weight \times \%\ M\ in\ Ore\ Feed}\right] \times 100 \quad \text{(B.1)}$$

Metal extraction values based on the pregnant leach solution based calculations were obtained using the equation below:

$$\text{Extraction\% of M} = \left[\frac{PLS\ volume \times M\left(\frac{mg}{L}\right)\ in\ PLS}{Ore\ Feed\ Weight \times \%\ M\ in\ Ore\ Feed}\right] \times 100 \quad \text{(B.2)}$$

Metal precipitation values from the pregnant leach solution were obtained using the equation:

$$\text{Precipitation\% of M} = \left[\frac{(Initial\ \ PLS\ volume \times Initial\ M\%) - (Final\ PLS\ volume \times Final\ M\%)}{Initial\ \ PLS\ volume \times Initial\ M\%}\right] \times 100 \quad \text{(B.3)}$$

APPENDIX C

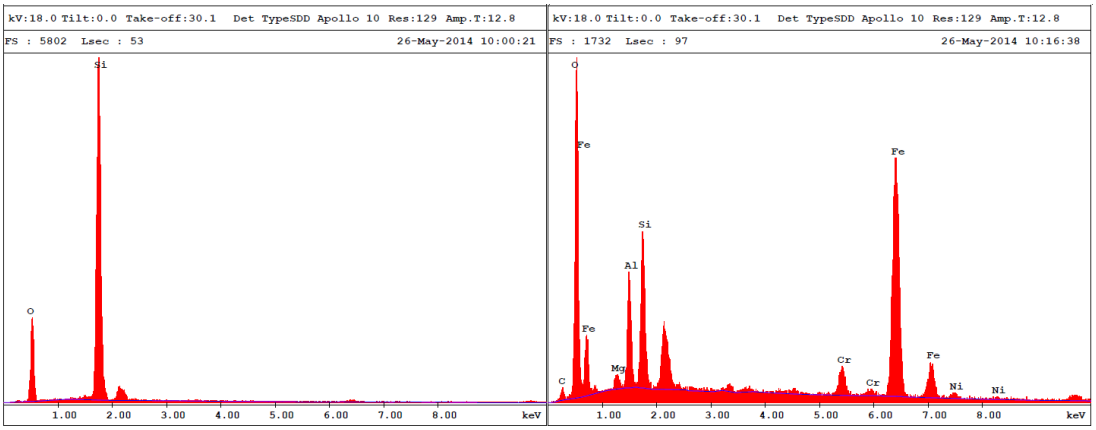

Figure 43: EDS results of images 1 and 2 in Figure 22 (pure crystalline silica and hematite with aluminum)

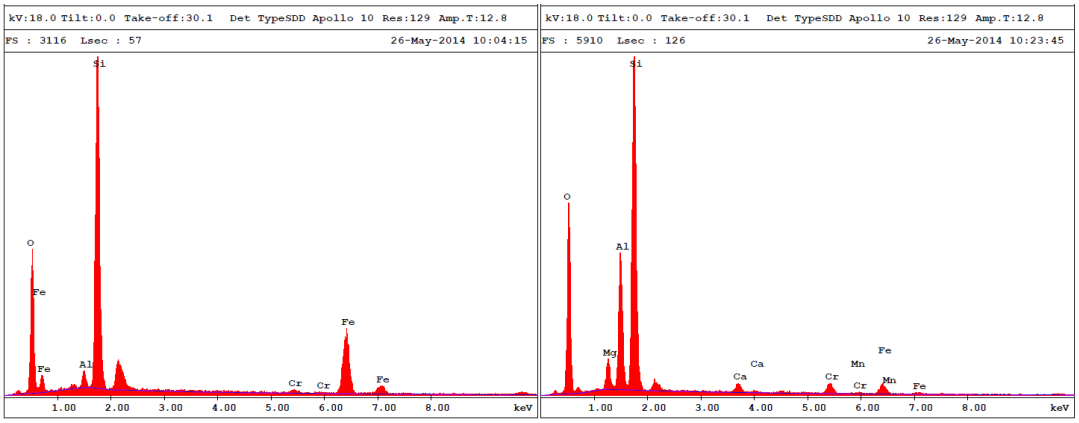

Figure 44: EDS results of images 3 and 4 in Figure 22 (silica covered goethite and alumina with silica)

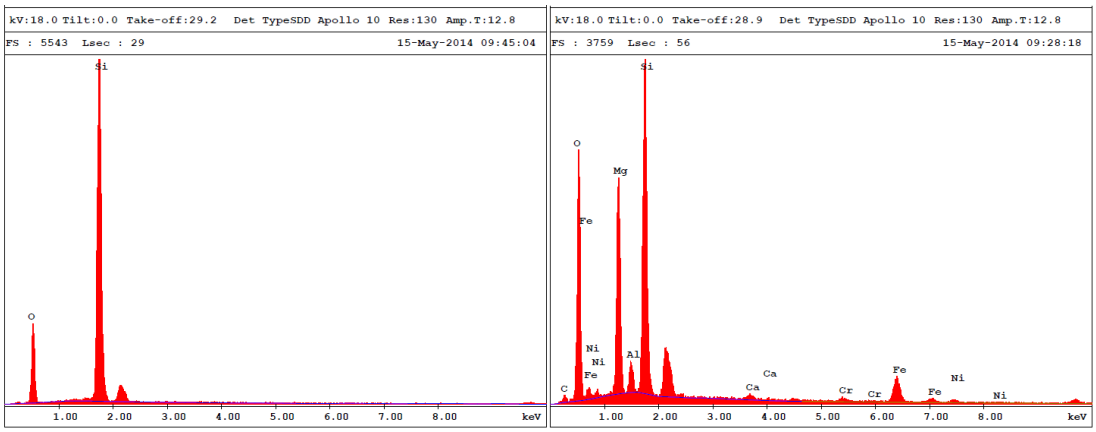

Figure 45: EDS results of images 1 and 2 in Figure 23 (pure crystalline silica and serpentine with magnesium)

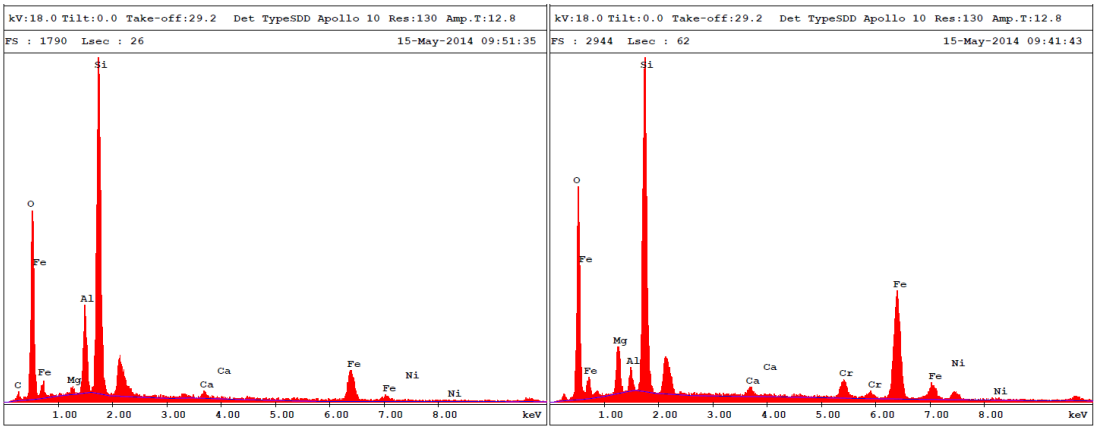

Figure 46: EDS results of images 3 and 4 in Figure 23 (goethite with aluminum,covered with silica and hematite with nickel)

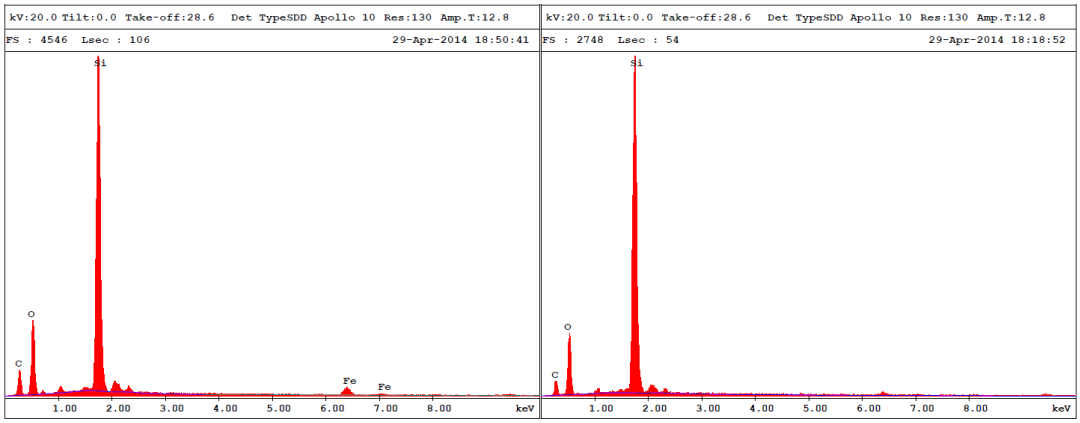

Figure 47 : EDS results of images 1 and 2 in Figure 39 (pure silica particles)

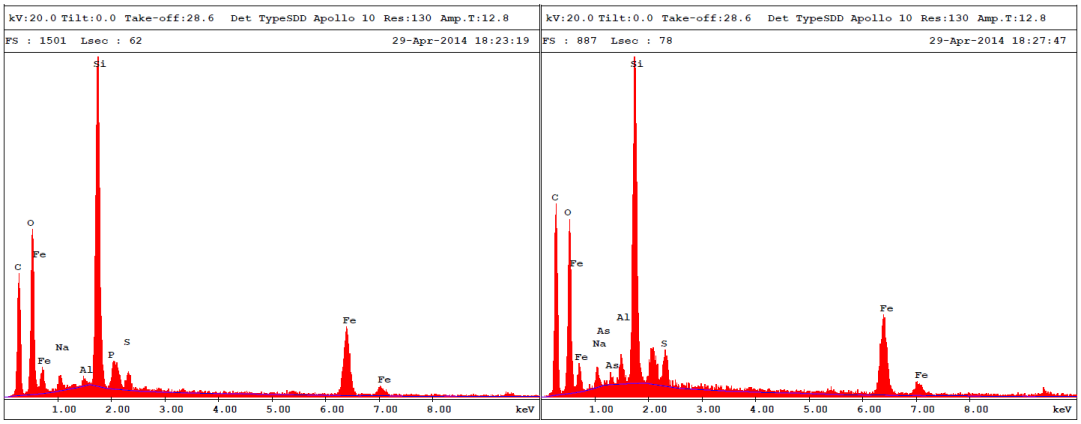

Figure 48: EDS results of images 3 and 4 in Figure 39 (hematite with Al and hematite with Al an As)

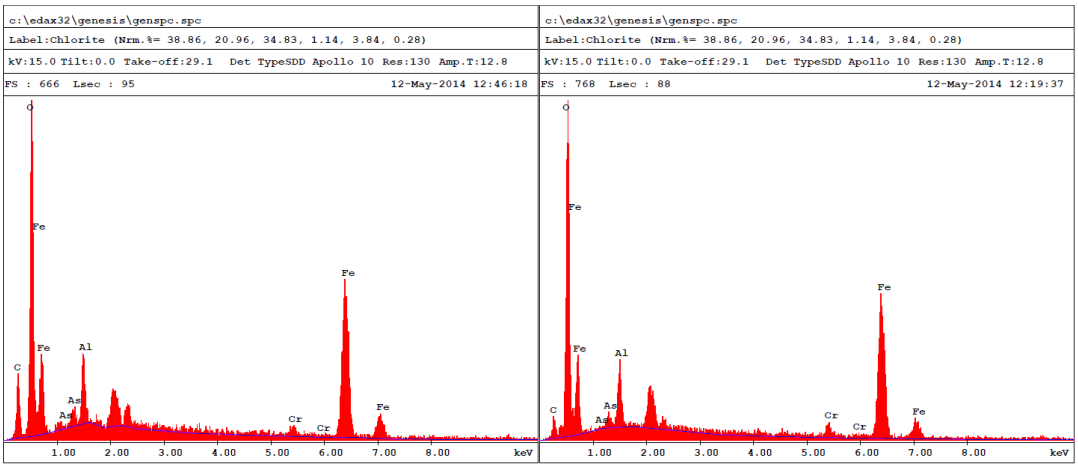

Figure 49 : EDS results of images 1 and 2 in Figure 44 (general view and goethite with Al, Cr and As)

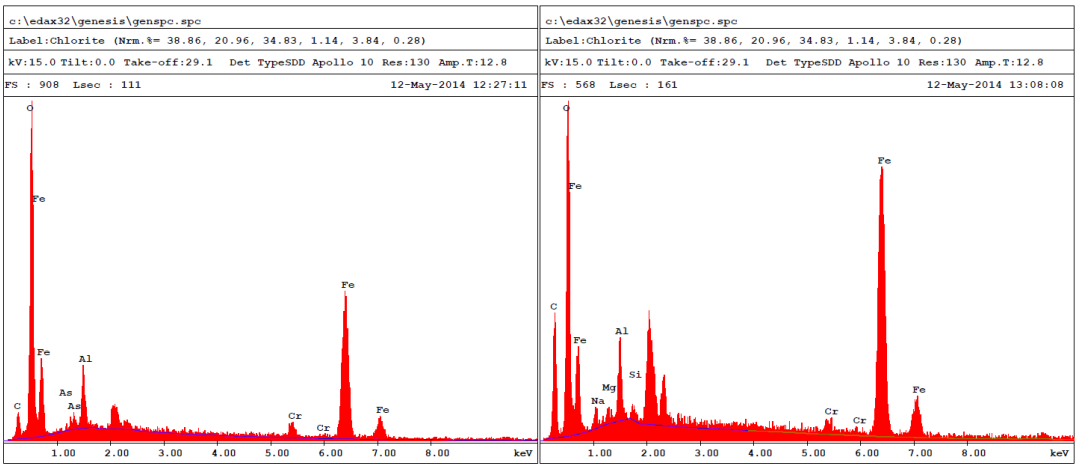

Figure 50: EDS results of images 3 and 4 in Figure 44 (goethite with Al, Cr and As and shiny goethite particle)